# Middle Rio Grande
# Isleta Reach:
## Isleta Diversion Dam to Rio Puerco
## Hydraulic Modeling and
## Silvery Minnow Habitat Analysis
## 1918-2016

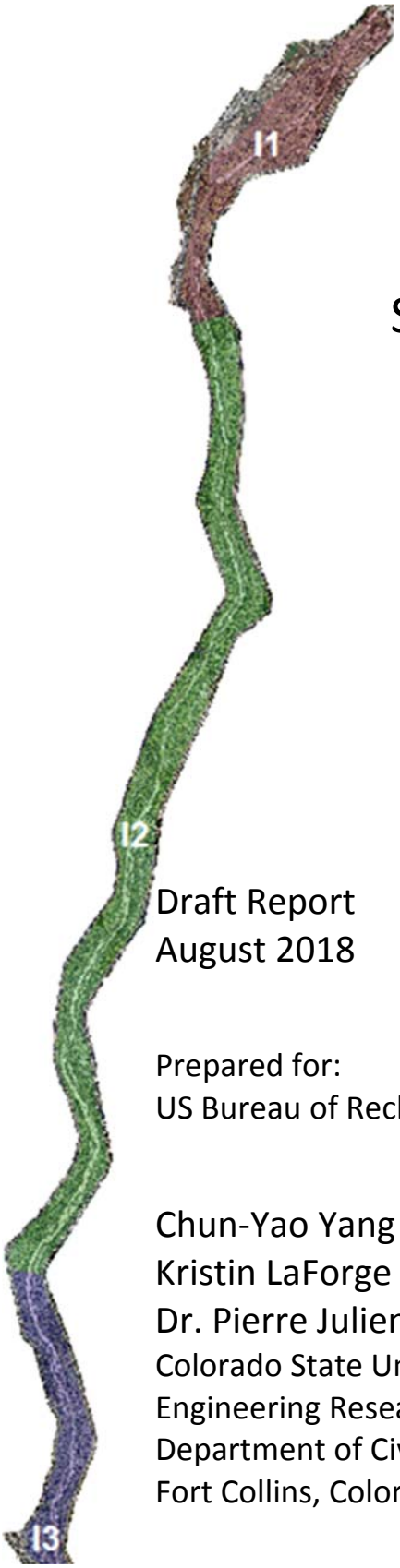



Draft Report
August 2018

Prepared for:
US Bureau of Reclamation

Chun-Yao Yang
Kristin LaForge
Dr. Pierre Julien
Colorado State University
Engineering Research Center
Department of Civil Engineering
Fort Collins, Colorado 80523

# Abstract

The Isleta Reach spans about 42 miles of the Middle Rio Grande, from the Isleta Diversion Dam to the confluence with the Rio Puerco, in central New Mexico. This reach report for the U.S. Bureau of Reclamation aims to better understand the morphodynamic processes of the reach and how this links to Rio Grande silvery minnow habitat. The reach is split into six subreaches (I1, I2, I3, I4, I5 and I6) to facilitate the analysis of spatial and temporal trends in channel geometry, morphology and habitat quality.

It is found that the hydrology and hydraulics have been in flux over the past century. For instance, the mean annual discharge decreased since the 2000s. Suspended sediment discharge has been declining since the 1970s, resulting in channel degradation.

The GIS analysis of aerial photographs as far back as 1918 and HEC-RAS analyses show geomorphic changes for each subreaches. The current channel width is less than one-fifth of what it was in 1918. This pattern is consistent throughout the subreaches. There is also a slight increase in sinuosity (the highest sinuosity occurs in I3), depth, velocity, and median grain size while the slope has decreased from 1972-2012. Also, a geomorphic conceptual model based on Massong et al. (2010) and Klein et al. (2018a) was considered to help to understand the channel evolution.

In addition, HEC-RAS and visual observations of aerial photographs with GIS were used to assess the habitat conditions in 1992, 2002, and 2012. HEC-RAS simulations show that the best "spawning" and "feeding/rearing" habitats are at 3500 cfs (compared to 600 and 1400 cfs). These habitats tend to occur in subreaches I1, I2, and I3 likely due to better floodplain connectivity. The area of "good" habitat is greatest at low flows of 600 cfs for subreaches I1-I4. The "good" habitat area also decreases from 1992 to 2012.

For the GIS analysis, the best scores are found in earlier years or when the flow is high enough to inundate the floodplain (>3500 cfs). Subreaches I2 – I4 have the highest scores when comparing all years. By comparing the aerial photographs that were taken under similar flow conditions (~600 cfs), it shows that subreaches I1 – I4 have the best habitat scores. The shoreline complexity was also analyzed with GIS. It does not have a consistent pattern over the years, but the highest score was found in 2005 with the flow just under 6000 cfs.

Comparing both HEC-RAS and GIS analyses for low flow conditions, it is found that subreaches I1-I3 have the best habitat and the overall habitat quality declines from 1992 to 2012. The decrease in habitat quality is likely due to: (1) a reduction in the frequency and magnitude of peak discharges; and (2) the channel narrowing and incising causing a loss of connectivity to the floodplain.

# Table of Contents

# List of Figures

# List of Tables

# 1. Introduction

The Middle Rio Grande is located in central New Mexico and spans about 170 miles from the Cochiti Dam to Elephant Butte Reservoir (Tetra Tech 2002). It has been heavily impacted over the past few centuries due to settlements along the river (Scurlock 1998). For instance, construction of levees, jetty jacks, and dams were put in place throughout the 1900's to control the flow and mitigate extreme floods and droughts. As a result this caused the river to become narrower and more incised than its previous braided and shallow planform (Larsen 2007). This has caused a plethora of problems for agriculture practices and the health of the river. These changes have recently caused a shift towards a more sustainable management of the river in the past few decades (Scurlock 1998; Tetra Tech 2014; Baird 2016).

In response to the decline of the silvery minnow, studies have been done to understand how the Rio Grande functions and how it has been changing (Baird 2014; Bauer 2000; Berry and Lewis 1997; Bovee et al. 2008; Crawford et al. 1993; Easterling 2015; Happ 1948; Horner 2016; Klein et al. 2018a; Larsen 2007; Makar 2010; Massong 2010; MEI 2002; Posner 2017; Richard 2001; Swanson et al. 2010; Tetra Tech 2014; Varyu 2016). These reports only comprise a few of those that have added to the body of knowledge of how the Rio Grande functions and how this affects silvery minnows. A report analyzing the geomorphology and silvery minnow habitat for subreaches within the Rio Puerco reach has not been done before. Therefore, this report intends to give an overview of the geomorphology and silvery minnow habitat for Rio Puerco subreaches.

Objectives of this report:

- Delineate the reach into meaningful subreaches
- Present the flow and sediment discharge history
- Compare the silvery minnow population to peak discharges
- Analyze the geomorphological drivers at a subreach level (sinuosity, width, braiding, bed elevation, bed material, volume change, and hydraulic parameters)
- Create a conceptual geomorphic model to help predict how the river will change in the future
- Analyze how the silvery minnow habitat changes with different flow regimes
- Analyze habitat quality of silvery minnows with remote sensing (GIS)

## 1.1. Literature Review

### 1.1.1. Middle Rio Grande History

Scurlock's commonly cited, comprehensive report on "An Environmental History of the Middle Rio Grande Basin", outlines relevant historical, climatic, and geomorphological events on the Middle Rio Grande. Since the 1400's the Rio Grande has undergone extreme fluctuations in climate. There have been intense floods that resulted in loss of establishments, livestock, and human life. These floods had negative impacts on settlements, but also provided them with benefits. The floods leached out salts and supplied rich alluvium to the farm land, and helped

maintain aquatic ecosystems by connecting the main channel flow to the floodplains. Droughts had major impacts as well. They sometimes forced settlements to abandon the area in search for better sources of water, which allowed the land to recover in their absence (Scurlock 1998).

Cultural shifts have also heavily impacted the river. Native Americans populated the land around the Middle Rio Grande and lived sustainably off the land for thousands of years. In the 1500's, Spaniards settled in this area and began taking over the farming land and employed irrigation systems. In these irrigation lands, mining and logging practices grew for hundreds of years. Starting in the 1800's, Anglo-Americans settled in the land. With the increase in land use of the years, regulations and agencies were necessary to deal with the growth. For instance, as more and more people settled in the land, the settlements became more permanent, so flooding and droughts needed to be mitigated. Starting in the 1900's levees, dams, and channelization techniques were used to control where and how much the river flowed. Towards the end of 1900's, there was a shift towards a more sustainable mindset that incorporated farming, water quality, water quantity and ecological needs (Scurlock 1998). This frame of mind is necessary moving forward as well. By focusing on the biological aspect of the river, such as saving endangered species like the silvery minnow, the health of the river can be improved.

### 1.1.2. Silvery Minnow

The Endangered Species Act of 1973 was enacted to prevent native plants and animals from becoming extinct and help preserve natural ecosystems. An ecosystems integrity often depends on species that are in danger of going extinct. The degradation of ecosystem functions is problematic because we benefit immensely from the services that healthy ecosystems provide, such as food production and water purification.

Silvery minnows became an endangered species in 1994 (Tetra Tech 2014; U.S. Fish and Wildlife Service 2010), and their decline is a harbinger of the declining ecological health of the Middle Rio Grande (Russo 2018). The southwestern willow flycatcher is also listed as an endangered species, and there are a plethora of invasive species on the Rio Grande. These are all signs that point towards an unhealthy riparian system. Dams, levees, and channelization of the river are likely causes of this (U.S. Fish and Wildlife Service 2007). Currently, the silvery minnow occupies about only seven percent of its historic range (U.S. Fish and Wildlife Service 2010). It is believed to only occur in the Middle Rio Grande from Cochiti Dam to Elephant Butte Reservoir (Bestgen and Platania 1991; Dudley et al. 2005). The San Acacia Reach falls inside of this range, which is one of the reasons is it being studied. Because silvery minnows are an indicator of the health of the river, great efforts have been made to protect them.

### 1.1.3. Silvery Minnow and the River

The relationship between the geomorphology and the riparian ecosystem is essential to understanding how to save the silvery minnow. The silvery minnow depends on certain characteristics of the Rio Grande to survive. The most important characteristic is the connection

of the main channel to the floodplain (Scurlock 1998; Cowley 2002; U.S. Fish and Wildlife Service 2010; Medley and Shirley 2013; Tetra Tech 2014; Dudley et al. 2016). Most of the spawning and rearing occurs in the floodplains, so silvery minnows need access to the floodplains to propagate. Silvery minnows depend on both the physical parameters of the river and hydrologic regime for floodplain connectivity. Spawning is stimulated by high flows in late April to early May, so these peak flows are very necessary (Cowley 2002).

The in-stream characteristic are also important. Silvery minnows most commonly occupy habitats with debris piles, pools and backwater. They thrive in mostly silt substrate and require low velocities and moderate depths. Their requirements as juvenile are also different than those as an adult (Dudley and Platania 1997).

Dams, levees and diversion structures have heavily impacted the hydraulics and fluvial processes of the river. Sediment size has gone up overall, the floodplain is less connected than it has been in the past, water quality has decreased, and the river has become fragmented by dams (Osborne et al. 2012; Larsen 2007). These factors all decrease the habitat quality of silvery minnows. This is evident when looking at the decline of silvery minnow genetic diversity, densities, catch rates, and habitat range (Horner 2016). To prevent the silvery minnow from going extinct, we must study the river processes, understand how this impacts the ecological health of the system, and how to improve it. Looking at smaller scales such as reaches, and subreaches may offer insight into how the rivers and minnows interact.

### 1.1.4. Why Save the Silvery Minnow

"It's hard to predict the effect of killing off a species unless you go ahead and kill it- and then it's too late to reverse it" (Marshall 2015). Without protecting species, the riparian ecosystem's diversity and resiliency will be negatively impacted. As a result, the health of the river could rapidly decline and its resources could become unusable. "Science is telling us that ecosystems provide us with a host of things we can't do without, and that the more diverse each ecosystem is, the better" (Marshall 2015). The more abundant, rich and resilient the ecosystems are, the more ecosystem services can be provided to people.

## 1.2. Site Description and Background

The lsleta Reach begins at the Isleta Diversion Dam to the confluence of Rio Puerco (Figure 1). The reach is about 42 miles and is relatively straight. The Isleta Diverison Dam was constructed in 1934 to control sedimentation and flooding (U.S. Bureau of Reclamation). The reach is relatively stable because of the bank stabilization and channelization during 1950s and 1960s. In addition, the floodplain is confined by a comprehensive levee system to protect the agricultural and municipal land on its perimeter (Posner 2017). Multiple sets of Kellner Jetty Jacks were placed on the bank to guide the flow and sediment to pass though the reach efficiently in order to protect the levee from erosion. As a result, sediment and vegetation filled the areas within the jack lines and the channel has become narrower (Varyu 2016).

In order to more easily analyze hydraulic trends along the Isleta Reach, the reach was segmented into six subreaches. These subreaches were determined by the cumulative plots of hydraulic variables including flow depth, velocity, slope and width with a flow of 3000 cfs. The location breaks of subreach are designated when there is noticeable change in slope in the cumulative plots. The variables were obtained by using HEC-RAS with the geometry files provided by the USBR. The geometry files of 1992, 2002, and 2012 were used. The breaks tend to coincide with the notable landmarks like confluences, geomorphic variables or bridges. Table 1 shows the subreach definition that is used in this study. This delineation is used in analyses throughout this report. The delineation is identified by aggredation/degredation lines (agg/deg line) which are "spaced approximately 500-feet apart and are used to estimate sedimentation and morphological changes in the river channel and floodplain for the entire MRG" (Posner 2017).

*Table 1: Isleta Reach subreach delineation.*

| Subreach Number | Agg-Deg Rangeline Numbers | Notable Geomorphic Controls and Comments |
|---|---|---|
| I1 | 657-700 | Isleta Diversion Dam (657)-Right Bank Drain Outfall (700) |
| I2 | 700-815 | Bend (815) |
| I3 | 815-964 | Straight reach, Abo Arroyo Confluence (964) |
| I4 | 964-1015 | No geomorphic control visible on aerial photograph |
| I5 | 1015-1053 | Highway 60 Bridge (1053) |
| I6 | 1053-1097 | Rio Puerco Confluence (1097) |

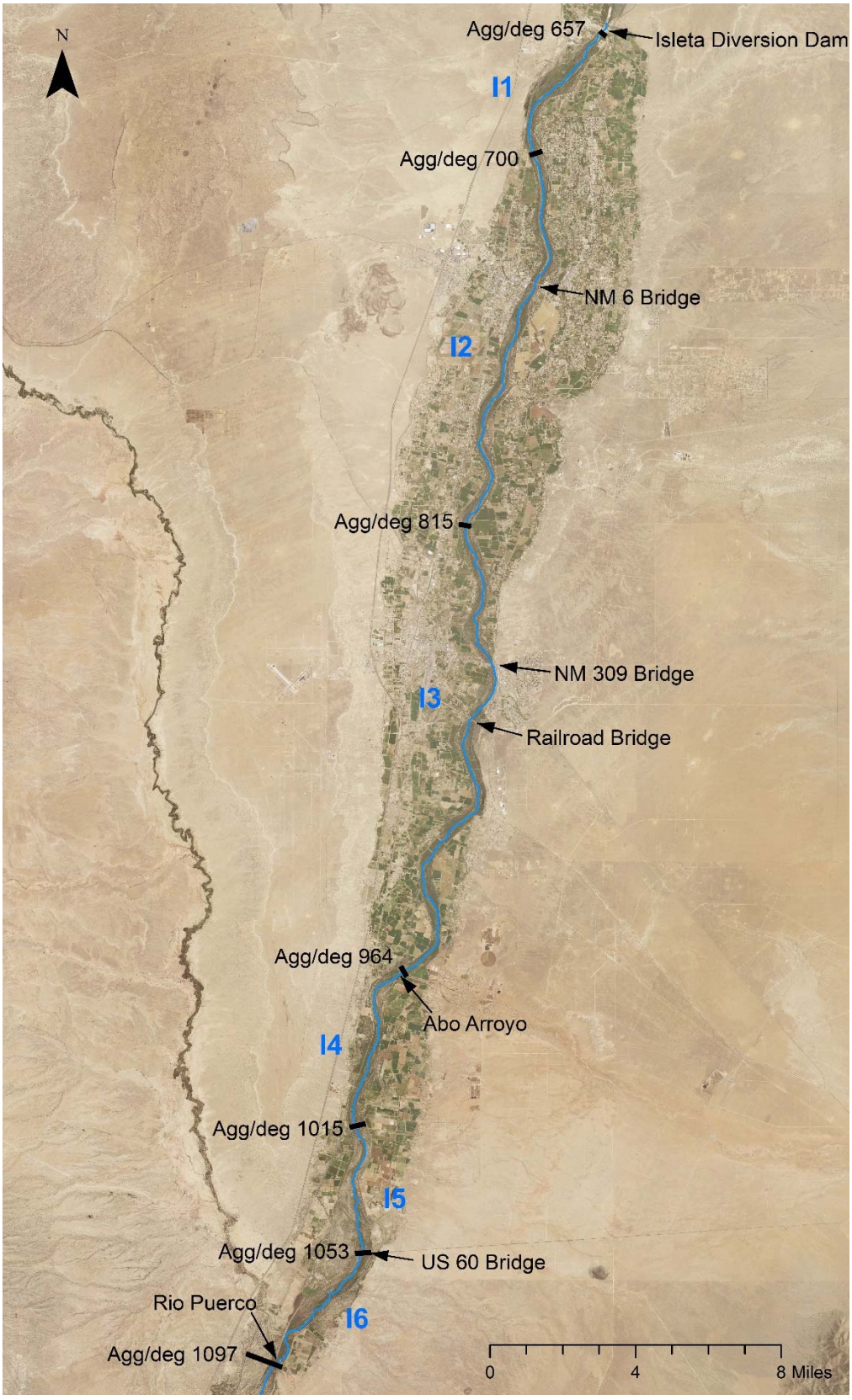


*Figure 1: Map of Isleta Reach and location of breaks of subreach.*

# 2. Flow and Sediment Discharge Analysis

Available gages near the study reach are found in the USGS National Water Information System. Table 2 lists the gages that were analyzed in this report.

*Table 2: List of USGS gages used in this study.*

| Station | Station # | Mean daily discharge | Suspended sediment |
|---|---|---|---|
| Rio Grande at Albuquerque | 08330000 | Oct 1989 - Current | Oct 1969 – Sep 2016 |
| Rio Grande at Isleta Lakes Near Isleta | 08330875 | Oct 2002 - Current | |
| Rio Grande Near Bosque Farms | 08331160 | Oct 2007 - Current | |
| Rio Grande at State HWY 346 near Bosque | 08331510 | Oct 2006 - Current | |
| Rio Grande Floodway Near Bernardo | 08332010 | Oct 1990 - Current | Oct 1964 – Sep 2015 |
| Rio Puerco near Bernardo | 08353000 | Sep 1939 - Current | Oct 1955 – Sep 2015 |
| Rio Grande Floodway at San Acacia | 08354900 | Oct 1958 - Current | Oct 1959 – Sep 2016 |

## 2.1. Discharge

The daily discharge of the Albuquerque (08330000), Bernardo (08332010) and San Acacia (08354900) are plotted as shown in Figure 2, Figure 3, and Figure 4. No data is available during July 2005 through September 2011 for the Bernardo gage. The plots show seasonal flow patterns: the high flow occurs in April through June, followed by low flow in July to October, and medium flow from November to March. The spring high flow is attributed to snow melt runoff. However, the spring flow significantly decreases after 2002. Recently, upstream reservoirs have reduced peak flows coming through the Isleta reach. The Rio Puerco is unregulated though, and has large peak flows. They are still lower than peak flows observed in the 1920's to the 1940's (MEI 2002 in Klein et al. 2018a).

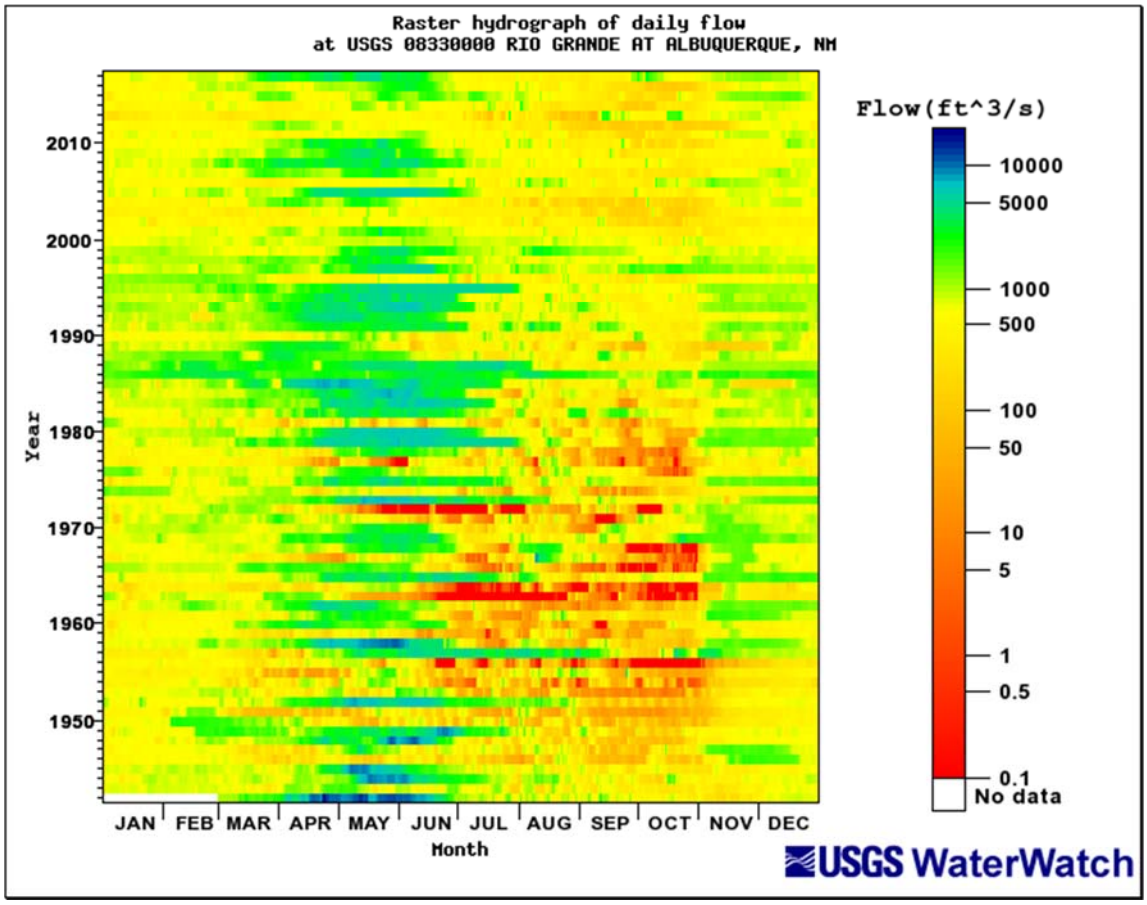


*Figure 2: Raster hydrograph for the Rio Grande at Albuquerque (08330000): 1942 to 2017.*

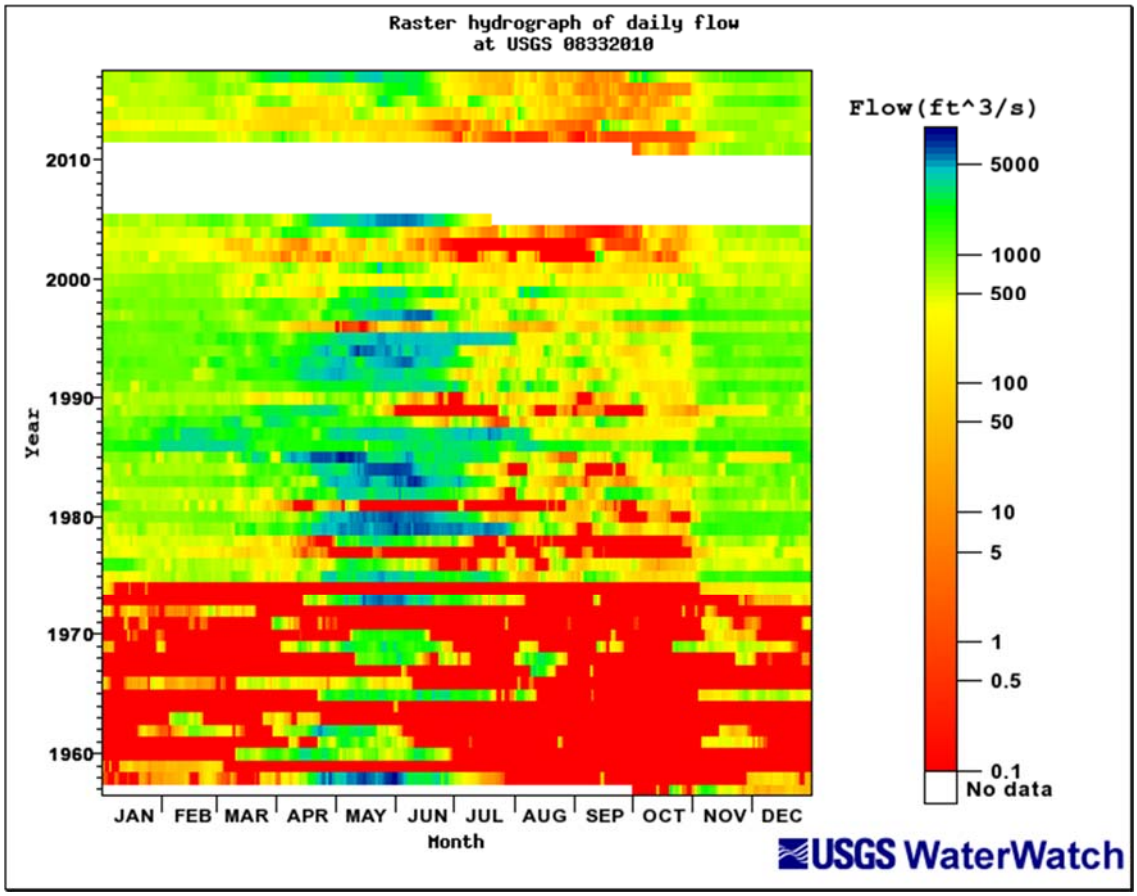


*Figure 3: Raster hydrograph for the Rio Grande floodway near Bernardo (08332010): 1958 to 2017.*

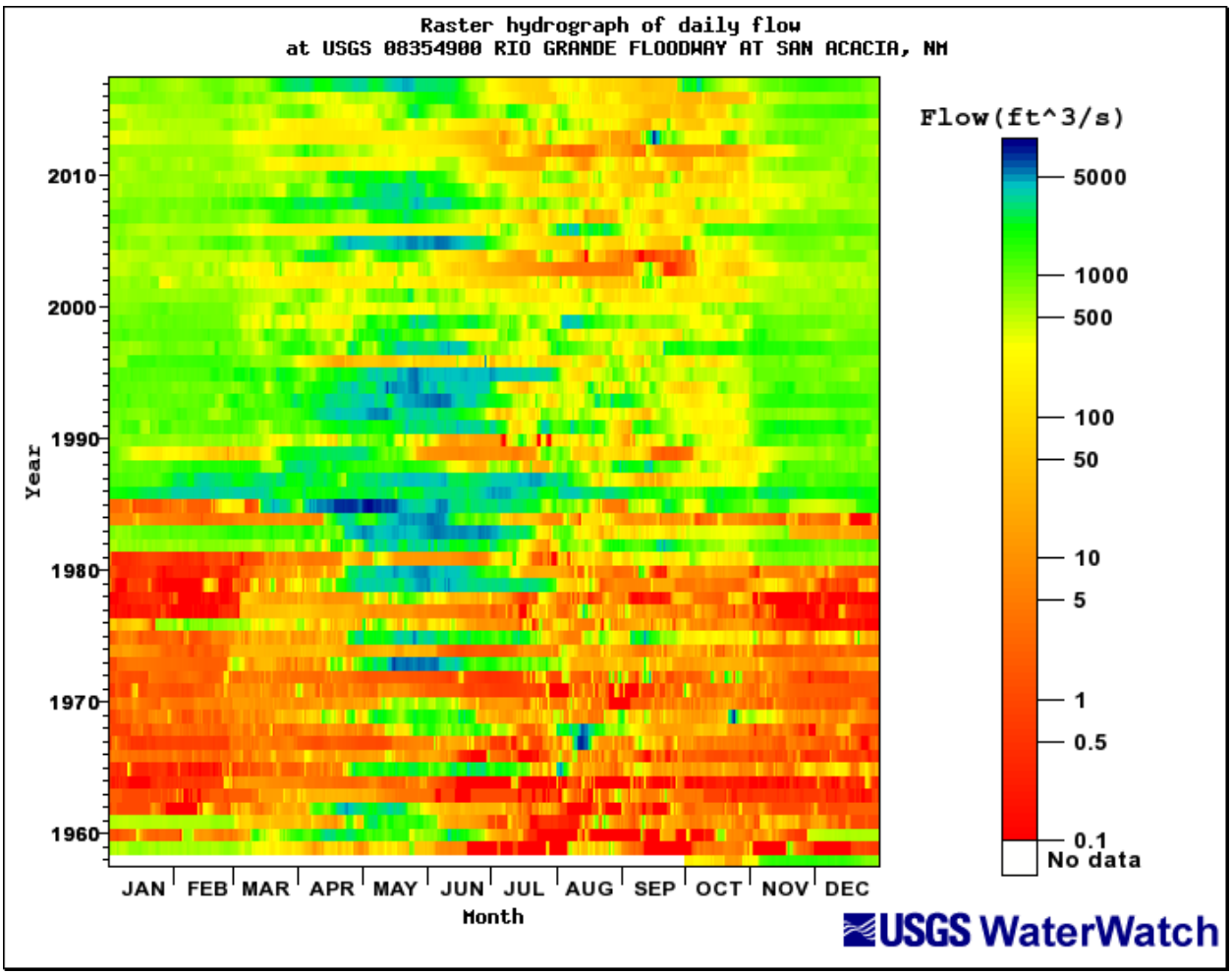


*Figure 4: Raster hydrograph for the Rio Grande floodway at San Acacia (08354900): 1958 to 2017.*

### 2.1.1. Single Mass Curves

Single mass curves are used to show changes in annual flow volume over time. The cumulative discharge is presented as a function of time in years. The slope of the line gives the mean annual discharge. Breaks in slope show changes in the flow volume. Figure 5 shows the flow mass curves of gages at Albuquerque, Isleta, Bosque Farms, Bosque, Bernardo, and San Acacia. The annual flow volume shows slight reduction in the downstream direction. The discharge mass curves are divided by the time periods 1942 to 1978, 1978 to 1980, 1980 to 1981, 1981 to 1987, 1987 to 1990, 1990 to 1995, 1995 to 2001, 2001 to 2004, 2004 to 2010, 2010 to 2014, 2014 to 2017. The average discharge of each period is listed in Table 2. For the Albuquerque gage (08330000), the annual flow increases from 0.74 million acre-feet to 1.21 million acre-feet after 1978. A decrease in discharge between 1995 and 2010 and another decrease in discharge is found after 2010. Similar trends are found in the other stations as well.

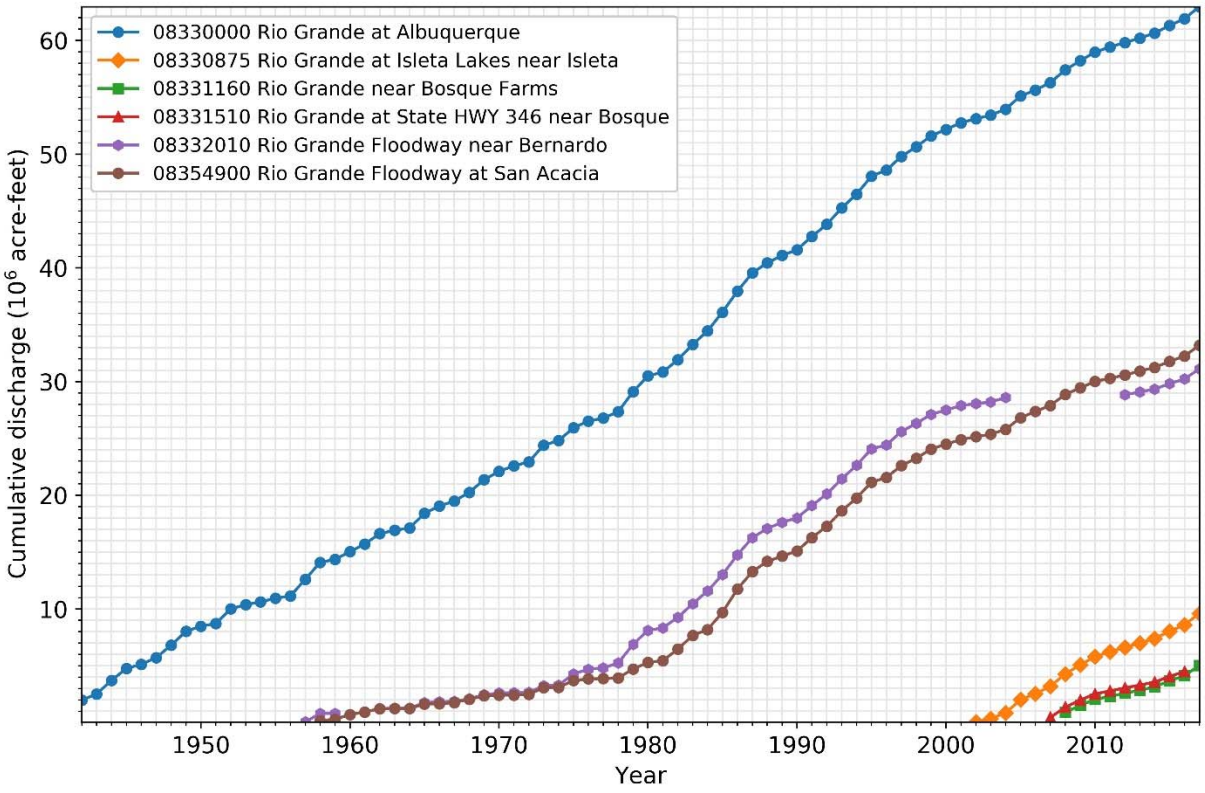


*Figure 5: Single mass curves with the cumulative water discharge on the y-axis and the year is on the x-axis.*

*Table 3: Average discharge at different time periods in million acre-feet.*

| Time | 08330000 | 08330875 | 08331160 | 08331510 | 08332010 | 08354900 |
|---|---|---|---|---|---|---|
| 1958 - 1978 | 0.74 | | | | 0.25 | 0.19 |
| 1978 - 1980 | 1.57 | | | | 1.44 | 0.68 |
| 1980 - 1981 | 0.34 | | | | 0.22 | 0.16 |
| 1981 - 1987 | 1.45 | | | | 1.32 | 1.30 |
| 1987 - 1990 | 0.68 | | | | 0.58 | 0.61 |
| 1990 - 1995 | 1.29 | | | | 1.21 | 1.21 |
| 1995 - 2001 | 0.78 | | | | 0.64 | 0.62 |
| 2001 - 2004 | 0.40 | 0.29 | | | 0.23 | 0.31 |
| 2004 - 2010 | 0.84 | 0.83 | 0.68 | 0.63 | | 0.70 |
| 2010 - 2014 | 0.42 | 0.40 | 0.28 | 0.26 | 0.25 | 0.31 |
| 2014 - 2017 | 0.78 | 0.73 | 0.63 | 0.46 | 0.59 | 0.65 |

### 2.1.2. Recurrence Interval

Using gages previously mentioned, recurrence intervals were calculated and presented in a report from the U.S. Bureau of Reclamation (USBR). The report by Klein et al. (2018a) is closely related to this report, but the USBR geomorphic analysis is not broken up into subreaches like it this one. Therefore, the USBR report provides a great deal of background and summary of this reach, so is referenced frequently. For example, Table 4 summarizes flood frequencies in the Klein et al. (2018a) report.

*Table 4: Return periods (Klein et al., 2018a).*

**Table 4: Discharge at different regulated flood frequencies for the study area modified from Wright (2010), MEI (2002), and Harris and AuBuchon (2016). Annual peak flow from the USGS was used in analysis.**

| Discharge (cfs) | 2 Year | 5 Year | 10 Year | 25 Year | 50 Year | 100 Year |
|---|---|---|---|---|---|---|
| **Albuquerque (MEI (2002))** | 5,410 | 7,600 | 8,940 | 10,100 | 11,600 | 12,600 |
| **Albuquerque (Wright (2010))** | 4,000 | 6,200 | 7,500 | 9,000 | 10,000 | 10,000 |
| **Albuquerque, 1993-2013** | 3,370 | 5,280 | 6,550 | 8,100 | 9,230 | 10,300 |
| **Bernardo (Wright (2010))** | 4,900 | 7,700 | 9,300 | 11,200 | 12,500 | 12,700 |
| **Bernardo, 1993-2013** | 3,290 | 5,610 | 7,090 | 8,820 | 10,000 | 11,100 |
| **San Acacia (Wright (2010)** | 7,800 | 12,000 | 14,500 | 17,400 | 19,300 | 20,100 |
| **San Acacia (Harris, 2016)** | 4,410 | 6,380 | 7,570 | 8,920 | 9,820 | 10,600 |

Days exceeding certain flow values was also examined. There is data at the Albuquerque, Bernardo and San Acacia gages. The data is analyzed in water years instead of the calendar years. From Figure 6 through Figure 8 we can see that the occurrence of high flow drops after 2002.

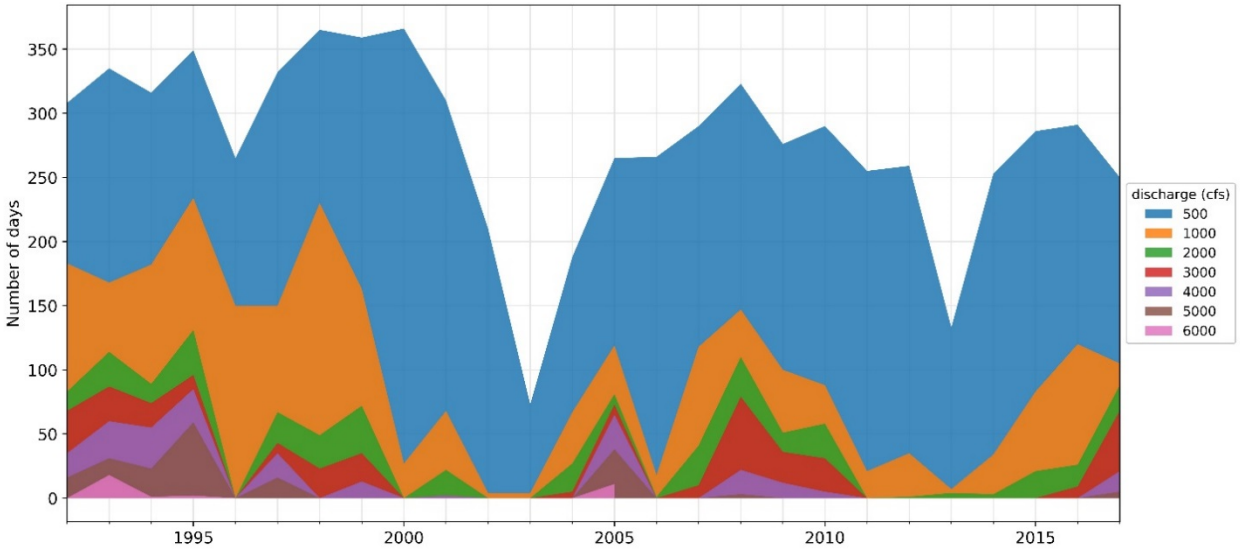


*Figure 6: Graph of days exceeding flow values at Albuquerque (08330000) (modified from Klein et al., 2018a).*

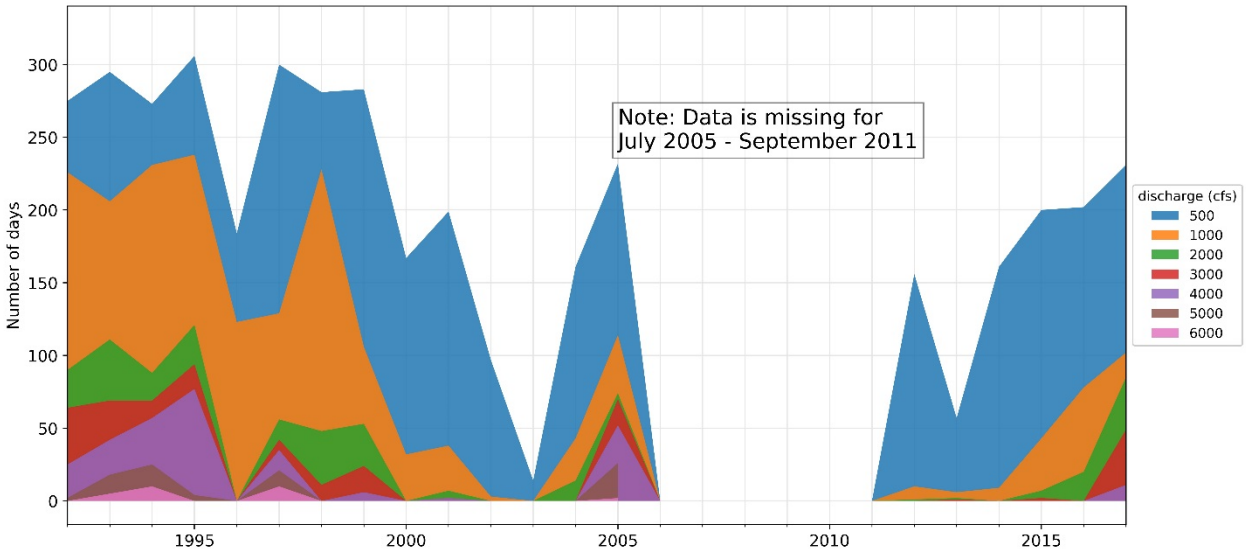


*Figure 7: Graph of days exceeding flow values at Bernardo (08332010) (modified from Klein et al., 2018a).*

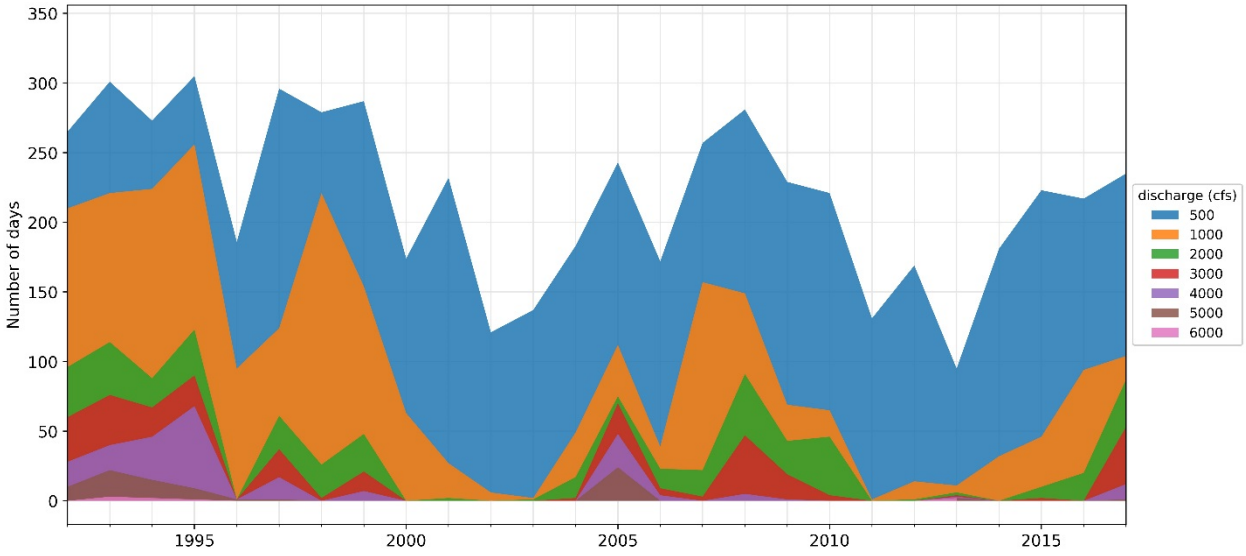


*Figure 8: Graph of days exceeding flow values at San Acacia (08354900) (modified from Klein et al., 2018a).*

### 2.1.3. Relation between flow and population of RGSM

According to Dudley et al., the population of RGSM is "closely related to the timing, magnitude, and duration of flows in spring and summer" (Dudley et al. 2016). Figure 9 shows the relation between the population density of RGSM, spring peak discharge, annual mean discharge, and occurrence of flow higher than 2000 cfs at Albuquerque. The change of fish population generally follows the magnitude of spring peak flow and the occurrence of high flow. Figure 10 shows the scatter plots of fish population vs spring peak discharge and fish population vs number of days that discharge is higher than 2000 cfs. This suggests the fish population is positively related to these two variables.

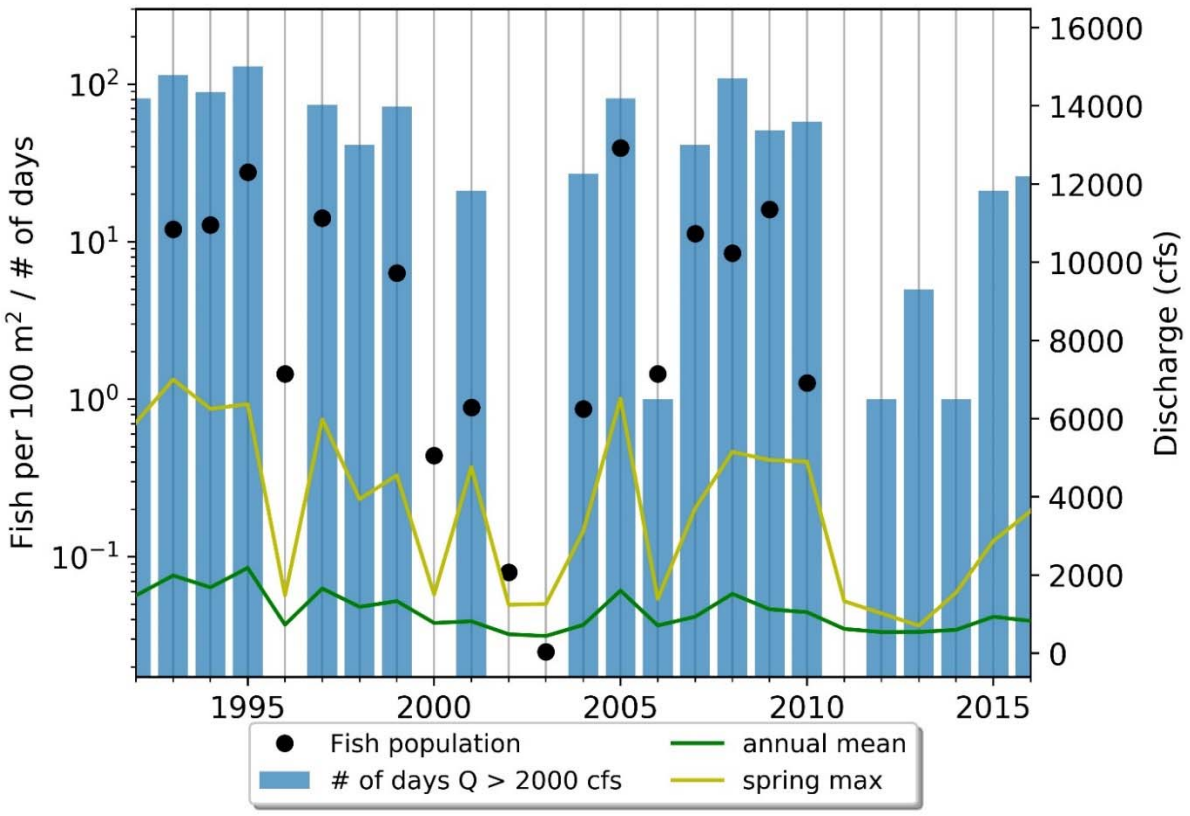


*Figure 9: Population of silvery minnow vs annual mean discharge vs spring peak flow vs number of days that discharge is greater than 2000 cfs.*

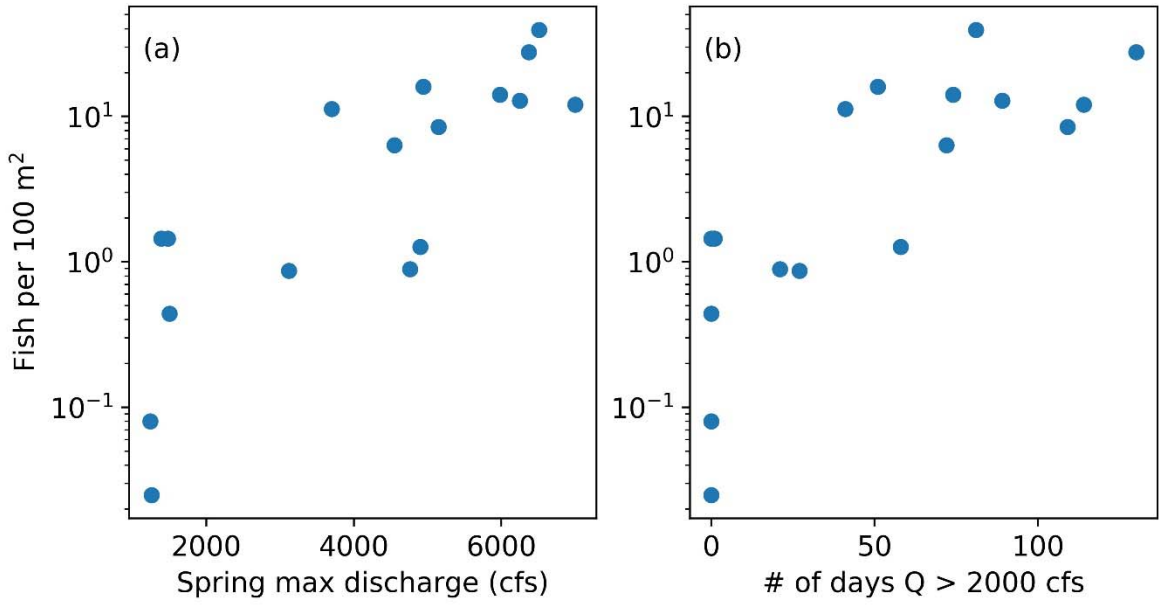


*Figure 10: (a) Fish population density vs spring peak discharge, and (b) Fish population density vs number of days discharge is higher than 2000 cfs.*

## 2.2. Precipitation

Precipitation data is collected from areas in between Los Lunas and Sevilleta. The data is from the Bosque Ecosystem Monitoring Program website (Klein et al. 2018a). The average annual and monthly data account for open and vegetated areas. The annual precipitation data summarized by USBR is shown in Figure 11.

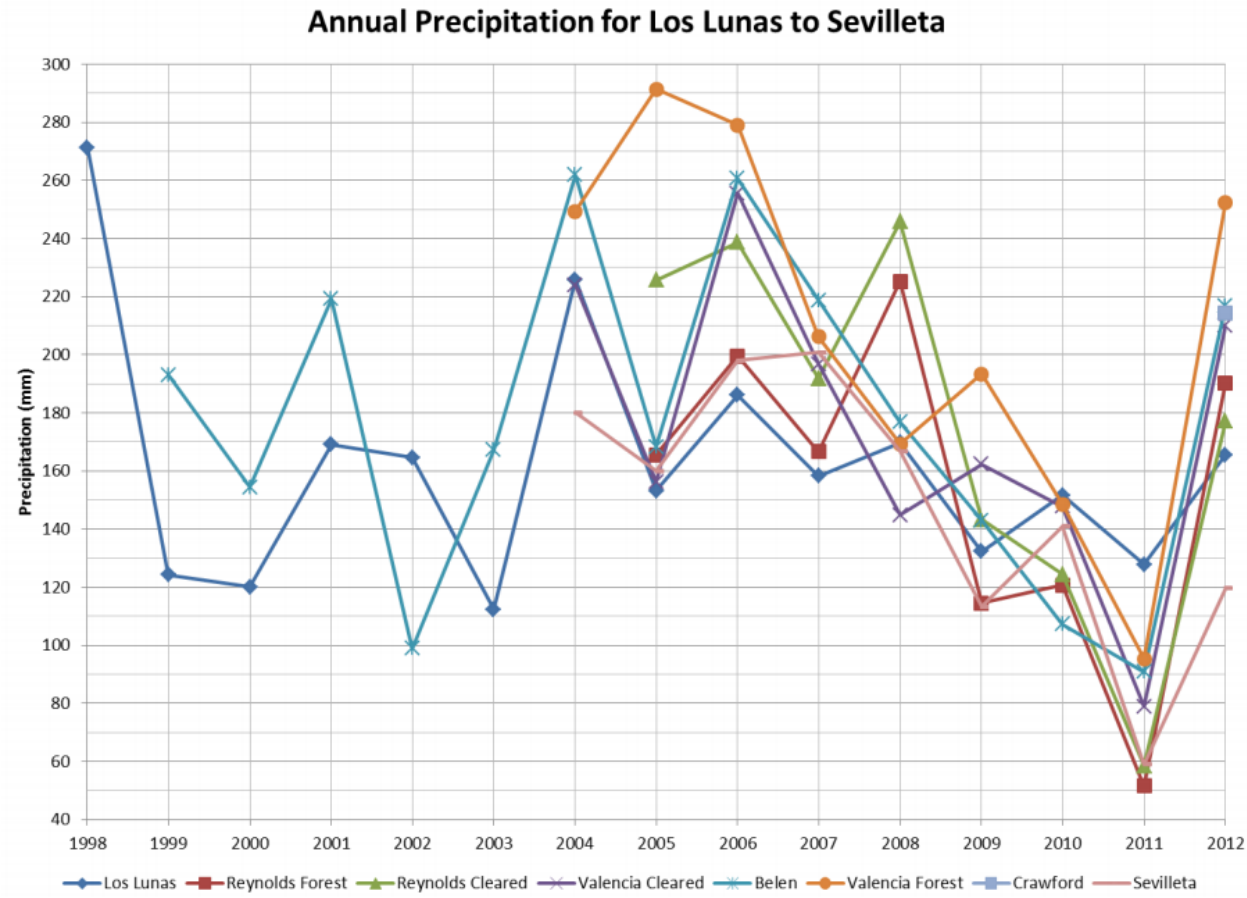


*Figure 11: Average annual precipitation graph from USBR from 1998-2012.*

The precipitation has a sinuous trend. It goes up and down over long periods of time. 1998, 2005 and 2012 have peaks in precipitation. The driest years are around 2002 and 2011. The monthly precipitation data summarized by USBR is shown in Figure 12.

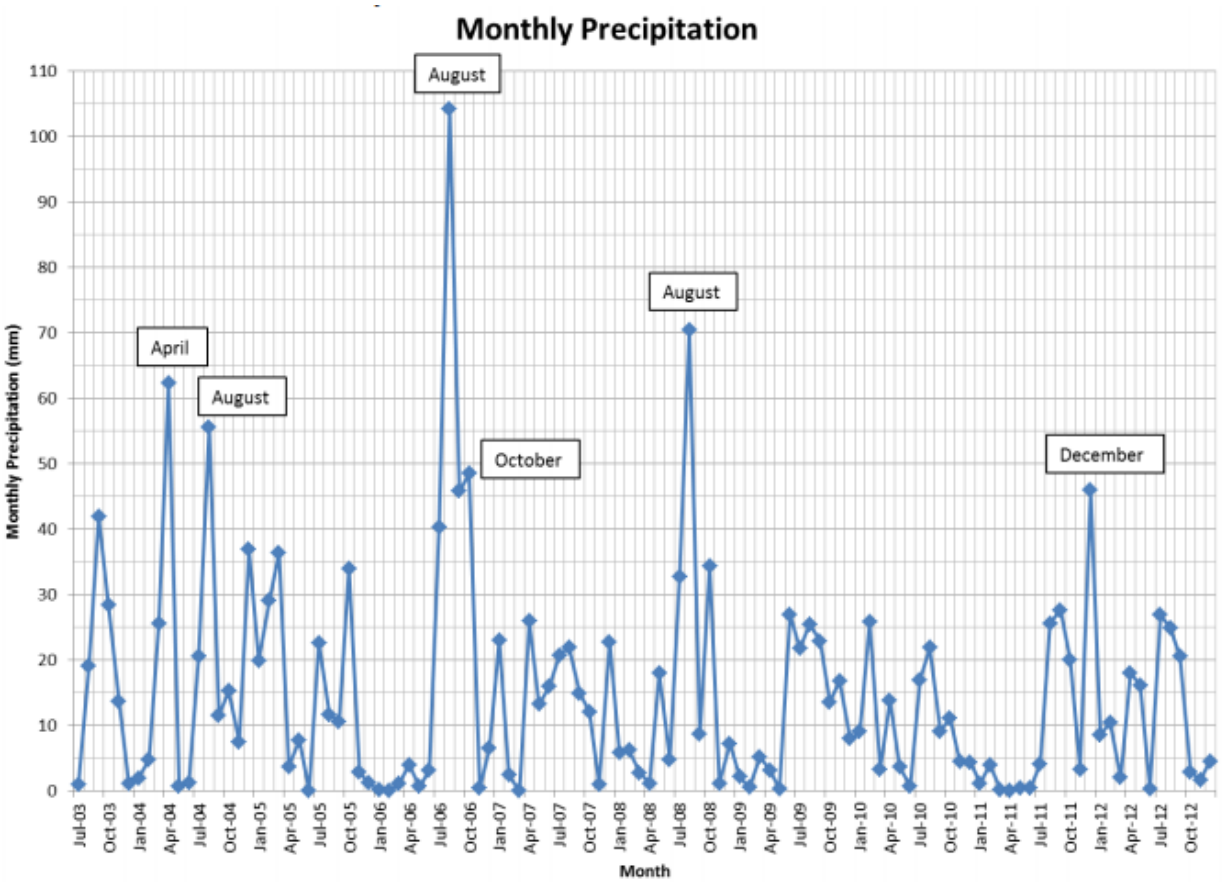


*Figure 12: Monthly precipitation graph from Los Lunas to Sevilleta (Klein et al. 2018a).*

The highest rainfall events tend to happen in late summer or early fall. Winter and early spring rain events still occur but are less common.

## 2.3. Suspended Sediment

Single mass curves are used to show how the tons of suspended sediment changes over time. Breaks in slope show these changes. USGS gages pertinent for suspended sediment in this reach are at the Albuquerque (08330000) gage and Bernardo (08332010) gage upstream of the Rio Puerco confluence. The Rio Puerco gage (USGS 0853000) is used for the Rio Puerco single mass curve. The data on the graph is based on annual sediment amounts. Figure 13-Figure 15 show the suspended sediment curves.

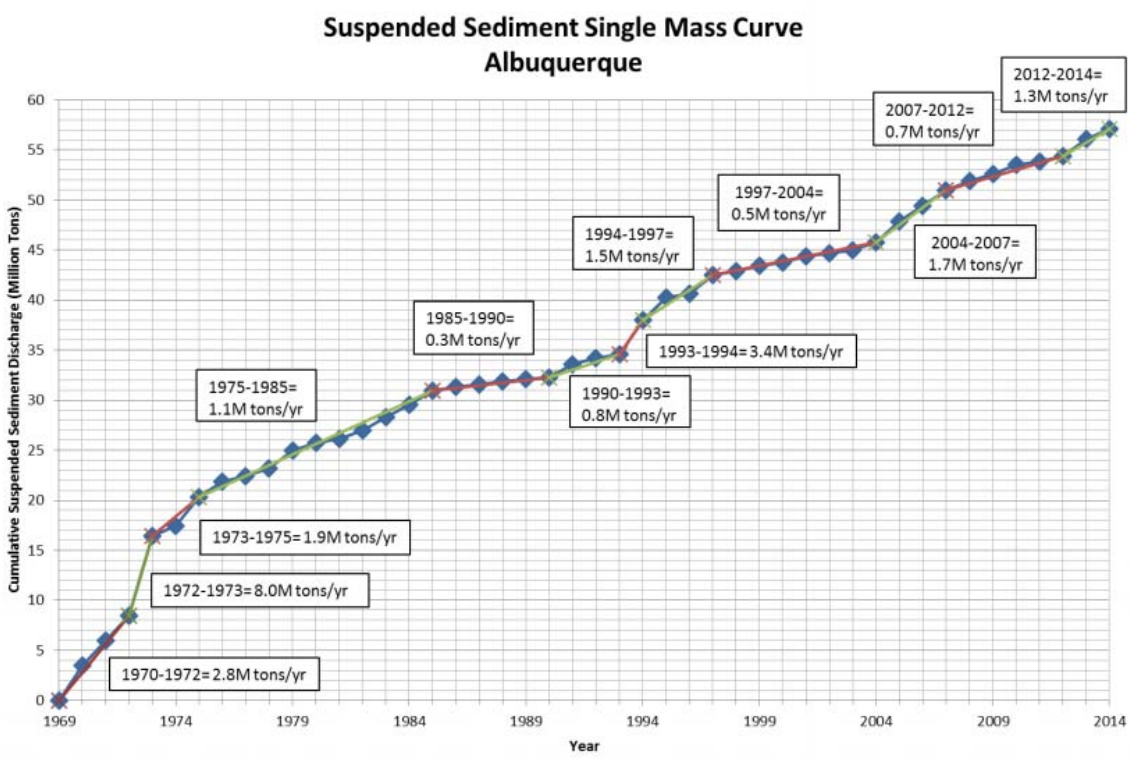


*Figure 13: Single mass curve at Albuquerque (08330000) for suspended sediment (Klein et al., 2018a).*

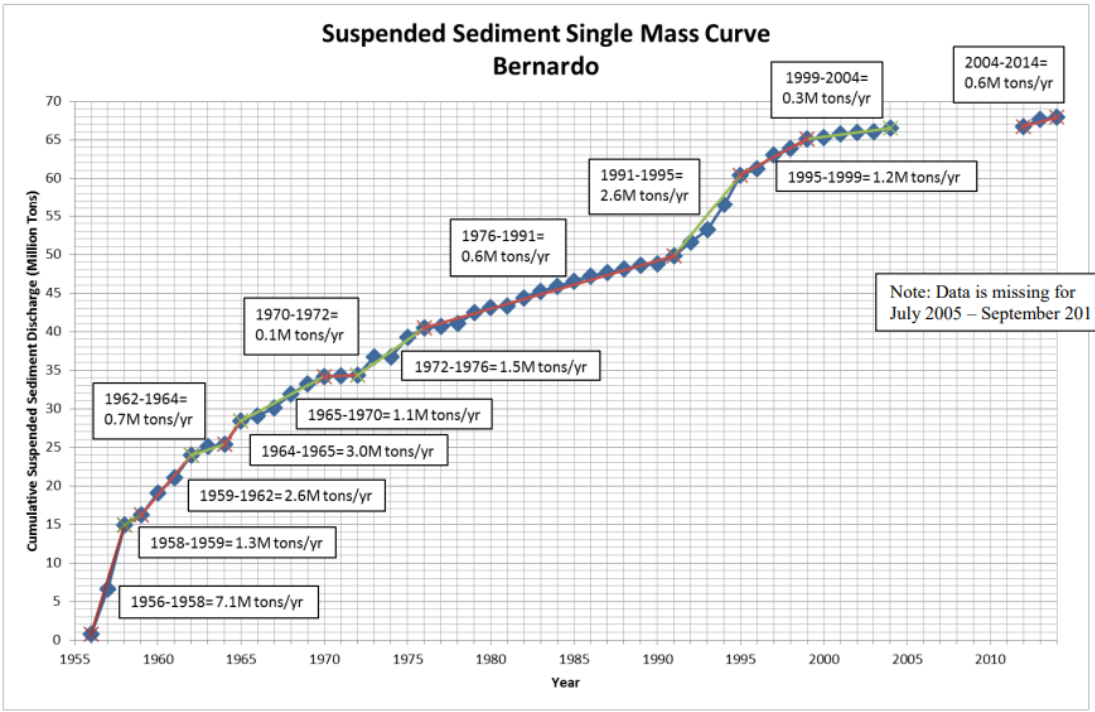


*Figure 14: Single mass curve upstream of the Rio Puerco (08332010) for suspended sediment (Klein et al., 2018a).*

For both the Albuquerque and Bernardo gages, there is a significant decrease in suspended sediment being transport starting around the 1970's. Also, from 1991 to 1995 there was a large increase in suspended sediment which then decreased and became constant after 1995. The Bernardo and Albuquerque gage have switched back and forth in terms of which one transports more suspended sediment. From the 1970's to the mid 1980's and from the mid 2000's through 2014 the Albuquerque gage showed more sediment yield. In-between those two time periods, the Bernardo gage recorded more suspended sediment transport.

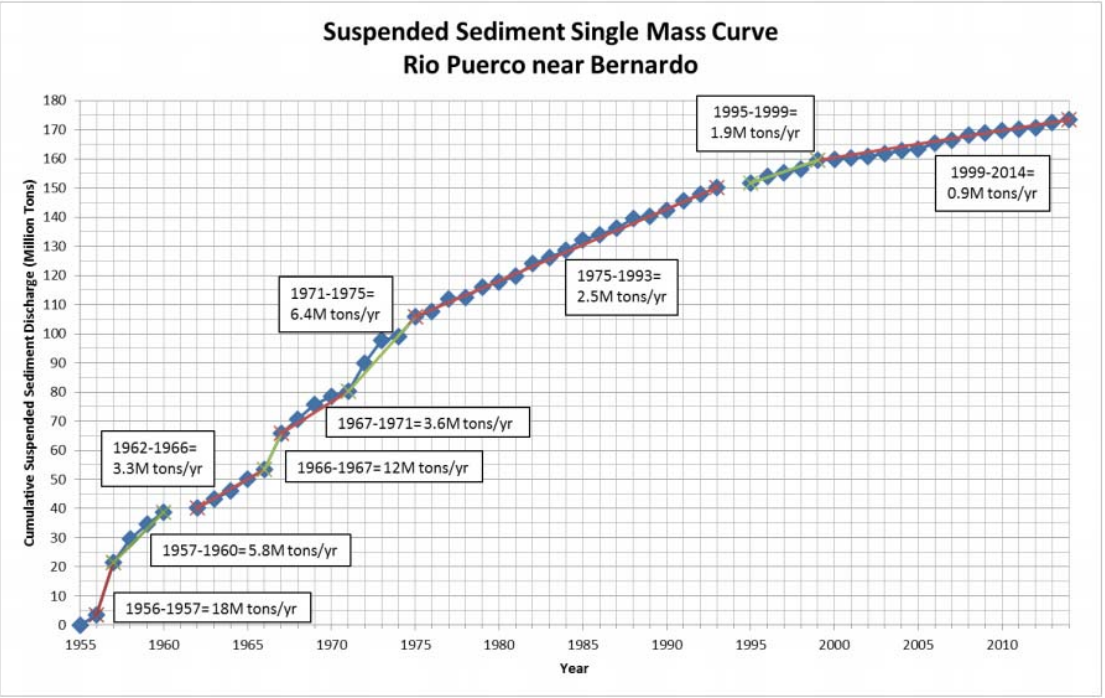


*Figure 15: Single mass curve for suspended sediment on the Rio Puerco (08353000) (Klein et al. 2018a).*

The Rio Puerco's sediment discharge has decreased since the 1970's. Still, it contributed 70% of the annual suspended sediment volume recorded at the San Acacia gage from the late 1970's through the early 1980's. Now it only contributes about 38% of the annual suspended sediment load (Klein et al. 2018a).

## 2.4. Double Mass Curves

Double mass curves are used to show how suspended sediment volumes pair with annual discharge volume. Overall, the mean annual suspended sediment concentration has decreased since the 1960's (Klein et al. 2018a).

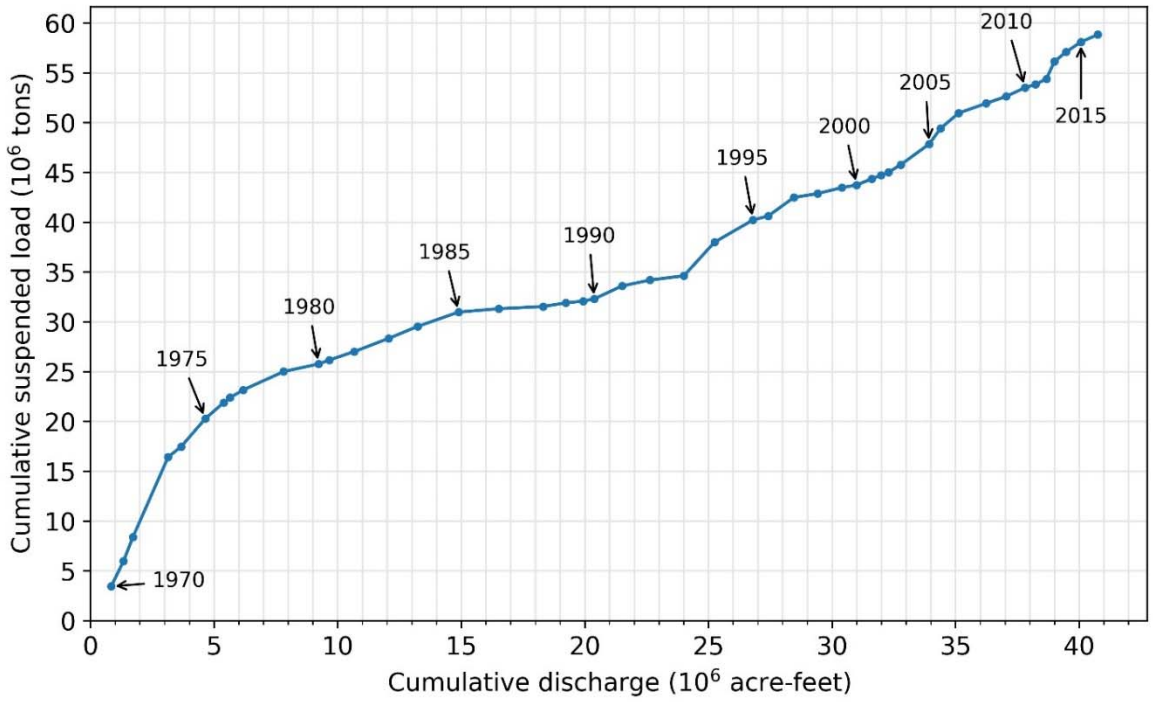


*Figure 16: Double mass curve at Albuquerque gage (08330000) from 1970 to 2016.*

The highest concentration occurred prior to 1975 at this gage. It decreased from 1985 to the 1990's and then increased again.

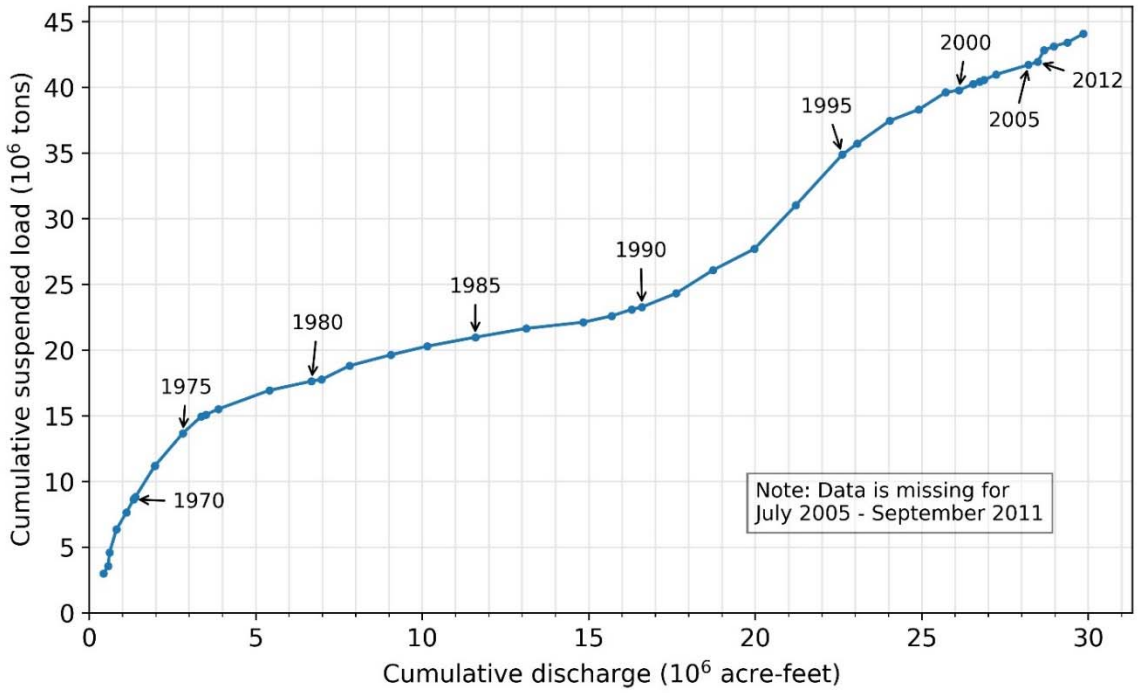


*Figure 17: Double mass curve at Bernardo gage (08332010) from 1965 to 2016.*

The Bernardo gage shows similar results as the Albuquerque gage. Although, there is a more distinct increase in sediment concentration in the early 1990's in the Bernardo gage.

## 2.5. Total Load

This section is a presentation of calculations, methods and results from the USBR report. Total load was calculated using BORAMEP with sediment data from the San Acacia gage downstream of the SADD. This is the only gage USBR used to calculate the total load, so it is the only data available for the Isleta Reach. The calculations using BORAMEP included the early 1990's through 2010 (Klein et al. 2018a).

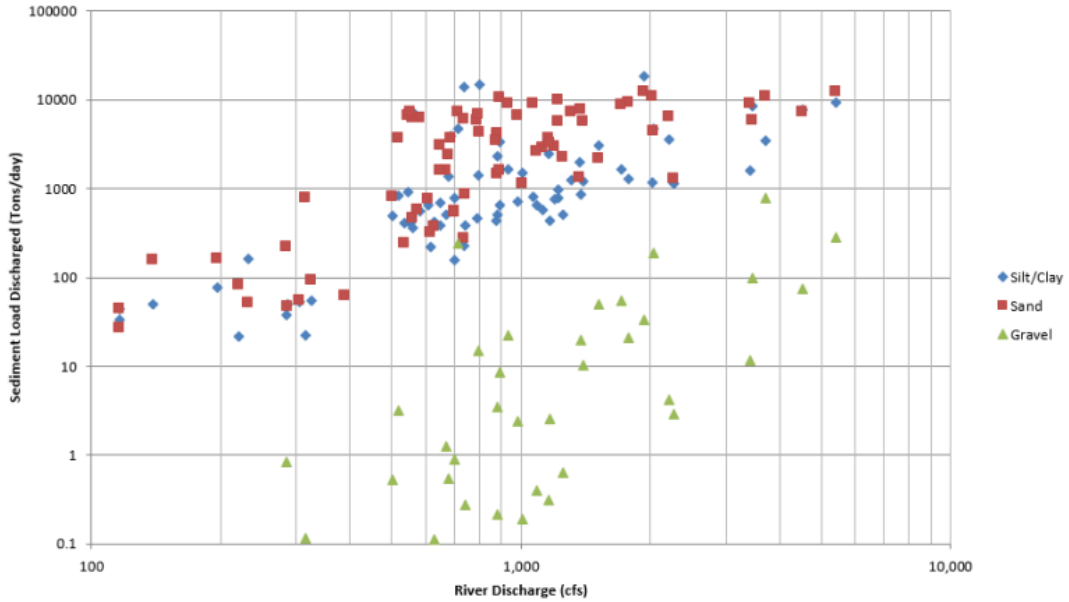


**Figure 60: Sediment load graph comparing sediment type for various river discharges at San Acacia for water years 1995 through 2010 (gravel data points below 0.1 tons/day have been omitted)**

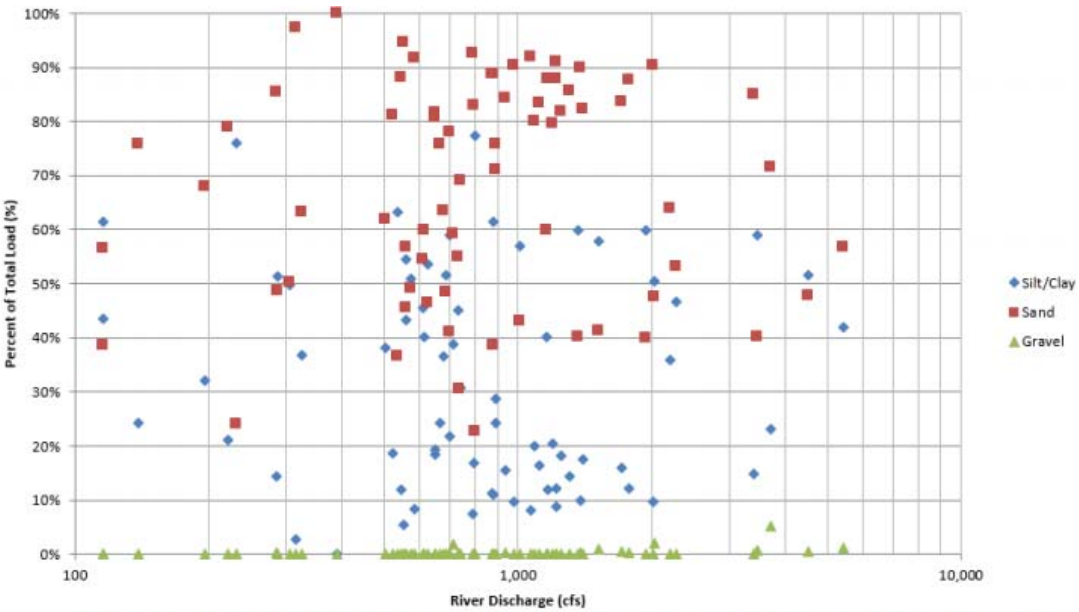


**Figure 61: Percent of total load graph comparing sediment type for various river discharges at San Acacia for water years 1995 through 2010.**

*Figure 18: Graphs of total load at the San Acacia gage from 1995-2010. Figure 60 shows the amount of sediment load discharged on the y-axis and figure 61 shows the percent of total load on the y-axis. They both show how particles move at different discharges (Klein et al., 2018a).*

The San Acacia gage shows that the predominant material being transported is sand. Silts and clays are transported less than sand, and gravel is less than 1% of the total load. Also, sand loads are 5 times greater during summer or fall rain events compared to spring snow-melt runoff periods. Gravel moves more during spring snow-melt periods (flows reach above 2000 cfs), whereas sand and smaller particles move during both spring and summer peak flow periods (Klein et al. 2018a).

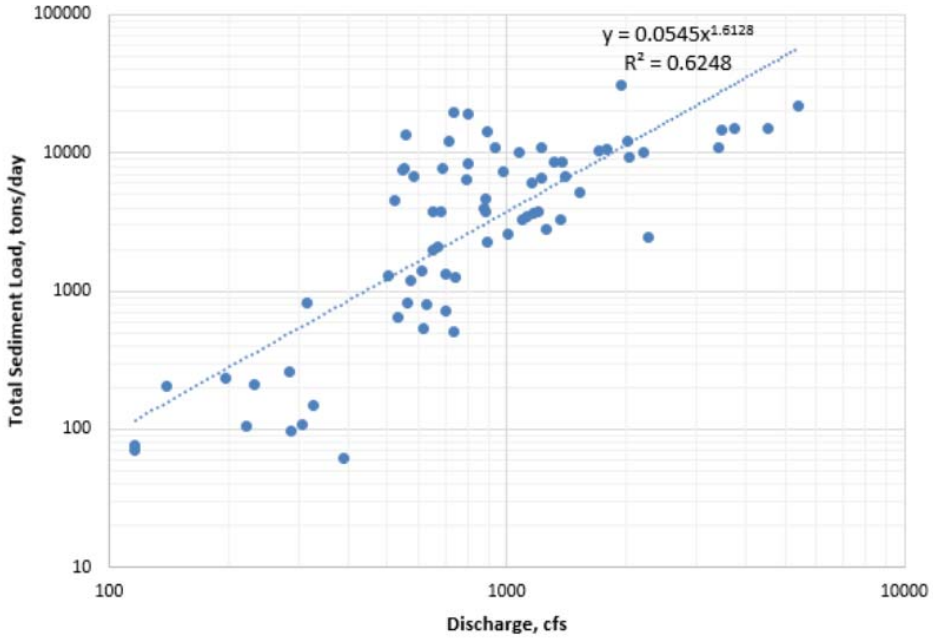


*Figure 19: Graph of total load rating curve at San Acacia for all total load points from 1995-2010 (Klein et al. 2018a).*

The effective discharge of 750 cfs was calculated from the total load rating curve trendline. The amount of sediment transported for each discharge was forecasted with the trendline and divided into bins. The results are shown in Figure 20.

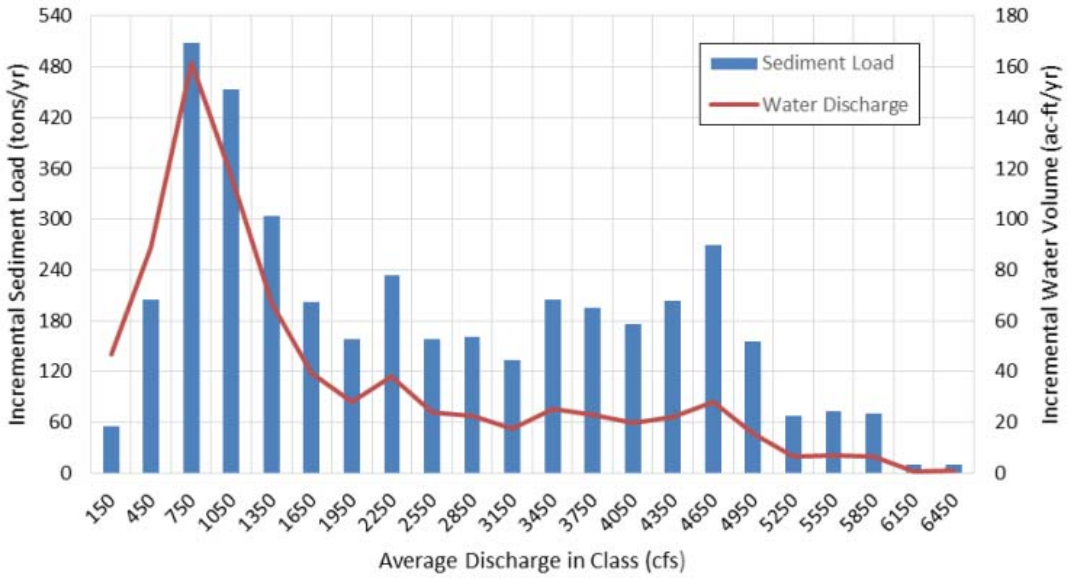


*Figure 20: Effective discharge curve at San Acacia from 1995-2010 (Klein et al. 2018a).*

# 3. Geomorphic and River Characteristics

Middle Rio Grande has been changing due to the dynamic of flow and sediment regimes, and the influence of human activities. In this section, the temporal change of the geomorphic attributes were analyzed. The analysis was conducted based on aerial photos, cross sectional surveys at agg/deg line and rangelines, and HEC-RAS simulations. The changes of the following parameters are present: sinuosity, active channel width, bed elevation, channel volume, and hydraulic variables.

## 3.1. Sinuosity

USBR collected data on sinuosity starting in the 1930's through 2016. Sinuosity has been increasing over time for the whole reach from the Isleta to the Rio Puerco since the 1930's.

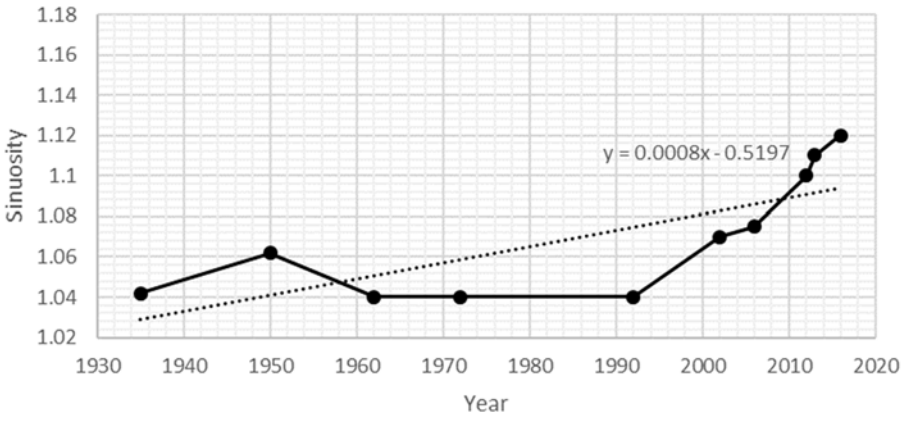


*Figure 21: Trend of sinuosity from the Isleta diversion dam to Rio Puerco. A positive slope of 0.0008 is observed. The data for this graph was extracted from a graph provided by USBR (Klein et al. 2018a).*

Figure 21 shows the Isleta to Rio Puerco reach with an overall positive slope. There is a small spike in 1950, then decreases and stays constant until about 1990 when it starts increasing. It follows this trend through 2016. Figure 22 shows the sinousity for each subreach. Overall, the sinuosity is near one which indicates a very straight channel.

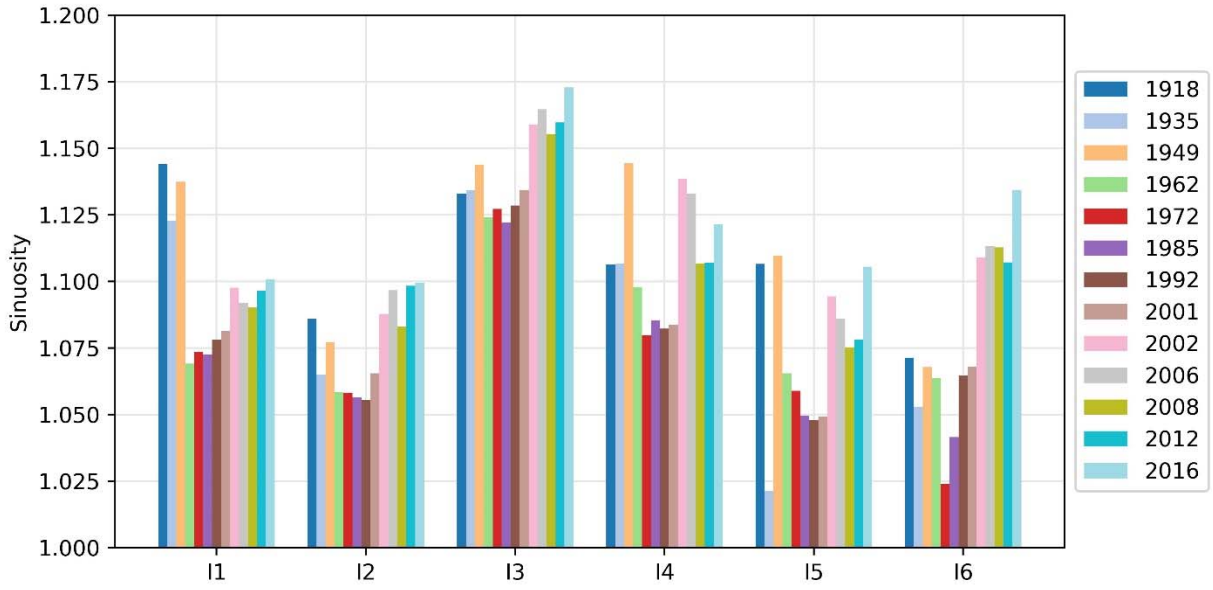


*Figure 22: Sinuosity at subreach scale.*

Subreach I3, Los Chaves to Abo Arroyo Confluence, is the most sinuous overall. The precipitous drop in sinuosity after 1949 in a few suberaches could be a result of channelization in the 1950's.

## 3.2. Width

The width has generally decreased over time since 1918 in this reach due to infrastructure building, channelization, reduction in peak flows, upstream sediment reduction and vegetation encroachment (Culbertson and Dawdy 1964; Crawford et al. 1993; Berry and Lewis 1997; Bauer 2000; MEI 2002; Bauer and Hilldale 2006; Tashjian and Massong 2006; Parametrix 2008; Bauer 2009; Makar 2010; Makar and AuBuchon 2012; Baird 2014 in Klein et al. 2018a). This has made the widths more uniform as well (Crawford et al. 1993; Parametrix 2008; Makar and AuBuchon 2012 in Klein et al., 2018a).

A schematic outlining basin morphology of the valley, levee and channel widths from 2007 and 2008 data helps present an overall reach perspective in Figure 23. The schematic is not to scale and provides an arbitrary centerline of the reach that doesn't account for sinuosity. It is used to get a perspective on the width of the active channel, levees and basin.

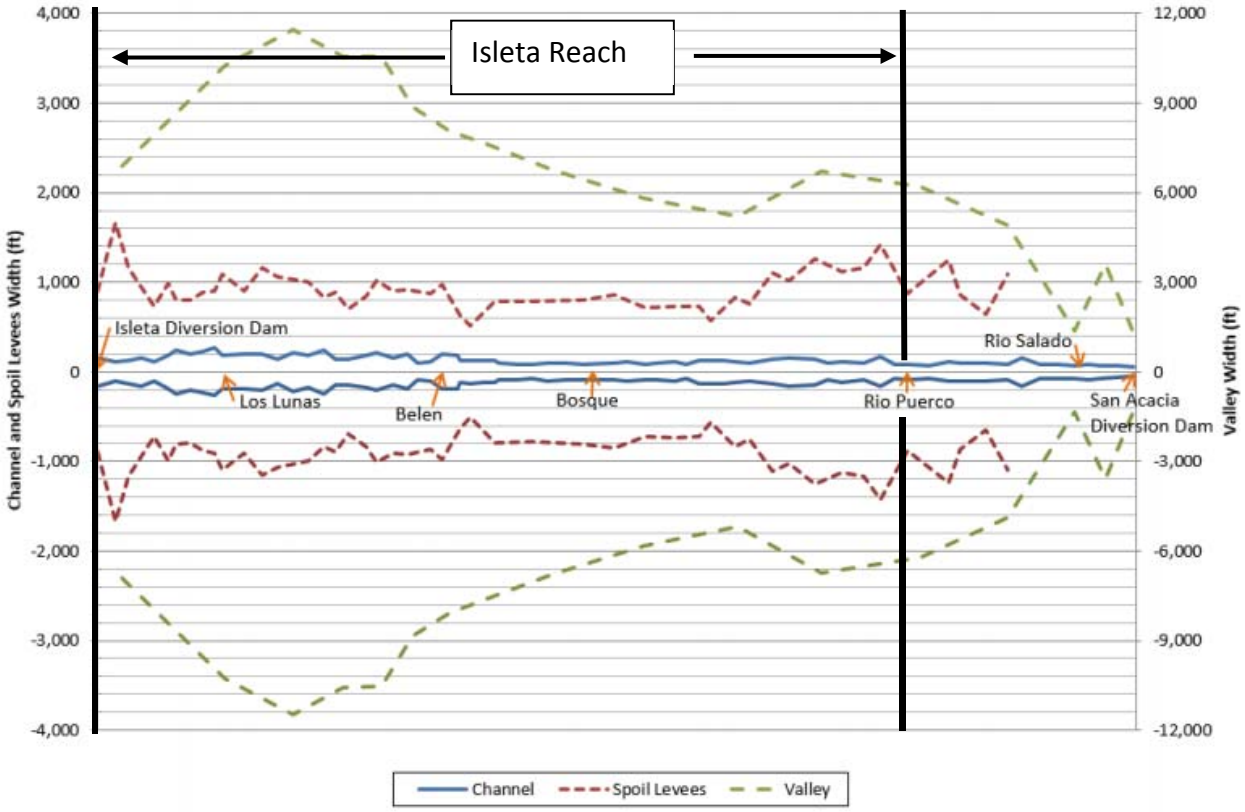


*Figure 23: Channel, spoil levees, and valley widths from the Isleta Diversion Dam to the San Acacia Diversion Dam. The figure is not to scale and just depicts relative widths. The Isleta reach is shown on the first ¾ of the graph going left to right from Isleta diversion Dam to Rio Puerco (Klein et al. 2018a).*

The valley width seems to have little effect on the channel width in the Isleta reach. The spoil levees control the floodplain width because they are between the valley and channel widths.

The active channel width is analyzed in more detail on a temporal scale between 1918 and 2016. The active channel is defined as non-vegetated channel and it is digitized by the USBR's GIS and Remote Sensing Group from the aerial photographs. The years analyzed include 1918, 1935, 1949, 1962, 1972, 1985, 1992, 2001, 2002, 2006, 2008, 2012, 2016 using agg/deg cross-sectional lines. Measurement of the active channel width is performed by clipping the agg/deg line coverage with the active channel polygon. Four lines (824, 873, 1061, and 1075) are deleted from the analysis because they are skewed with respect to the active channel for all years. The average width for each subreach is calculated by averaging the width of all agg/deg lines in the subreach (Figure 24).

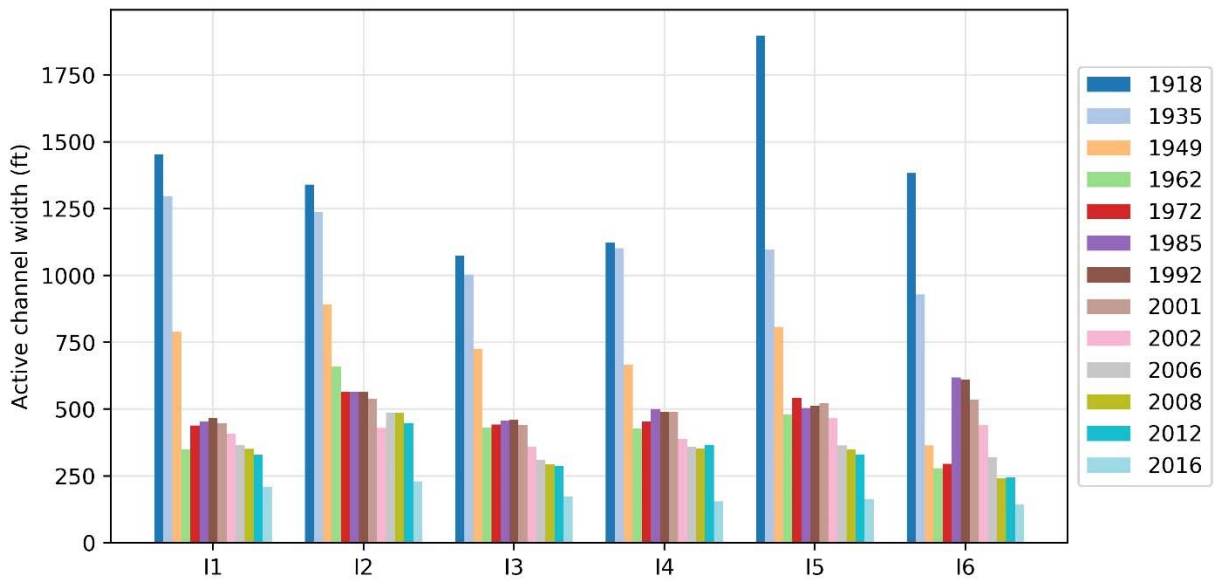


*Figure 24: Reach averaged active channel width.*

For each subreach, the width has decreased since 1918. The decline in channel width from 1918 to 1962 is the most significant and the biggest decrease is found at subreach I5: 1417 feet over 44 years. The widths across subreaches tend to drop off dramatically after 1949 because channelization with installation of jetty jack systems started around the 1950's (Easterling Consultants LLC 2015). There is an increase in channel width around the 1980's which is believed to be due to mechanical removal of vegetation (which stopped in the 1980's) and larger spring runoffs (Bauer and Hilldale 2006; Parametrix 2008 in Klein et al. 2018a). The average width began decreasing again starting in about 1992. The decreasing rate ranges from 5.9 ft/year (I2) to 18.3 ft/year (I6) between 1992 and 2012. There is an even steeper decrease starting in the 2010's, ranging from 25.2 ft/year (I6) to 54.5 ft/year (I2). The trend is similar to the Cochiti Reach reported in Richard (2001).

## 3.3. Braiding

The number of channels at each agg/deg line is measured from digitized planforms. The average number of channels is calculated for each subreach and presented in Figure 25.

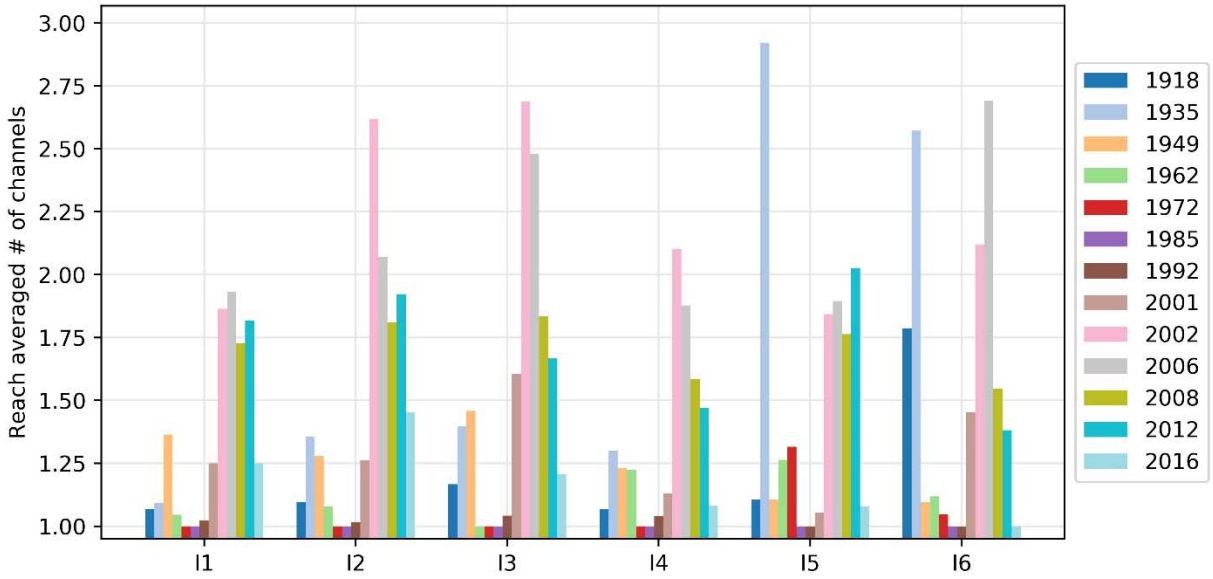


*Figure 25: Average number of channels at each subreach.*

The Isleta reach was a single threaded channel with occasional bars before 1940s. After 1940s, the reach transitioned into a braided channel. The number of channels is low for 1962, 1972, and 1982, because the digitized planforms for these years did not capture the bars or islands in the channel. The actual number should be higher. After 2012, the number of channels decreased.

## 3.4. Bed Elevation

The mean bed elevation is used to compare the change in long profile in this report. Cross-section geometry models along agg/deg lines were developed by the Bureau of Reclamation, Albuquerque Area Office. The geometry models are available for 1962, 1972, 1992, 2002 and 2012. For the models prior to 2012, the cross-section geometry is captured using photogrammetry techniques. The 2012 model is from LiDAR (Klein et al. 2018a). In addition, an underwater prism was developed (Varyu 2013). All the models were using the NAV88 vertical datum.

Figure 26 shows the long profiles of 1962, 1972, 1992, 2002, and 2012.

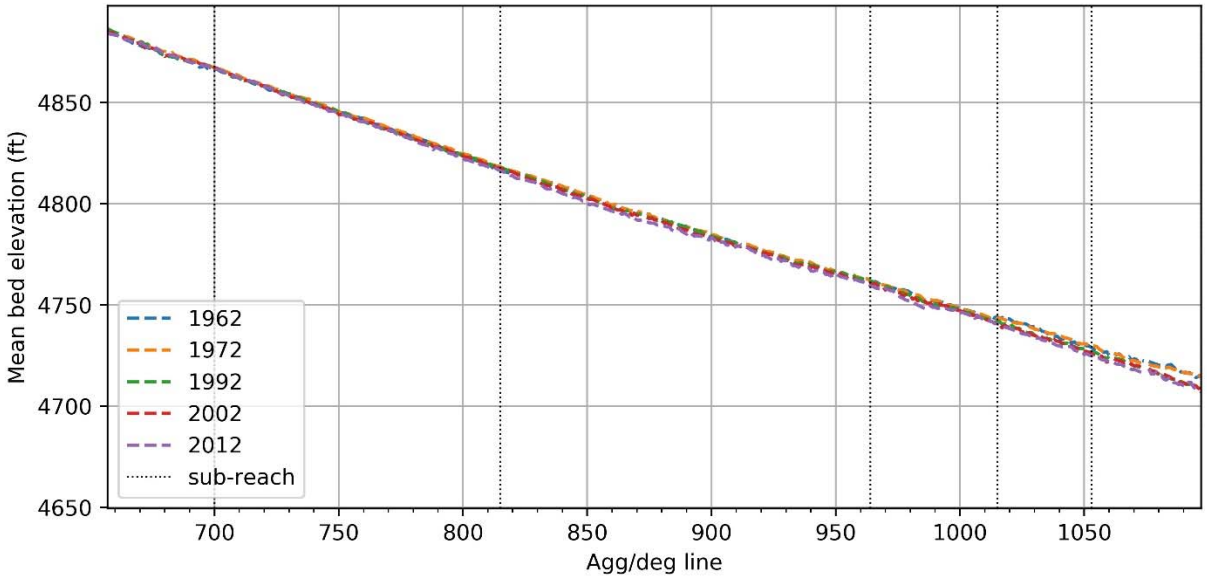


*Figure 26: Long profiles for 1962, 1972, 1992, 2002, and 2012.*

The long profiles of subreaches I1 and I2 are very similar between 1962 and 2012. Channel incision is found at subreaches I3, I4 and I5 after 1972. The average change in mean bed elevation for each subreach is listed in Table 5 and plotted in Figure 27.

*Table 5: Change in mean bed elevation (ft).*

| Subreach | 1962 - 1972 | 1972 - 1992 | 1992 - 2002 | 2002 - 2012 |
|---|---|---|---|---|
| I1 | 1.32 | -0.72 | -0.06 | -0.16 |
| I2 | 0.68 | -0.89 | -0.13 | -0.42 |
| I3 | 0.55 | -0.82 | -0.74 | -1.28 |
| I4 | 0.09 | -1.10 | -0.43 | -1.18 |
| I5 | 0.22 | -2.81 | -0.52 | -1.01 |
| I6 | -0.25 | -3.70 | -0.02 | -1.29 |

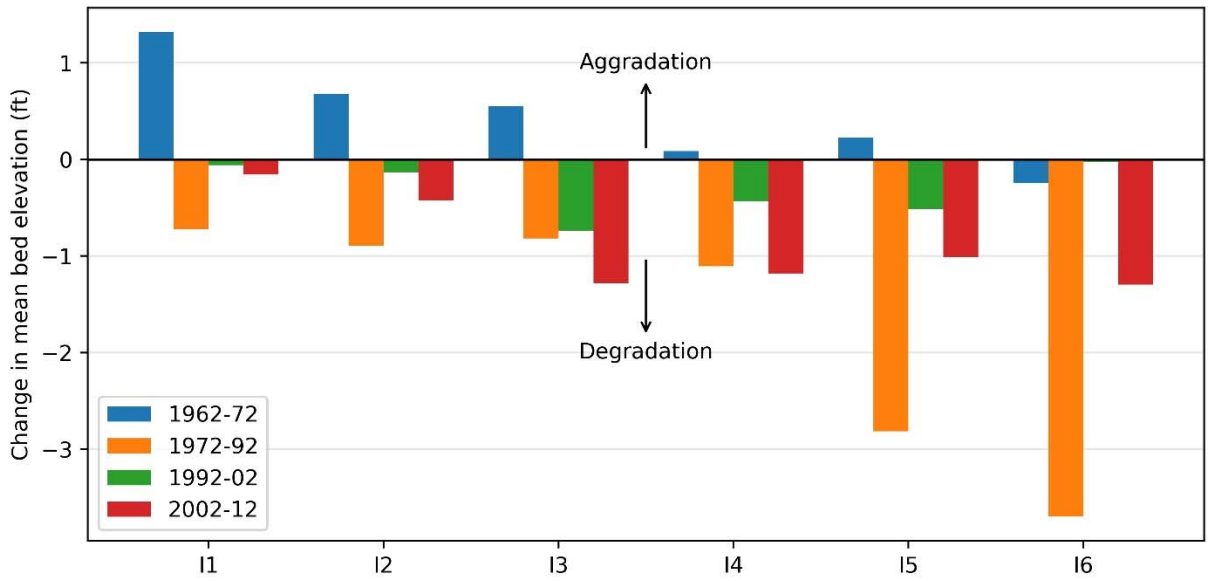


*Figure 27: Change in bed elevation.*

From 1962 to 1972, the channel aggraded in every subreach except in I5. I1 has the highest aggradation amount of 1.32 ft. The average aggradation varies from -0.25 ft to 1.32 ft. All of the reaches degraded following construction of Cochiti dam (November 1973). I6 has the highest degradation amount of 3.7 ft, during 1972 and 1992. Besides the influence of Cochiti dam, the degradation is likely associated to the decline in sediment load in Rio Puerco after 1975.

## 3.5. Volume Change

The change in main channel sediment volume for the time periods 1962 to 1972, 1972 to 1992, 1992 to 2002, and 2002 to 2012 is analyzed. This analysis follows a procedure by Varyu (2013) which provides an example of how to calculate the volume change. The extent of main channel is determined based on banklines. Banklines are given in the geometry models and are where the active channel intersect the agg/deg line. Due to the dynamic nature of the channel, banklines are likely to shift from year to year. The portion of the cross section within the outer-most right and outer-most left location of the banklines from two input datasets are defined as the main channel. The volume change is calculated as the difference in cross section area between two years multiplied by the length. The length is determined as half of distance of a cross section to its upstream cross section plus one-half the distance to the downstream cross section.

Figure 28 presents the main channel volume change of each subreach. The change generally follows the trend in mean channel bed elevation.

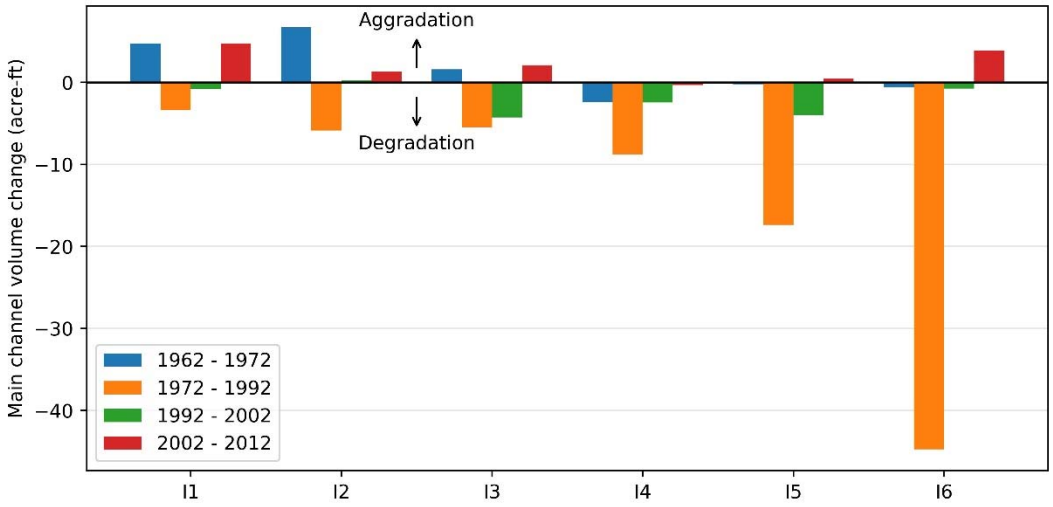


*Figure 28: Main channel volume change.*

Notice that from 2002 to 2012, most of the reaches show aggradation based on volume change but degradation based on the elevation change. It suggests that the channel is narrowing and incising.

## 3.6. Bed Material

Bed material samples were collected at rangelines that differ from the agg/deg lines. These rangelines don't date back as far as the agg/deg lines and are also spaced out further. They are used in this analysis because bed material has been surveyed in these rangeline cross-sections. The sediment samples are grouped by decade and the statistical summary of the median grain size $d_{50}$ is shown in Table 6. The typical $d_{50}$ are medium sand (0.25 mm to 0.5 mm). Although there are no samples in some subreaches, the grain size in 2010s seems coarser than 2000s.

*Table 6: Median grain size statistics from the bed material samples in Isleta reach.*

| | Subreach | Min (mm) | Max (mm) | Mean (mm) | # of samples | # in sand | # in gravel |
|---|---|---|---|---|---|---|---|
| 1990s | I1 | | | | | | |
| | I2 | | | | | | |
| | I3 | 0.03 | 0.96 | 0.36 | 366 | 366 | 0 |
| | I4 | 0.19 | 0.46 | 0.32 | 13 | 13 | 0 |
| | I5 | 0.36 | 0.18 | 0.24 | 8 | 8 | 0 |
| | I6 | | | | | | |
| 2000s | I1 | | | | | | |
| | I2 | 0.34 | 0.45 | 0.37 | 14 | 14 | 0 |
| | I3 | | | | | | |
| | I4 | | | | | | |
| | I5 | | | | | | |
| | I6 | | | | | | |
| 2010s | I1 | 0.004 | 0.68 | 0.4 | 10 | 10 | 0 |
| | I2 | 0.49 | 0.6 | 0.54 | 2 | 2 | 0 |
| | I3 | 0.39 | 0.46 | 0.42 | 6 | 6 | 0 |
| | I4 | 0.42 | 0.46 | 0.44 | 2 | 2 | 0 |
| | I5 | 0.44 | 0.44 | 0.44 | 1 | 1 | 0 |
| | I6 | 0.39 | 0.41 | 0.4 | 3 | 3 | 0 |

## 3.7. Flow depth, Velocity, Width, Wetted Perimeter and Slope

Flow depth, velocity, width, wetted perimeter, and slope are obtained by using HEC-RAS 5.0.3 with the discharge of 3,000 cfs. Available years of analysis with HEC-RAS include 1972, 1992, 2002, and 2012. The average value of each variable at subreach scale is plotted in Figure 29. The change between ranges of years is summarized in Table 7.

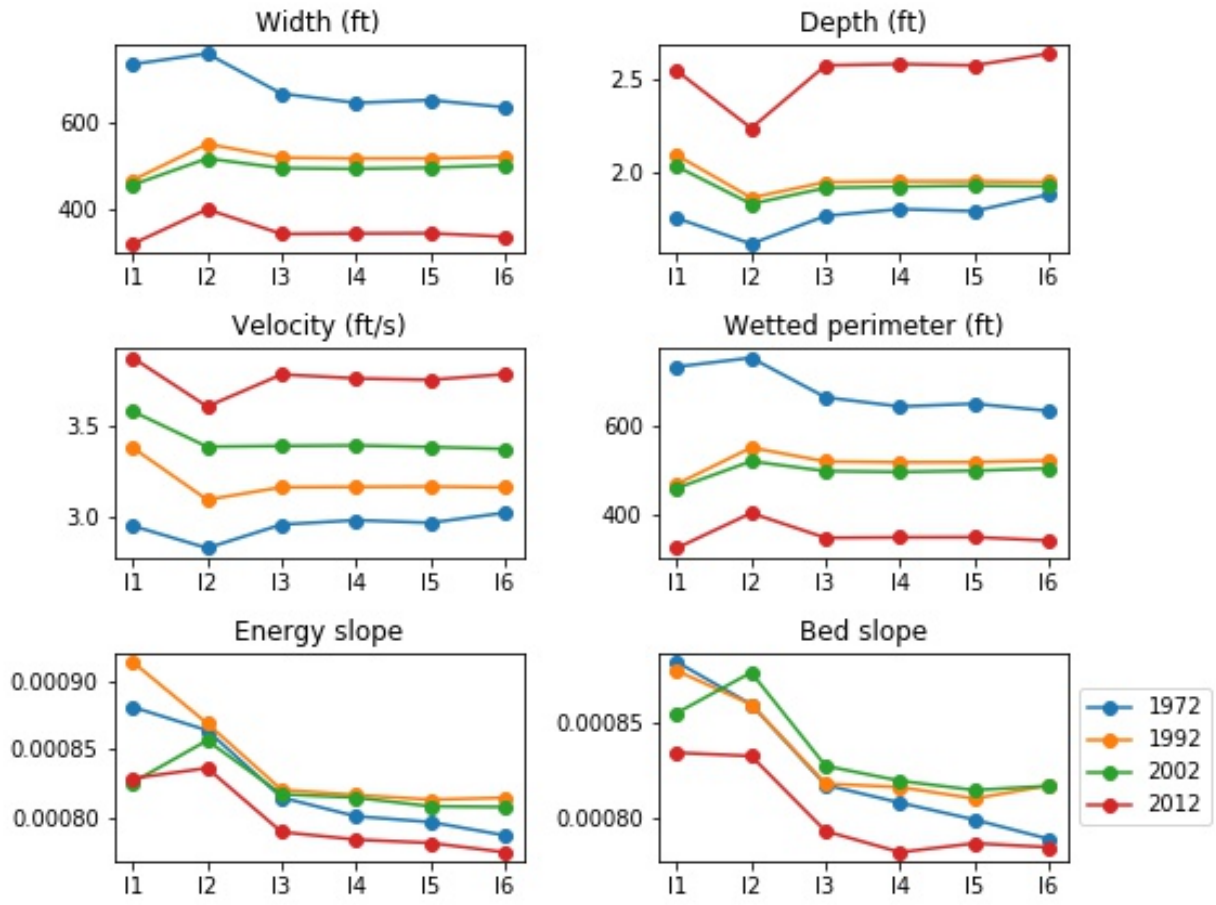


*Figure 29: Width, depth, velocity, wetted perimeter, energy slope, and bed slope at each subreach for 1972, 1992, 2002, and 2012 at 3000 cfs.*

The widths and wetted perimeter have decreased about 420 ft since 1972. Depth and velocity are both inversely proportional to width and wetted perimeter. The bed and energy slope generally increased from 1992 to 2002 but decreased in 2012. The range of decrease is between 0.00003 and 0.00005. I2 has a different geometry than the other subreaches because there is a spike up or down in each of the parameters.

The sinuosity tends to increase in 2002 which coincides with an increase in number of channels shown in Figure 25. Also, the channel's energy and bed slope increase from 1972-2002 and then dramatically decreases from 2002-2012 as shown in Figure 29. A braided channel is generally steeper than a single sinuous channel (Julien 2002), so it is expected that the channel becomes more sinuous like it does when the slope decreases from 2002-2012. Although, from 1972-2002 the slope increases, but the channel becomes more sinuous. Therefore, there must be another driver causing this trend.

*Table 7: Isleta Reach channel geometry temporal change summary (+: increase in parameter value; -: decrease in parameter value).*

| Reach | Year | Width | Bed slope | Depth | Velocity | Volume | Bed elev. |
|---|---|---|---|---|---|---|---|
| I1 | 1972 - 92 | - | - | + | + | + | - |
| | 1992 - 02 | - | - | - | + | + | - |
| | 2002 - 12 | - | - | + | + | - | - |
| I2 | 1972 - 92 | - | = | + | + | + | - |
| | 1992 - 02 | - | + | - | + | - | - |
| | 2002 - 12 | - | - | + | + | - | - |
| I3 | 1972 - 92 | - | = | + | + | + | - |
| | 1992 - 02 | - | + | - | + | + | - |
| | 2002 - 12 | - | - | + | + | - | - |
| I4 | 1972 - 92 | - | + | + | + | + | - |
| | 1992 - 02 | - | + | - | + | + | - |
| | 2002 - 12 | - | - | + | + | + | - |
| I5 | 1972 - 92 | - | + | + | + | + | - |
| | 1992 - 02 | - | + | - | + | + | - |
| | 2002 - 12 | - | - | + | + | - | - |
| I6 | 1972 - 92 | - | + | + | + | + | - |
| | 1992 - 02 | - | = | - | + | + | - |
| | 2002 - 12 | - | - | + | + | - | - |

## 3.8. Geomorphic Conceptual Model

Massong et al. (2010) developed a channel planform evolution model for the Rio Grande. The sequence of the planform evolution is outlined in Figure 30.

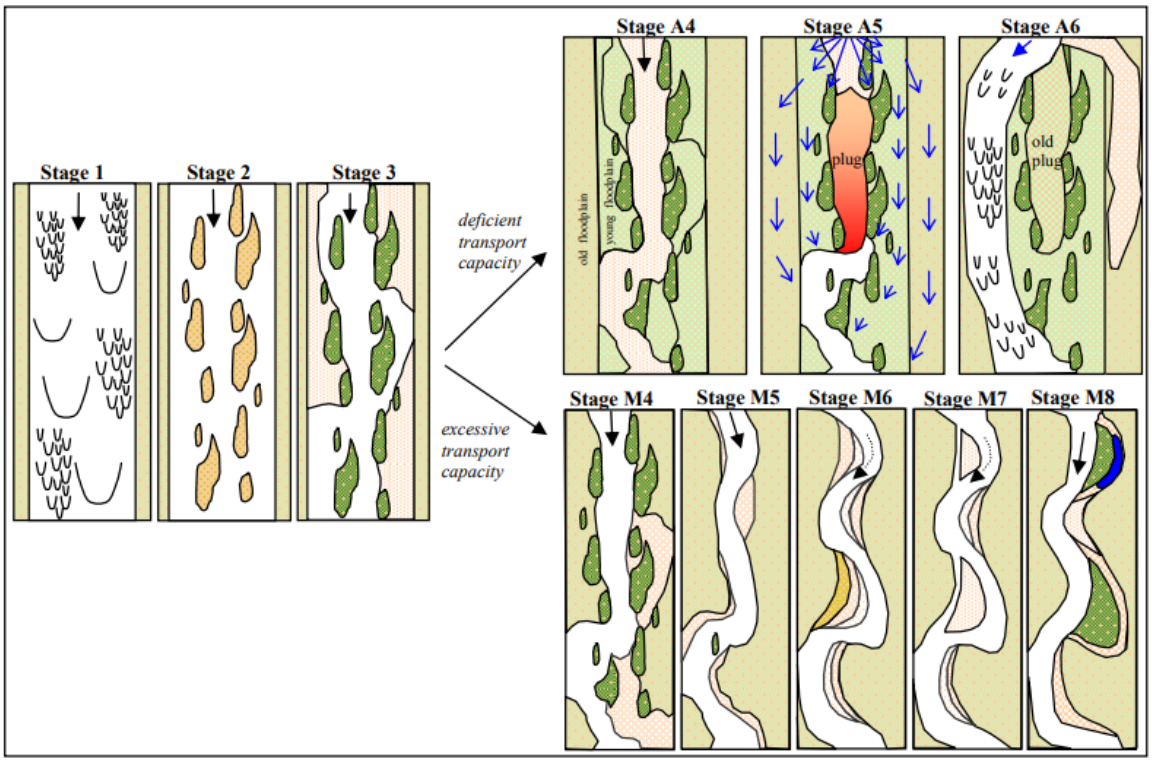


*Figure 30: Planform evolution model from Massong et al. The river undergoes stages 1-3 first and then A4-A6 or M4-M8 depending on the transport capacity.*

Stages 1-3 are generally more braided and have a wider planform than later stages. Stage 1 starts with bedforms, then during drought periods stage 2 occurs. Sedimentation and mid-channel bars result in stage 2 due to low flows and deficient transport capacity. Stage 3 occurs when vegetation forms on the mid-channel bars and islands. In the rest of the stages, the river becomes much more channelized. If there is a deficient transport capacity, A4-A6 occur. In A4-A6 the excess amount of sediment settling on the river bed forms plugs and causes avulsions. If there is an excessive transport capacity, M4-M8 occur. M4-M8 are relevant to the Isleta Reach because it has an excessive transport capacity (Massong et al. 2010).

The entire reach has undergone or is undergoing stages 1-3. Stage 1 and 2 occurred on a large amount of the Middle Rio Grande from 1999-2004. In 2005, high flows provided the environment vegetation needed to encroach on the bars, thus forming stage 3 (Massong et al. 2010). The latest classification of the Isleta reach has been M5, and has undergone various stages since the early 1900's. USBR assinged planform stages to the Isleta reach over multiple years based on aerial photography in their report from 2018. Their results are in shown in Table 8.

*Table 8: Planform classification by stages (Klein et al., 2018a).*

**Table 14. Channel Classification for the Isleta to Rio Puerco geomorphic reach**

| Years | Massong et al. (2010) | Schumm (1977, 1981) |
|---|---|---|
| **1918** | 2 | 3 |
| **1935** | 1 | 3 |
| **1949** | 2 | 3 |
| **1962** | 3 | 2 |
| **1972** | 3 | 2 |
| **1985** | 3 | 8/9 |
| **1992** | 3 | 8 |
| **2002** | 3 | 9 |
| **2012** | M4 | 8 |
| **2016** | M5 | 7 |

Using these years of data and the classification from Massong et al. (2010), a conceptual model was formed. The intent of this is to understand how the river is changing and where it will end up in the future. The model is formed from a plan view and cross-sectional view of a typical cross-section, and presented with the stages assigned by Klein et al. The conceptual geomorphic model for this reach was formed using agg/deg line 939 and spans from 1962-2016. The plan view was obtained using GIS, and the cross-section was from HEC-RAS.

The conceptual model only dates back to 1962 for a few reasons. First, aerial photography was not available before 1936. Also, the years of cross-sectional data analyzed with HEC-RAS include 1936, 1952, 1962, 1972, 1992, 2002 and 2012. Although there are seven year of available data, the analysis could only start with 1962. Determining which agg/deg cross-section was which before 1962 was difficult because the surveys were not consistent between the earlier years. This may be due to the agg/deg lines being established in 1962 (Posner 2017).

The cross-sections at agg/deg line 939 are not compared after station 2600 because it is far away from the main channel. Also, there is very little variation in that area from year to year. 2016 data was acquired from AutoCAD from rangeline CC-939 which is in the same location as agg/deg line 939. The CC-939 data does not cover as much distance because the survey was not as extensive as the agg/deg surveys in previous years. A comparison of the results are shown in Figure 31 and Figure 32 show the conceptual model with the cross-section and plan views.

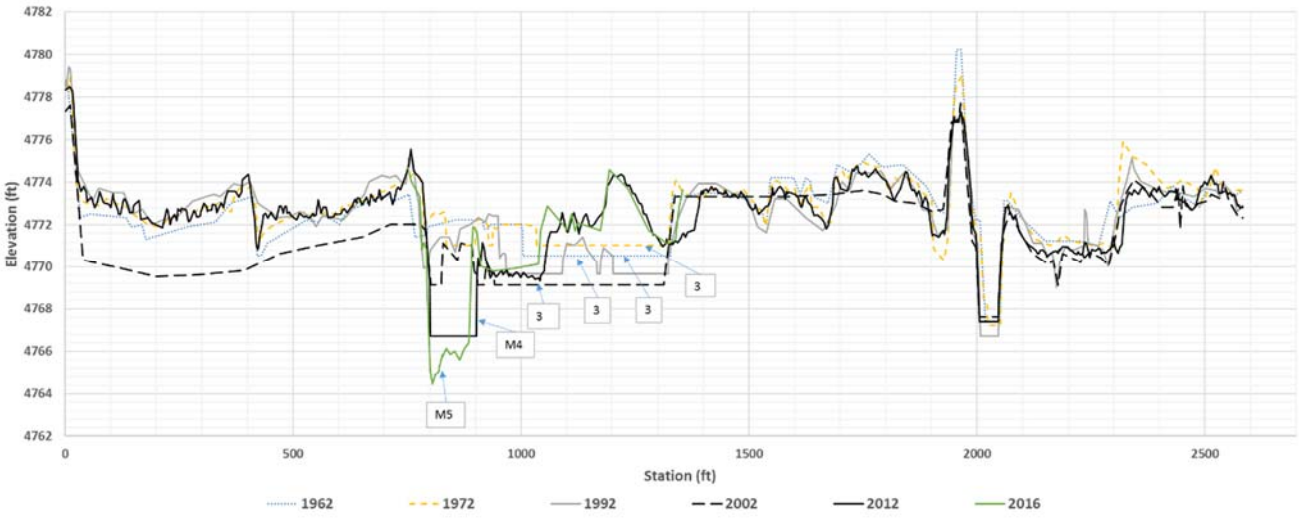


*Figure 31: Comparison of cross-section 939 from 1962-2016. Each stage classified by USBR is in a box and has an arrow pointing to the cross-section that it describes.*

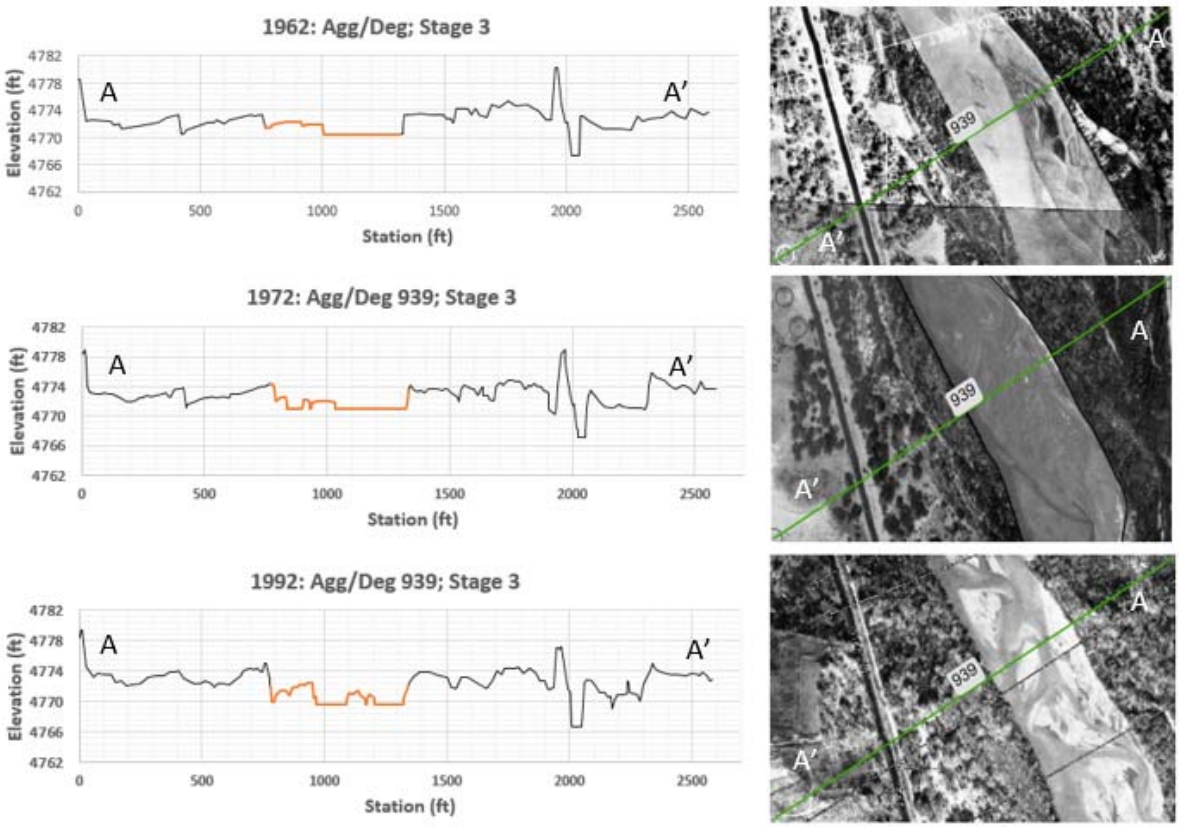


*Figure 32: 1962, 1972, and 1992 cross-section and planform views (planform to the right of each corresponding year). A denotes the left bank and A' denotes the right bank. The active channel is in orange the stage is denoted at the top of the graph.*

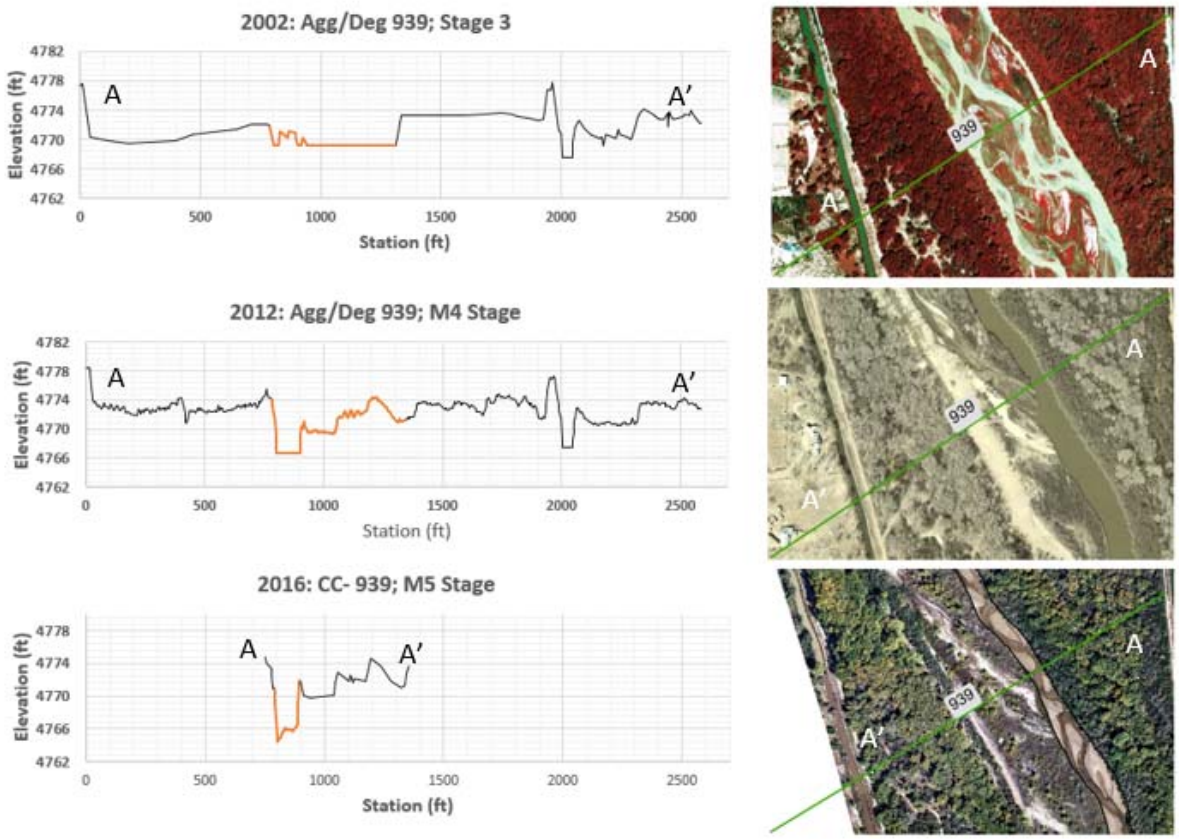


*Figure 33: 2002, 2012 and 2016 cross-section and planform views (planform to the right of each corresponding year). A denotes the left bank and A' denotes the right bank. The active channel is in orange the stage is denoted at the top of the graph.*

Over time the active channel has become narrower and more incised. This makes sense as the stages progress from 3-M5 and become more of a narrow, single-threaded channel. The active channel width is based on planforms provided by USBR in GIS, and they may differ based on the flow when the photograph was taken. For instance, 1992, 2002, and 2012 are all around 650 cfs. 1972 is around 5 cfs and 2016 is at 40 cfs. The flow in 1962 is also about 650 cfs (Swanson et al. 2010).

# 4. HEC-RAS Silvery Minnow Hydraulic Modeling

Flow depth and velocity determine the quality of habitat of RGSM. In this study, we use HEC-RAS 5.0.3 to analyze the flood extent and hydraulic condition at different flow discharges. The depth and velocity from HEC-RAS model are used to quantify the location and area of the habitat.

## 4.1. Habitat Criteria

The classification of habitat for silvery minnow used in this section is based on criteria and descriptions of habitat from Tetra Tech (2014). To understand the quality of silvery minnow habitat and how it is changing, it is useful to classify it into different types. These types of habitats indicate how good the habitat is and what it is used for. For instance, feeding, rearing and spawning habitats are necessary for silvery minnows to propagate. Feeding habitats for silvery minnows include benthic food sources, which includes organic detritus, algae, diatoms, and small invertebrates. For "feeding/rearing" habitat to form, it requires low velocity flow so that the river bed is stable (< 0.5 ft/s) and sufficient sunlight so the algae can grow. Also, spawning habitat is better if it is warm and has a low velocity so eggs don't drift downstream. The warm water triggers spawning and provides the energy for algae to grow and therefore ensures food supply for larval development. "Spawning" is a rare habitat that has a velocity less than 0.05 ft/s and a depth less than 1.5 ft which ensures survival of eggs and larvae. This is why inundated floodplains are the perfect habitat for spawning. Other categories include "good", "adequate", and "inadequate". "Good" habitat describes the area where the silvery minnow is commonly found. Studies have shown that the silvery minnow is most commonly collected from water less than 1.6 ft (USFWS 2010 from Tetra Tech 2014). "Inadequate" meets none of the ideal habitat criteria and "adequate" meets some of the criteria.

These descriptions of habitats are translated into numerical ranges that fit certain depths and velocities. Flow depth is divided into four groups: 0 ft – 1.5 ft, 1.5 ft – 1.6 ft, and > 1.6 ft. Velocity is broken down into four tiers, 0 – 0.05 ft/s, 0.05 – 0.5 ft/s, 0.5 – 1.5 ft/s, and > 1.5 ft/s. Also, the ideal habitat for RGSM should have flow depth between 0.16 ft (5 cm) and 1.5 ft (45 cm) and flow velocity less than 1.5 ft/s (Baird 2016). A summary of the depth and velocities and which habitats they represent is described in Table 9.

*Table 9: Habitat Classification based on flow depth and velocity*

| Depth (ft) | Velocity (ft/s) | | | |
|---|---|---|---|---|
| | 0 – 0.05 | 0.05 – 0.5 | 0.5 – 1.5 | > 1.5 |
| 0 - 1.5 | Spawning | Feeding/rearing | Good | Inadequate |
| 1.5 – 1.6 | Adequate | Adequate | Adequate | Inadequate |
| >1.6 | Inadequate | Inadequate | Inadequate | Inadequate |

## 4.2. Method

The amount of “inadequate”, “adequate”, “good”, “feeding/rearing”, and “spawning” habitat and where it is can be visualized and analyzed from the process outlined in this section. By looking at the simulated velocities and depths of the range of flows, we can have insight into silvery minnow habitat and how it changes with different flow regimes, spatially, and temporally.

HEC-RAS is employed to analyze the hydraulic condition at different flow conditions. Spring flow is targeted because the population of RGSM is highly correlated to the connectivity to floodplain in spring. The connectivity depends on the flow magnitude, flow duration and channel geometry. The flows used in HEC-RAS were based on past analyses and practicality. For instance, the 25-day exceedance spring runoff peak flow for dry, mean, and wet year are identified by MEI (2006) to be 1400, 3500, and 5600 cfs, respectively. Spring runoff for the last decade has been lower than the past runoffs, so we chose 600, 1400 and 3500 cfs for the fish habitat analysis. 600 cfs was chosen because several years with aerial photographs were taken with the flow discharge around this value (1992 at 650 cfs, 2002 at 600 cfs, 2006 at 580 cfs and 2012 at 740 cfs). This allows the comparison of HEC-RAS results with aerial photographs which is discussed in the conclusion in section 8.

The available years of HEC-RAS geometries around when fish population started being collected include 1992, 2002, and 2012. The HEC-RAS geometry cross sections were developed by USBR. An example of a cross-section from 2002 is shown in Figure 34. The 1992 and 2002 are derived by using photogrammetry and the 2012 geometry was derived from LiDAR. The reach from Isleta Diversion Dam to San Acacia was extracted from the entire Middle Rio Grande HEC-RAS file with additional 10 cross sections adjacent to upstream and downstream ends. Modifications were made to the main channel designation and levee stations to more accurately reflect the flood extent in the aerial photographs (Figure 34). Aerial photographs from April of 2005 (4500 cfs), 2006 January (580 cfs), and 2008 July (1630 cfs), and a digitized flood map of 2005 June (5980 cfs) were used to identify the location of levees. Manning n was set as 0.019 for the main channel and 0.1 for the floodplain according to Klein et al. (2018b). The simulation was run under uniform steady condition.

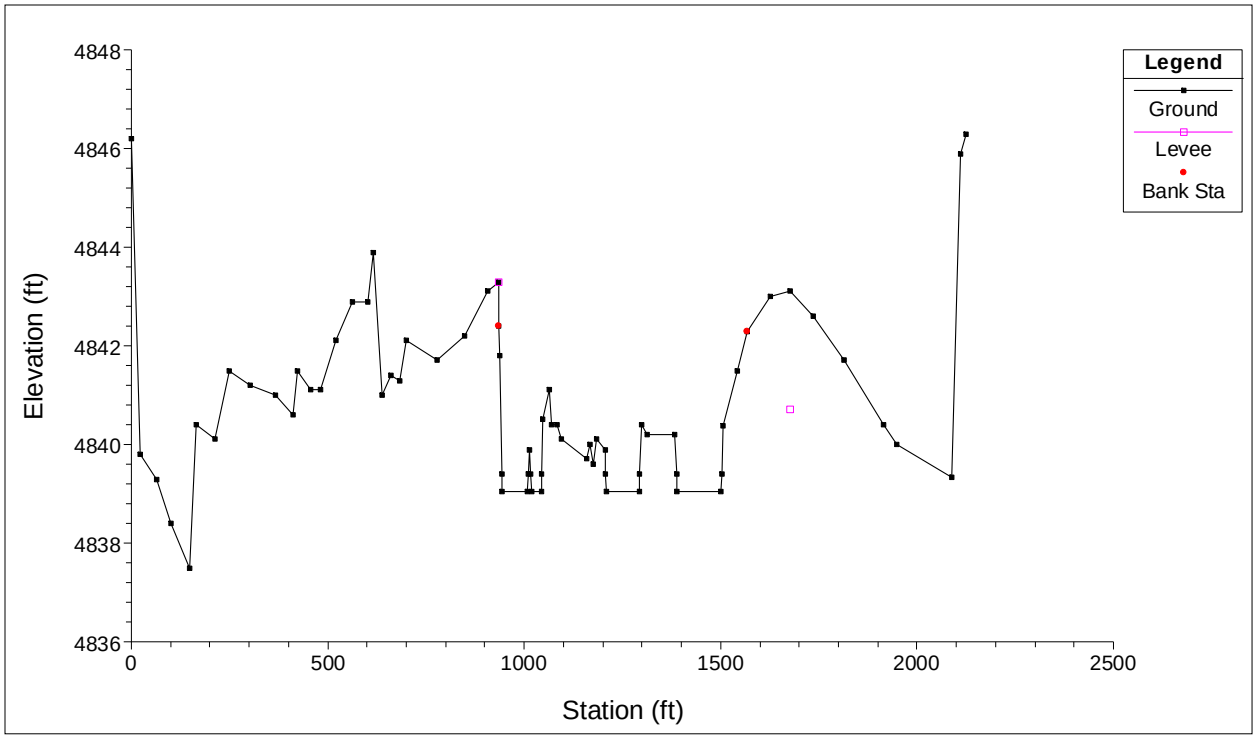


*Figure 34: Example of modified levee station: agg/deg 764 (river station 1177) in 2002. The 2005 flood map shows that the flow only overtopped at the right bank. Furthermore, the right bank side channel is found inundated in April of 2005 but not in the aerial photos in January of 2006, so the levee on the right bank is placed between side channel and main channel and at the elevation with flow between 1500 cfs and 3150 cfs. The levee on the left bank is placed at the top of the main channel banks.*

Flow depth and velocity for each station are exported to ArcGIS to analyze the habitat spatially. The habitat quality is broken up into subreaches and compared. Because the HEC-RAS geometries are not geo-referenced, a program is developed to compute the coordinate for every station. A point polygon with flow depth, flow velocity, and xy-coordinate for a given flow condition can be generated. The point feature is used to create a TIN to generate surface features for depth and velocity. Lastly, depth and velocity are classified and combined based on Table 9.

## 4.3. Results & Discussion

Figure 35 and Figure 36 illustrate the simulation results of flow depth and velocity at subreach I1 with discharges at 600, 1400, and 3500 cfs in 2012. As shown in Figure 37, we can identify the location with the flow depth and velocity that is suitable for silvery minnows according to Table 9.

From the previous sections we learned that the Isleta reach transitioned from braided to single thread from 1992 to 2012. In addition, the channel width is decreasing. From the simulation, we saw that the main channel is narrower, and velocity and depth become greater over the years (figures in Appendix A). There are areas with slow and shallow water around bars in 1992

and 2002. This feature is much less in 2012. As a result, we found loss of habitat over time, especially from 2002 to 2012.

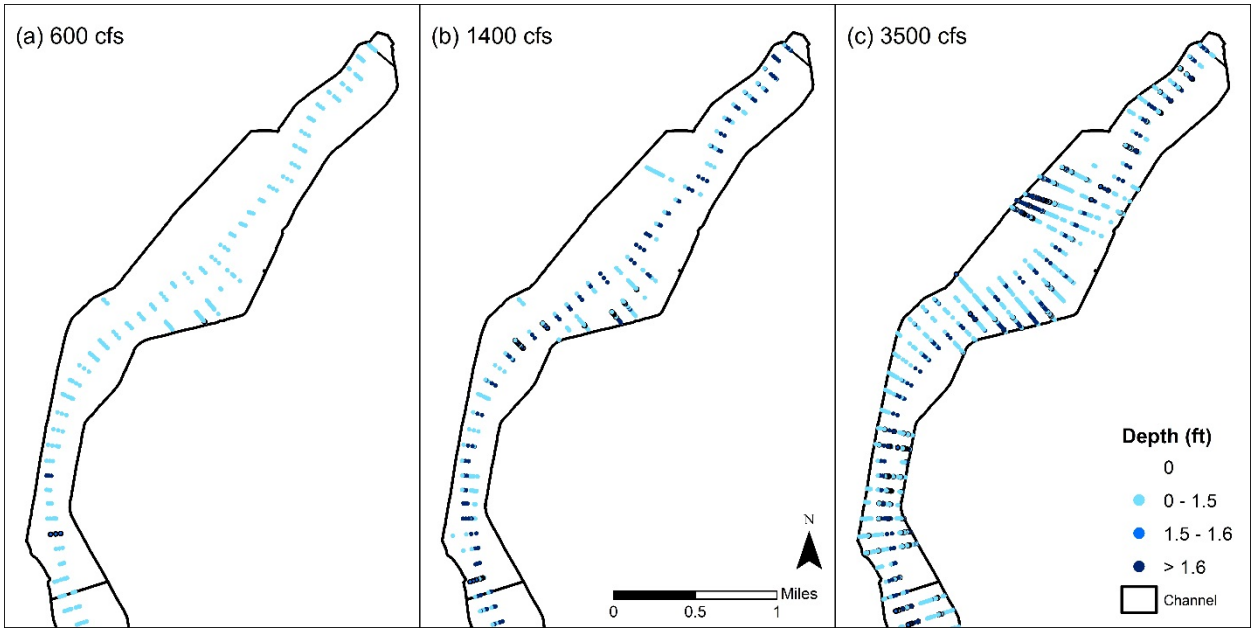


*Figure 35: Simulated depth at subreach I1 at flow rate 600, 1400, and 3500 cfs in 2012.*

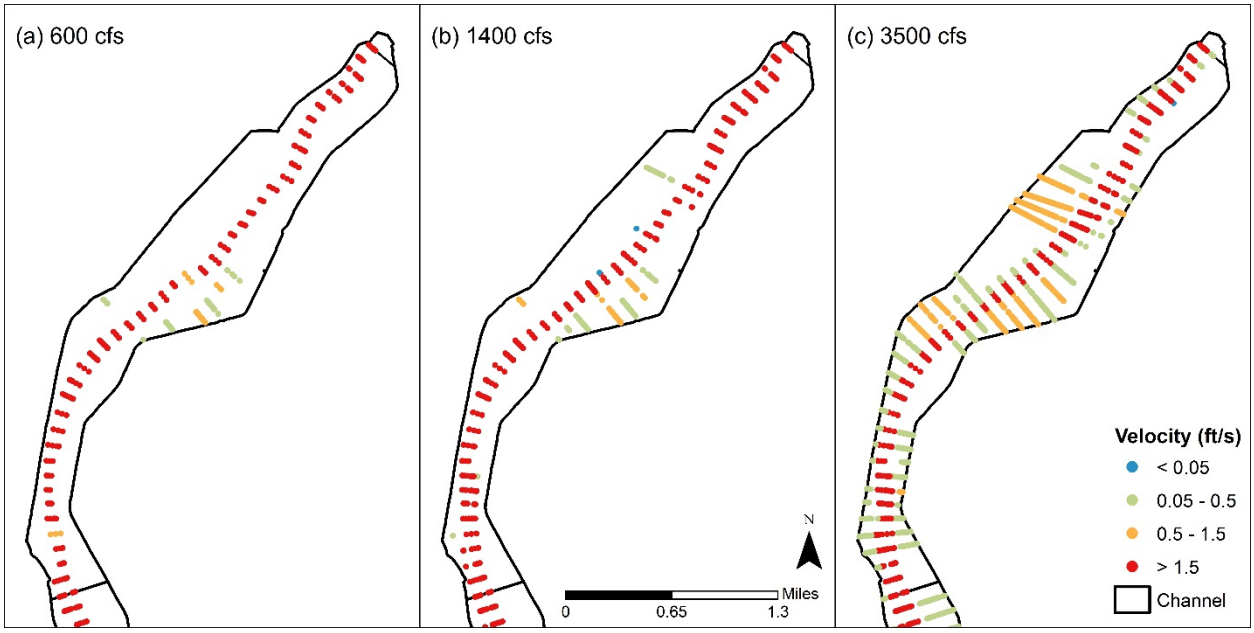


*Figure 36: Simulated velocity at subreach I1 at flow rate 600, 1400, and 3500 cfs in 2012.*

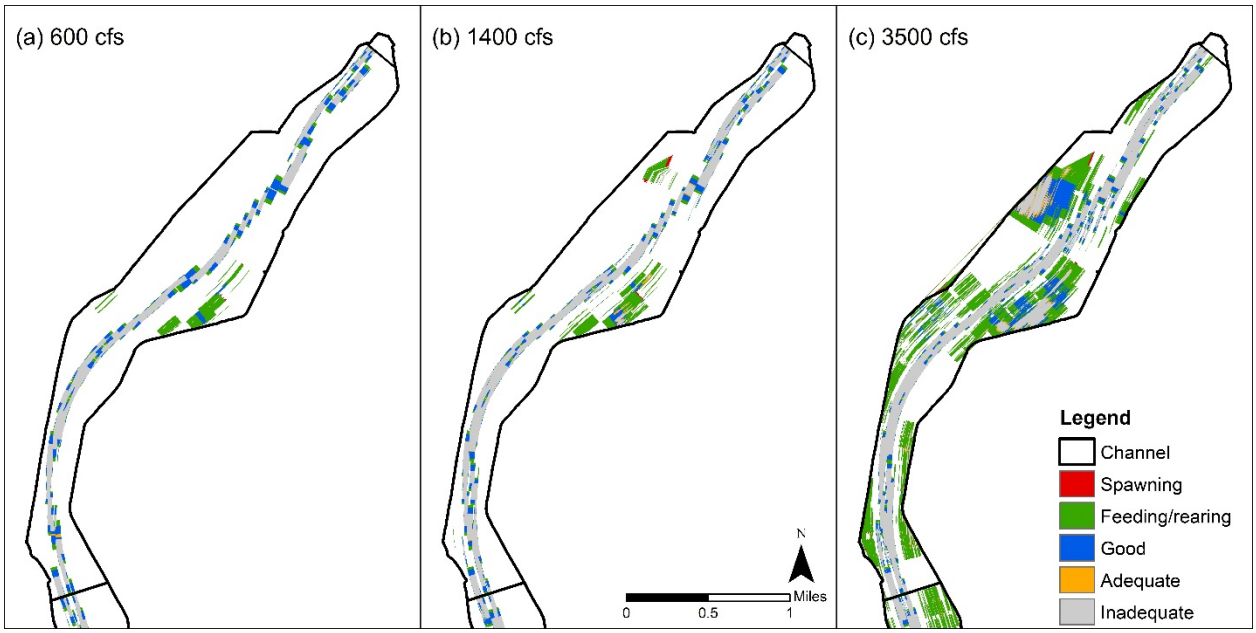


*Figure 37: Hydraulic habitat at subreach I1 at flow rate 600, 1400, and 3500 in 2012*

Figure 38, Figure 39, and Figure 40 shows the areas and densities of "spawning", "feeding", and "good" habitat respectively of each subreach. The habitat density depicted in (b) in these figures gives a more meaningful representation of the habitat quality because it is weighted by subreach area.

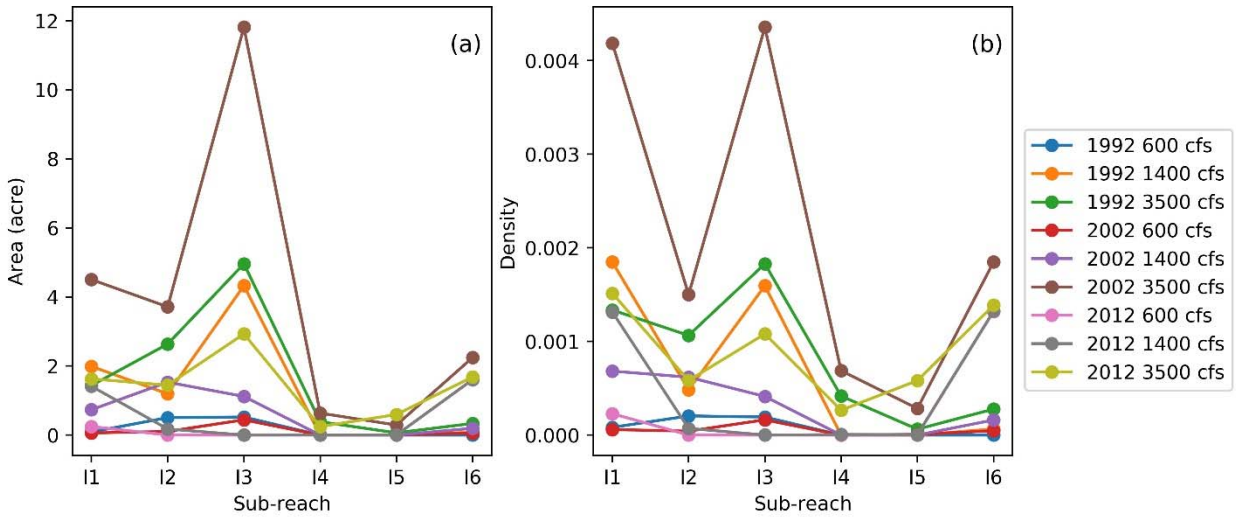


*Figure 38: "Spawning" habitat: (a) area, (b) density (area of habitat divided by area of subreach).*

For all simulated years, the area of "spawning" habitat is largest when the flow is 3500 cfs (5.0 acre in 1992, 11.8 acre in 2002, and 2.92 acre in 2012 at I3). Figure 38b shows that I1 and I3 have the highest weighted area by subreach of "spawning" habitat. Also, while 2002 has the

highest amount of “spawning” habitat at 3500 cfs, it has the least amount of “good” habitat at that flow compared to other years as shown in Figure 40.

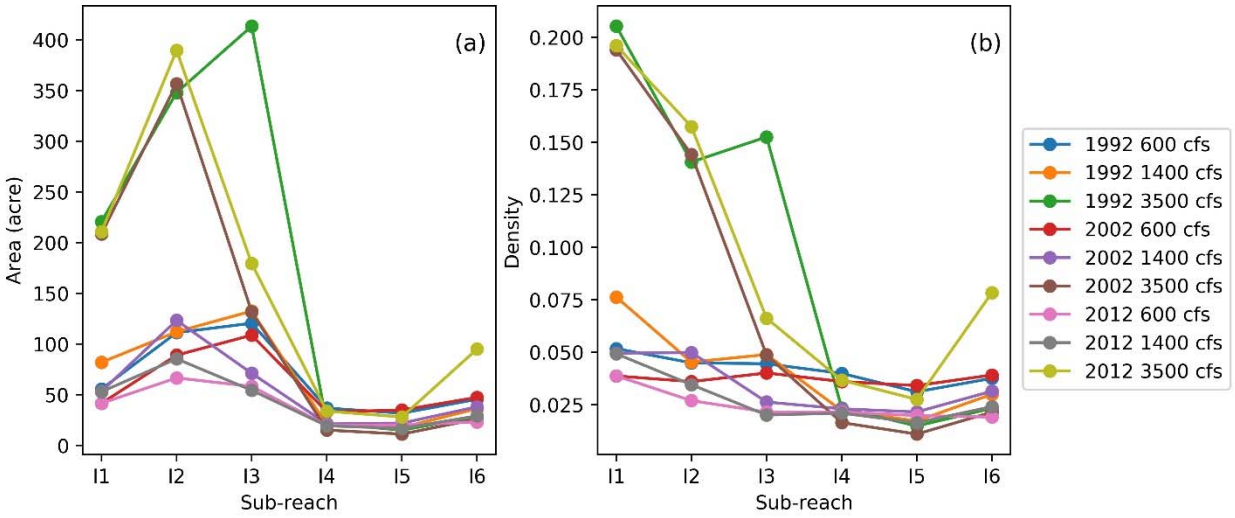


*Figure 39: “Feeding/rearing” habitat: (a) area, (b) density (area of habitat divided by area of subreach).*

Area of “feeding/rearing” habitat shows a similar pattern to the spawning habitat. The best “feeding/rearing” habitat occurs in I1, I2 and I3 at 3500 cfs as shown in Figure 39. The increase is attributed to floodplain inundation. Floodplain inundation begins at 3500 cfs for this reach, and as a result habitat quality increases (Tetra Tech 2014). This explains why there is more “feeding/rearing” and “spawning” habitat at 3500 cfs in this simulation.

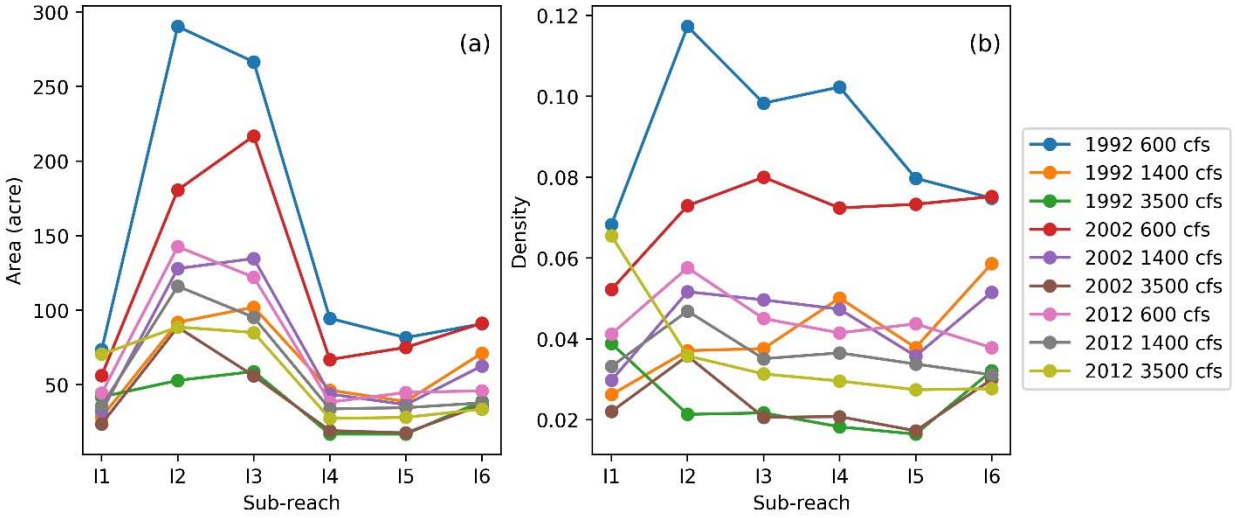


*Figure 40: “Good” habitat: (a) area, (b) density (area of habitat divided by area of subreach).*

For the “good” habitat, the area is negatively related to discharge. Therefore, the highest density of “good” habitat is at the lowest flow of 600 cfs for all years. This could be due to more accessible channels in the main channel, and shallower areas at low flow providing better habitat. Also, subreaches I2-I4 appear to have the majority of “good” habitat, but there is not an obvious trend when looking at the weighted area in Figure 40b.

When the discharge increases, the area of low velocity in the channel decreases and therefore the area of “good” habitat decreases until floodplain inundation occurs. It would be expected that the “good” habitat would be lowest at 1400 cfs and higher at 3500 cfs when the floodplain becomes inundated (Bovee et al. 2008; Tetra Tech 2014), yet this does not occur. The “good” habitat is lowest at 3500 cfs. This is most likely because a very small amount of inundation occurs starting at 3500 cfs (Tetra Tech 2014), so that area become all “feeding/rearing” and “spawning” habitat. When significant inundation begins at flows such as at 5000 cfs, greater amounts of “good” habitat would be expected.

Overall, subreaches I1, I2, and I3 provide more in-channel and overbank habitat than I4, I5, and I6. The highest “spawning” and “feeding/rearing” habitat is at 3500 cfs. The majority of “good” habitat occurs at 600 cfs. As for the dry scenario (600 cfs), the greatest area for all habitats are found in 1992, followed by 2002, and the least in 2012 at all subreaches. The middle flow level of 1400 cfs never has the highest habitat area, and usually has the least amount of quality habitat.

# 5. Silvery Minnow Habitat Criteria

## 5.1. Introduction

This section outlines how silvery minnow habitat can be analyzed with GIS from aerial photography. It covers the methods, results and discussion of the findings. The analysis is based on finding what habitat features silvery minnows thrive in, identifying those features in the same reach over different years, and seeing how the habitat changes spatially and temporally. The ultimate goal in the future is to link this analysis to how fish population densities have changed with the habitat.

## 5.2. Methods

### 5.2.1. Data used/Aerial Photography

Analyzing orthographic aerial photography over many years can show how silvery minnow habitat has changed over time. Once we know how the habitat is changing and how this is related to fish population, habitat suitability can be improved. A link between habitat and population trends can be determined by looking at population data from population monitoring reports by Dudley and Platania (1997). They have been collecting data on the fish population throughout the Middle Rio Grande since 1993. The following years of aerial photography will be used to analyze habitat quality (1992 is also analyzed because it is the closest year to 1993 of aerial photography available):

*Table 10: The year, month and flow corresponding aerial photographs used for this study. Data from Klein et al., 2018a, Swanson et al., 2010 and GIS metadata provided by USBR.*

| Year | Month | Flow (cfs): |
|---|---|---|
| 2016 | October | 40[SA] |
| 2012 | January | 740[SA] |
| 2008 | July | 1630[I] |
| 2008 | June | 4990[I] |
| 2006 | January | 580[SA] |
| 2005 | June | 5980[I] |
| 2005 | April | 4500[I] |
| 2002 | February | 600[SA] |
| 2001 | February | 687[A] |
| 1992 | February | 650[SA] |
| [I] Isleta gage daily average discharge | | |
| [SA] San Acacia gage daily average discharge | | |
| [A] Albuquerque gage daily average discharge | | |

The years analyzed are based on availability of data from USBR starting with 1992, so there is not a consistent spacing of years. The uncertainty created by varying image quality is also a limitation of analyzing the photographs. This is a known limitation based on many other studies using aerial photography to map fish habitat quality (Holmes and Hayes 2011; Perschbacher 2011). Other limitations include the flow being variable within the reach and between years,

limited amounts of data, the analysis being subjective, limited data aids such as LiDAR and thermal imagery, and ability to ground truth the data (Holmes and Hayes, 2011; Perschbacher 2011).

An effort can be made to address these limitations. For instance, picking only years that have the same flow can allow the habitat analysis to be compared. 1992, 2001, 2002, 2006, and 2012 all have flows around 650 cfs so these ones are chosen to compare to each other. To keep it as consistent as possible, 2001 is not used because it uses flow data from a different gage than the rest.

Though it would be useful to analyze habitat that meet the needs of different life history stages of silvery minnows, it is not plausible to do a thorough analysis of this with the given set of aerial photography. High flows around the same value across many years would be necessary to see how much the floodplain inundates and how the habitat quality changes over time. Aerial photography analyzed during low and peak flows can still be analyzed because this can give insight into habitat quality spatially and across different flow regimes. Still, the focus must be on analyzing adult silvery minnow habitat in the main channel because that is the available habitat for the comparable photographs at 650 cfs. Though there are a limited amount of photographs to work with, analyzing this low flow of 650 cfs may be very useful because the Middle Rio Grande has experienced lower and less peak flows than it has in the past. This trend is expected to continue, so focusing on lower discharges that don't lead to floodplain inundation may be more a more realistic focus for improving silvery minnow habitat (Drew Baird, personal communication, June 19$^{th}$, 2018).

To make the analysis as objective as possible, a detailed description of discernable habitat features will be given. This is still a challenge because distinctions between features such as islands, bars, bedforms and shoreline complexity are not always clear. Also, if more LiDAR or thermal imagery data were available that would help as well. Lastly, ground truthing to test the analysis with actually field surveys can be done in the future.

Even with limitations, there are advantages of using remote sensing for habitat analysis. The amount of habitat that can be mapped in a short amount of time can be very useful (Holmes and Hayes 2011; Perschbacher 2011). For this study, it took less than a day to map 50 miles of river habitat. This mapping technique allows a researcher to take a cursory look at a large area and find large-scale trends. Also, this exact type of habitat analysis for this exact reach has not been done before. Therefore, this analysis may yield interesting results (Torres 2007; Klein et al. 2018a).

### 5.2.2. Criteria Development

The criteria developed is based on literature that discusses physical features of silvery minnow habitat. That criteria from research is then simplified and shortened based on ability to analyze it based quality of aerial photography and practicality. Physical features determined to be important based on literature include: bankline complexity, main channel complexity, side

channels, backwater, bars, islands, confluences, pools, limited suspended sediment, suitable amounts of vegetation, and a correct range of temperatures. These features are important because they are representative of suitable silvery minnow habitat that requires low velocities, shallow depths, diverse habitat, silt and sand substrate, and good water quality (Tetra Tech 2014; Cluer and Thorne 2014; Bovee et al. 2008; Bestgen et al. 2003; Dudley and Platania 1997).

Even though all of these features are important, only a handful of these can be accurately measured from aerial photography using GIS. The habitat requirements gets narrowed down to low velocities, shallow depths, and habitat diversity (In this criteria diverse habitat is defined as anything that adds to complexity and diversity of the physical habitat topographically or with features such as debris piles). This creates of analyzable features that only include bankline complexity, main channel complexity, side channels, backwaters, bars, islands, and confluences.

There are a few reasons why certain features are not included. For instance, suspended sediment can sometimes be analyzed by looking at the color of the water, yet the aerial photographs vary so much spatially and temporally, it is impossible to analyze visually. Substrate is too hard to analyze because aerial photography from most years is not detailed enough. Also, temperature is something that cannot be seen on the imagery. Isolated pools can be seen from aerial imagery, but it is hard to determine how connected the pools are to the main channel so they are removed as well.

Vegetation is not included in this list because vegetation is incorporated indirectly through certain habitat features. For instance, vegetation indicates complexity on bars, shorelines, or islands which affects habitat scores. It also affects how wide side channels are, which impacts the habitat area, and the likelihood that a channel would be inundated during high flows. It further adds complexity because vegetation provides shade to regulate temperatures and produces leaf litter. Leaf litter provides nutrients to feed algae and diatoms that in turn feed silvery minnows. Temperature regulation is also very important for the minnow (Tetra Tech 2014; Bovee et al. 2008; Bestgen et al. 2003; Dudley and Platania 1997). Therefore, vegetation density in the active channel is incorporated through other habitat features.

Also, though runs and pools would be useful to identify (Dudley et al. 2016), they are unable to be identified from the set of aerial photography given. Identifying runs and pools have been a focus of other studies identifying habitat features with remote sensing. They were able to do this by using ground truthing to identify where the pools and runs were and use that information to identify the features in aerial photography (Holmes and Hayes 2011; Perschbacher 2011). Ground truthing was not an option for this study. Using agg/deg cross-sectional data from HEC-RAS to identify pools and runs could be an option as well, but these lines are far apart so the data would not be as accurate.

The following schematic in Figure 41 shows the main features that were considered for the criteria.

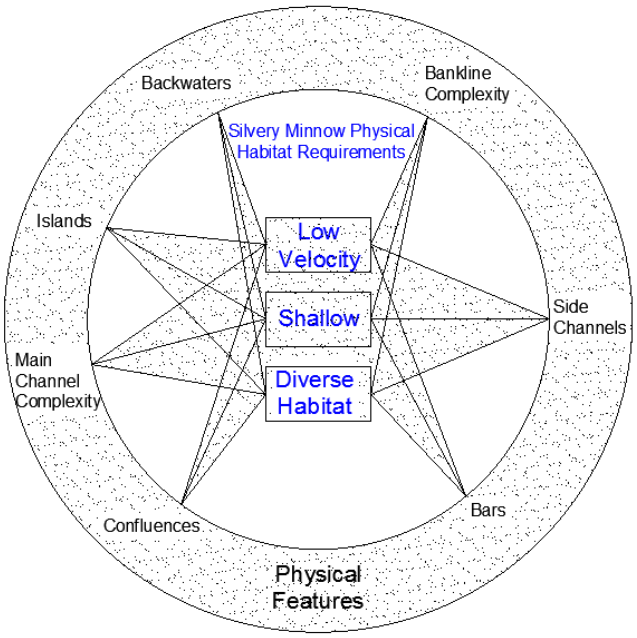


*Figure 41: Habitat requirements that can be seen from aerial photography. All of the physical features have three lines coming out of it and meeting the three requirements listed in the middle of the circle.*

Overall, certain physical features that may indicate good quality silvery minnow habitat can be analyzed with GIS from aerial photography. These include features such as backwaters, secondary channels, and debris piles. These components of the river create low velocities, shallow depths and diverse habitats that are crucial for silvery minnow survival. By identifying features in the river, giving those features a score based on habitat suitability, and comparing the scores spatially and across time we can see how the physical habitat is changing.

### 5.2.3. General Guidelines for Scoring and Mapping

Each habitat feature is identified with a point using GIS and identified with a criteria that has a number and letter. The criteria is correlated with a habitat feature (number), subdivided into the quality of that feature (letter), and given a score based on the quality of the habitat. The score is determined from literature review and is outlined in Appendix B. Table 11- Table 13 outline and briefly describe the criteria, what type of habitat it is and the score it receives. The entire outline of features which pictures and a description of what they are is given in Appendix B.

*Table 11: Habitat type, criteria and scores. Scores range from 1-5 and are further explained in Table 13.*

| | Shoreline Complexity | | | Main Channel Complexity | | Side Channels | | | | | Backwater | | Bars | | | Islands | | | | | | Confluences | |
|---|---|---|---|---|---|---|---|---|---|---|---|---|---|---|---|---|---|---|---|---|---|---|---|
| Criteria: | 1a | 1b | 1c | 2a | 2b | 3a | 3b | 3c | 3d | 3f | 4a | 4b | 5a | 5b | 5c | 6a | 6b | 6c | 6d | 6e | 6f | 7a | 7b |
| Score: | 4 | 3 | 2 | 4 | 3 | 4 | 3 | 2 | 3 | 5 | 5 | 4 | 5 | 2 | 1 | 3 | 2 | 1 | 1 | 4 | 3 | 4 | 3 |

*Table 12: Brief description of habitat types.*

| | |
|---|---|
| Complex Shoreline | 1a |
| Less Complex Shoreline | 1b |
| Less Complex, Less Accessible Shoreline | 1c |
| Main Channel Complexity (Large) | 2a |
| Main Channel Complexity (Small) | 2b |
| Large, Easily Accessible Dry Side Channel | 3a |
| Medium, Easily Accessible Dry Side Channel | 3b |
| Small, Less Accessible Dry Side Channel | 3c |
| Non-Complex Wetted Side Channel | 3d |
| Complex Wetted Side Channel | 3f |
| Large Backwater | 4a |
| Small Backwater | 4b |
| Complex Bar | 5a |
| Simple Vegetated Bar | 5b |
| Simple Unvegetated Bar | 5c |
| Large Unvegetated Island | 6a |
| Small Unvegetated Island | 6c |
| Large Vegetated Island | 6b |
| Small Vegetated Island | 6d |
| Large Complex Island | 6e |
| Small Complex Island | 6f |
| Active Confluence | 7a |
| Inactive Confluence | 7b |

*Table 13: Score Criteria. Each category depicts habitat that is beneficial to silvery minnows. 5 provides the most optimum habitat and 1 provides the least amount of benefits.*

| ***Score*** | ***Habitat Description*** |
|---|---|
| 1 | Low chance of becoming inundated, in main channel, small features, and low complexity of topography. |
| 2 | Low chance of becoming inundated, in main channel or could be in margins, bigger features than 1 or smaller than 3, and low complexity of topography. |
| 3 | Medium chance of becoming inundated, in main channel or near shoreline, bigger features than 2 or smaller than 4, and medium complexity of topography. |
| 4 | High likelihood of becoming inundated on side channel, or inundated but not very complex in main channel. Bigger features than 3 or smaller than 5. |
| 5 | Areas that are currently inundated with water and form complex flow with shallow areas and low velocities. Tend to be isolated from the main channel. Large features with high topographic complexity. |

The amount of points given for a feature is based on agg/deg polygons (area between each line). For instance, if an island spans over two agg/deg polygons it is given two points. The same is done for every feature including side channels. The longer the side channel, the more points it gets because it provides more silvery minnow habitat. Figure 42a. depicts scoring with islands and channels across agg/deg lines.

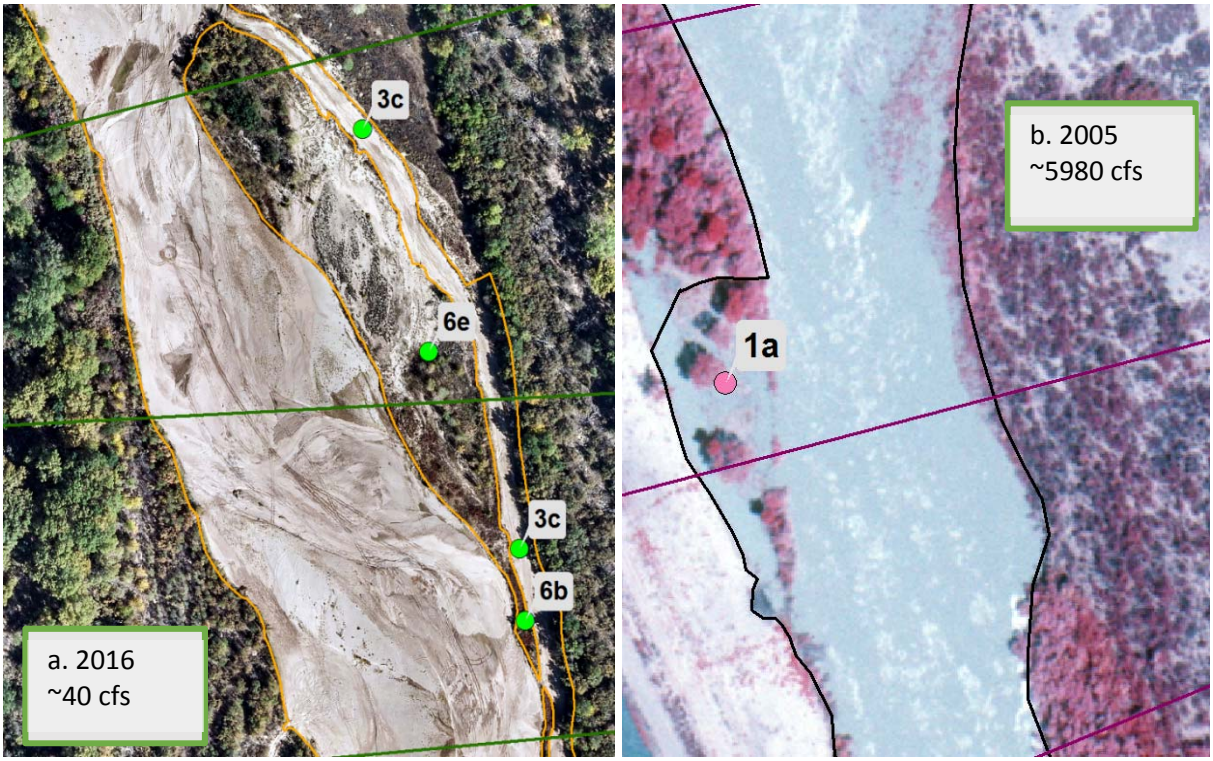


*Figure 42: a. A dry side channel (3c) and islands (6b and 6e) are depicted above in an aerial photograph from 2016. Agg/Deg lines are shown in green lines perpendicular to the main channel. The active channel is outlined in orange. b. 1a depicts shoreline complexity in an aerial photograph from June of 2005. Agg/Deg lines are shown in purple perpendicular to the main channel. The active channel is outlined in black. The flow is going to the bottom of the page for both images.*

In Figure 42a., the channel and the island span over two polygon lengths so they are each given a point in each polygon. The criteria is not exact, but instead an estimate of how many features there are. The criteria is not meant to be exact and map feature areas, but instead depict the amount of features that offer suitable habitat to get a general idea of how change is occurring. In Figure 42b. 1a is counted once instead of twice in this example. Even though the channel complexity spans over two agg/deg polygons, it only occupies the length of one agg/deg polygon so it is counted once.

For each year, the points are mapped and the scores are assigned. The results are compiled and compared in a few different ways shown in the following sections.

## 5.2.4. Methods of Analysis

### 5.2.4.1. Overall Habitat Score

An overall score for each year was calculated as well as a count for how many of each habitat types there were in the Isleta reach.

### 5.2.4.2. Subreach Delineation

Each year with available photographs is analyzed. The points are broken up and grouped into subreaches using ArcGIS. Scores given to different habitat types are added up within each subreach and compared across years. Because the subreaches have different areas, the scores are weighted by area by computing the score per square ft. The score is divided by the area and multiplied by a multiple of 10 that makes the data easy to work with. Below is a sample calculation:

$$Raw\ score\ for\ I1\ in\ 1992: 493$$

$$Area\ for\ I1: 46{,}386{,}142\ ft^2$$

$$Multiple\ of\ 10: 10{,}000{,}000$$

$$Normalized\ score: \frac{493}{46{,}386{,}142 ft^2} * 10{,}000{,}000 = 106$$

Also, the number of points in each subreach are counted and grouped into categories such as shoreline complexity, side channels, backwater etc. These scores are weighted as well. The following habitat features are grouped into the associated categories in Table 14 This is done to reduce the amount of graphs needed to compare how the habitat changes over time. When the habitat types are quite similar and mainly vary by size instead of quality they were grouped.

*Table 14: Habitat types grouped into broader categories.*

| | |
|---|---|
| Complex Shoreline | 1a, 1b, 1c |
| Main Channel Complexity | 2a, 2b |
| Easily Accessible Dry Side Channels | 3a, 3b |
| Less Accessible Dry Side Channels | 3c |
| Non-Complex Wetted Side Channel | 3d |
| Complex Wetted Side Channel | 3f |
| Backwater | 4a, 4b |
| Complex Bars | 5a |
| Simple Bars | 5b, 5c |
| Unvegetated Islands | 6a, 6c |
| Vegetated Islands | 6b, 6d |
| Complex Islands | 6f, 6e |
| Active Confluence | 7a |
| Inactive Confluence | 7b |

### 5.2.4.3. Agg/Deg Line Delineation

Using ArcGIS, the points were broken up and grouped into agg/deg polygons divided by each agg/deg line. Each polygon was given one value. This value is the summation of the criteria score given to the points based on the type of habitat outlined in section 5.2.3. The polygon

was given a color based on its value. The colors in agg/deg polygons were visualized in the six subreaches using ArcGIS.

## 5.3. Results

### 5.3.1. Overall Habitat Score

Table 15 summarizes the analysis for overall habitat score.

*Table 15: Summary of total habitat score, flows, and number of habitat types for each year. The comparable years are highlighted in blue.*

| | | | | Shoreline Complexity | | | Main Channel Complexity | | Side Channels | | | | | Backwater | | Bars | | | Islands | | | | | | Confluences | |
|---|---|---|---|---|---|---|---|---|---|---|---|---|---|---|---|---|---|---|---|---|---|---|---|---|---|---|
| Year | Month | Total Habitat Score | Flow (cfs) | 1a | 1b | 1c | 2a | 2b | 3a | 3b | 3c | 3d | 3f | 4a | 4b | 5a | 5b | 5c | 6a | 6b | 6c | 6d | 6e | 6f | 7a | 7b |
| 1992 | February | 4025 | 650[SA] | 23 | 6 | 7 | 85 | 88 | 0 | 3 | 1 | 211 | 184 | 9 | 7 | 42 | 103 | 58 | 3 | 0 | 11 | 2 | 180 | 147 | 0 | 1 |
| 2001 | February | 3300 | 687[A] | 26 | 6 | 0 | 125 | 103 | 0 | 0 | 3 | 111 | 111 | 1 | 1 | 45 | 26 | 8 | 5 | 6 | 26 | 8 | 216 | 83 | 1 | 1 |
| 2002 | February | 4335 | 600[SA] | 17 | 10 | 0 | 153 | 45 | 0 | 10 | 4 | 181 | 142 | 3 | 12 | 73 | 158 | 28 | 19 | 7 | 16 | 16 | 293 | 45 | 0 | 0 |
| 2005 | April | 3447 | 4500[I] | 138 | 16 | 5 | 168 | 59 | 8 | 2 | 4 | 84 | 84 | 2 | 0 | 101 | 8 | 0 | 0 | 1 | 0 | 10 | 118 | 81 | 3 | 0 |
| 2005 | June | 4395 | 5980[I] | 340 | 8 | 1 | 55 | 50 | 8 | 16 | 7 | 64 | 128 | 16 | 2 | 140 | 23 | 0 | 0 | 9 | 5 | 24 | 147 | 79 | 1 | 1 |
| 2006 | January | 3081 | 580[SA] | 45 | 33 | 2 | 42 | 76 | 8 | 75 | 3 | 124 | 65 | 21 | 14 | 24 | 140 | 33 | 6 | 2 | 16 | 7 | 156 | 56 | 2 | 1 |
| 2008 | June | 3050 | 4990[I] | 81 | 9 | 0 | 30 | 22 | 0 | 0 | 1 | 193 | 39 | 8 | 1 | 143 | 16 | 1 | 0 | 33 | 0 | 33 | 148 | 82 | 2 | 0 |
| 2008 | July | 2905 | 1630[I] | 38 | 35 | 11 | 7 | 35 | 7 | 31 | 24 | 165 | 123 | 12 | 8 | 17 | 40 | 13 | 3 | 109 | 9 | 54 | 128 | 45 | 1 | 1 |
| 2012 | January | 3501 | 740[SA] | 65 | 35 | 5 | 68 | 57 | 23 | 146 | 11 | 82 | 89 | 6 | 5 | 43 | 79 | 29 | 14 | 58 | 19 | 35 | 135 | 76 | 2 | 0 |
| 2016 | October | 719 | 40[SA] | 16 | 9 | 9 | 11 | 25 | 0 | 7 | 0 | 33 | 10 | 4 | 4 | 7 | 32 | 41 | 5 | 12 | 36 | 3 | 10 | 3 | 0 | 6 |

Note: Flows at different gages are given the follow subcripts: [I] Isleta gage daily average discharge, [SA] San Acacia gage daily average discharge, [A] Albuquerque gage daily average discharge

Overall, June of 2005 had the highest score and 2016 had the lowest score. The flows in the photographs in these years are also the highest and lowest respectively. The overall scores in between these two flows and those respective years vary and there is not a consistent trend. 1992 and 2002 also have high scores compared to the rest of the years.

Out of the comparable years, 1992 and 2002 are very similar and have higher scores than 2006 and 2012, which have close scores to each other as well.

June of 2005 has the highest amount of “shoreline complexity” (1a) followed by April of 2005 because in both of those years the floodplain gets inundated, but less so in April. April of 2005 has the most “large main channel complexity features” (2a), and 2001 has the most “smaller main channel complexity features” (2b). In 1992, the channel has the greatest amount of “wetted side channels” (3d and 3f). The most “dry channels” occur in 2012. There are not any standout amounts of backwater or bars in any of the years. In July of 2008, the most “vegetated islands” occur (6b, 6d). There is not a trend for most “non-vegetated island”. More “complex islands” occur earlier in time (6e,6f), and there is not a trend with “confluences”.

## 5.3.2. Subreach Delineation

*Table 16: Total weighted score by subreach. Summation of all years combined.*

| Subreach | Score |
|---|---|
| I1 | 771 |
| I2 | 863 |
| I3 | 884 |
| I4 | 840 |
| I5 | 591 |
| I6 | 649 |

Table 16 shows that I3 and I2 have the highest scores followed by I4. I5, I6 and I1 are the lowest. The total scores for the four years with photographs taken around 650 cfs are compared in Figure 43.

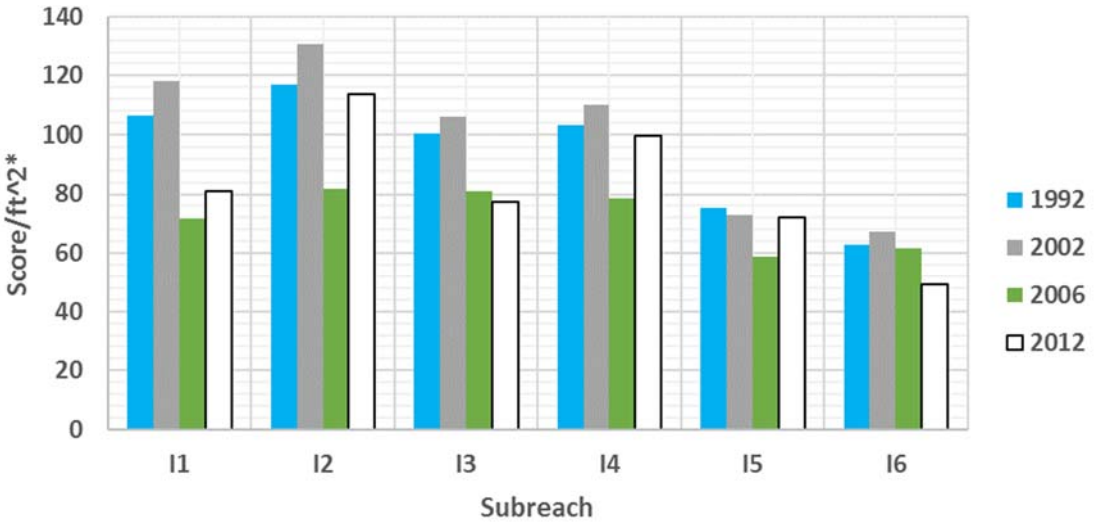


*Figure 43: The column graph shows the overall habitat scores in each of the four comparable years in each subreach. *Score/ft$^2$ is the score weighted for area of the subreach as discussed in section 5.2.4.2.*

Figure 43 shows subreach I2 has overall highest scores for all years, whereas I5 and I6 contain the lowest scores of each of the years. For instance, in I6, the lowest scores occur for all of the years except for 2006 which occurs in I5. The scores in 2006 and 2012 generally tend to be lower than those in 1992 and 2002, but there is not a dramatic change over the years.

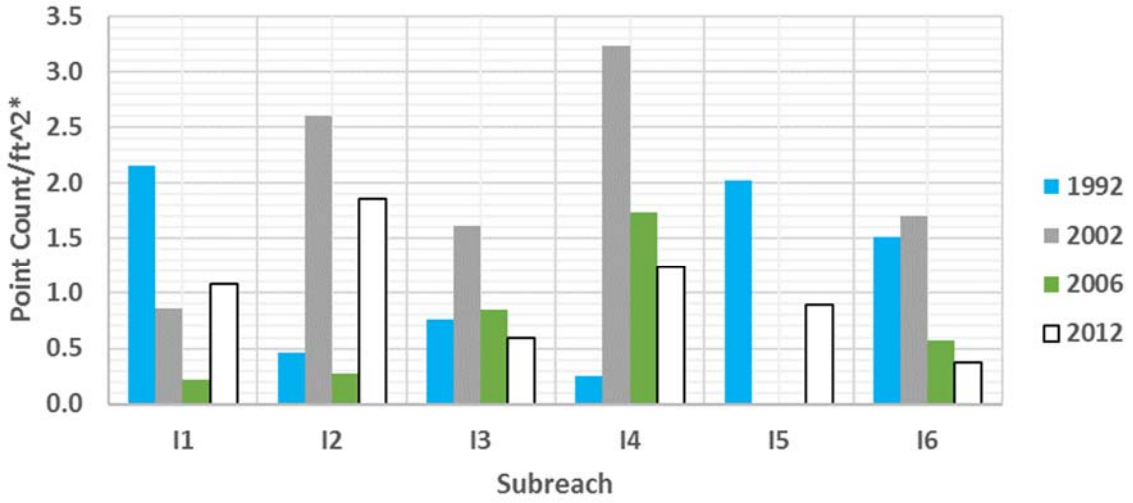


*Figure 44: The column graph shows the amount of complex bars in each of the four comparable years in each subreach. *The point count/ft$^2$ is the number of points counted and weighted for area of the subreach as discussed in section 5.2.4.2.*

As seen in Figure 44, the complex bars have shown to be decreasing over time. Complex bars seem to be more abundant in 1992 and 2002 compared to 2006 and 2012. Looking at similar graphs like this one that are listed in Appendix C, there are other trends that can be analyzed. For instance, complex islands, non-complex wetted side channels, and bedforms have generally decreased over time. Shoreline complexity, easily accessible dry side channels and vegetated islands have increased over time. The rest of the parameters don't show consistent enough patterns to draw conclusions from.

The overall scores comparing all years are shown in Figure 45.

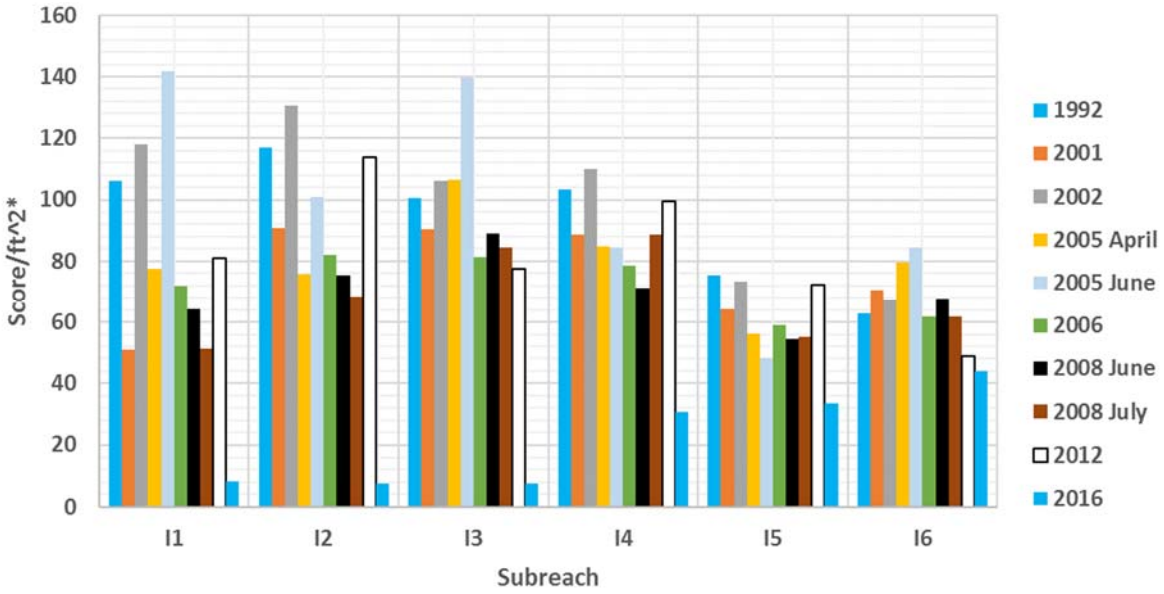

*Figure 45: The column graph shows the overall score in every year in each subreach. * Score/ft$^2$ is the score weighted for area of the subreach as discussed in section 5.2.4.2.*

The highest scores in the subreaches tend to occur in 1992, 2002, and June of 2005. The lowest scores occur in 2016 and July of 2008 somewhat consistently. All other years and flows vary and are middle of the range of high and low point counts/ft$^2$. Comparing the different habitat types does not prove very useful, because there are too many variables to find any trends. I3 has the highest cumulative score when adding all years together. It is closely followed by I2. I5 and I6 have the lowest scores.

## 5.3.3. Agg/Deg Line Delineation

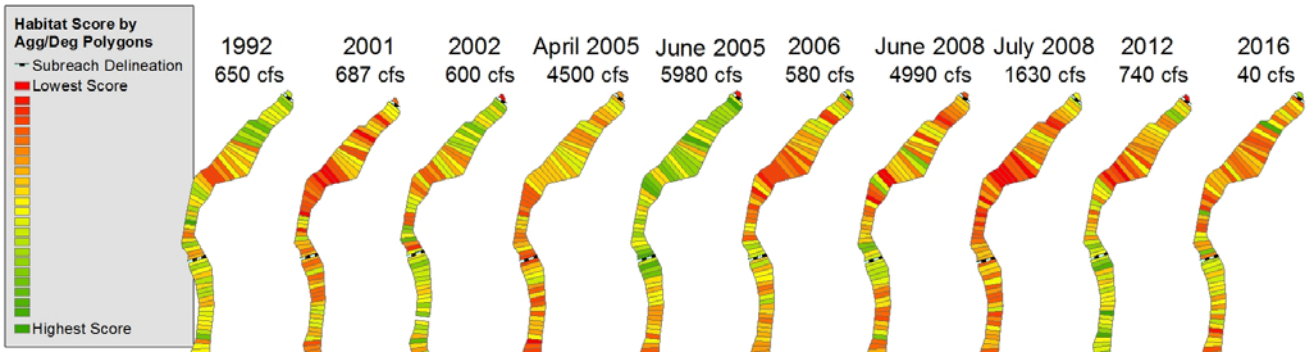


*Figure 46: Subreach I1 summation of habitat scores indicated by the color scheme in the legend and separated by agg/deg lines. All years are shown here with the discharge when the photographs used for this scoring scheme were taken. I1 is at the upper half of the images and the lower portions below the subreach delineation are part of the next subreach (I2).*

Green represents the highest scores, red is the lowest score, and yellow falls in the middle range of scores on the spectrum as shown in Figure 46. In Figure 46, the highest scores are shown in June of 2005 for subreach I1 because it appears to have the highest proportion of green polygons. 1992 and 2002 also have a high proportion of green and yellow polygons compared to other years, showing higher scores in more places. July of 2008 appears to have the lowest scores for the I1 subreach. The rest of the subreaches for the Isleta reach are in Appendix E.

All the subreaches vary in habitat quality over the years. There are not strong trends, but some years have more consistently higher or lower scores than the others. For instance, 2006, 2008 of July, and 2016 have higher proportions of red polygons. Also, 1992, 2001, 2002 June of 2005, and 2012 tend to have more green polygons in their subreaches.


*Figure 47: Subreach I1 summation of habitat scores indicated by the color scheme in the legend and separated by agg/deg lines. Only years around 650 cfs are shown. 2001 is excluded because location of the gage is far away from this study site, so this information is not as accurate.*

Looking at four years with around the same flow, 1992 and 2002 appear to have higher scores in this subreach compared to later years (Figure 47). Subreaches I2-I6 are in Appendix F. There is not a consistent trend when compared these four years over the whole reach. By taking a cursory look at how many green polygons appear in each subreach in each year, the order of higher to lower quality habitat can be estimated. 1992 has the most amount of green polygons, then 2012 and 2002 are very similar and 2006 has the lowest scores.

## 5.4. Discussion

The overall habitat score, subreach delineation scores, and agg/deg line delineation figures generally share the same results. Looking at the comparable years, 1992 and 2002 have better habitat than 2006 and 2012. This makes sense because habitat quality for silvery minnows in the Middle Rio Grande has been decreasing over time (Scurlock 1998; Bovee et al. 2008; Tetra Tech 2014).

When comparing all the years 2002, June and April of 2005, and 1992 consistently have the highest scores. 2006, July of 2008 and 2016 generally have the lowest scores. By subreach, I1-I3 have the highest scores for these years.

2016 has the lowest score by far because the river is dry for a lot of this reach, so it provides minimal habitat for silvery minnows. June of 2005 has the highest score mostly likely because of its high flow. By looking at the aerial photography, it is evident that the floodplain is inundated. This is further supported by the fact that there is significant overbank inundation at 5000 cfs in this reach (Tetra Tech 2014) and the aerial photographs in this year are taken when the flow was 5980 cfs. Habitat quality also increases with discharge from 3500 cfs- 7000 cfs (Tetra Tech, 2014) as mentioned before. Floodplain inundation is extremely important for the survival of silvery minnows, especially during their spawning stages (Dudley and Platantia 1997; Tetra Tech 2014; Bovee et al. 2008; Klein et al. 2018a). Also, it has been shown that “prolonged high flows during spring were most predictive of increased density” (Dudley et al. 2016). It is also interesting to note that there are no other photographs that captured a flow above 5000 cfs which may be why the other sores are not as high as June in 2005. April of 2005 also has a flow that causes a small amount of inundation which would explain why it has higher habitat scores.

The scores may be low in July of 2008 due to the flow of 1630 cfs. This flow is suboptimum for silvery minnow as suggested by a study done on silvery minnow by Bovee et al. (2008). The study was done in 2008 in a few small reaches (1-2 km each) downstream of the Rio Puerco and upstream of the San Acacia Diversion dam. They mapped out adult and juvenile hydraulic habitat in the study areas at flows up to 1000 cfs. Looking at connectivity, woody debris, depths and velocities, they found that habitat areas were reduced when flows exceeded 150 cfs mainly because of flow depth and velocity as shown in Figure 48. In stream habitat such as connectivity and woody debris decreased over time as well for flows exceeding 150 cfs (Bovee et al. 2008).

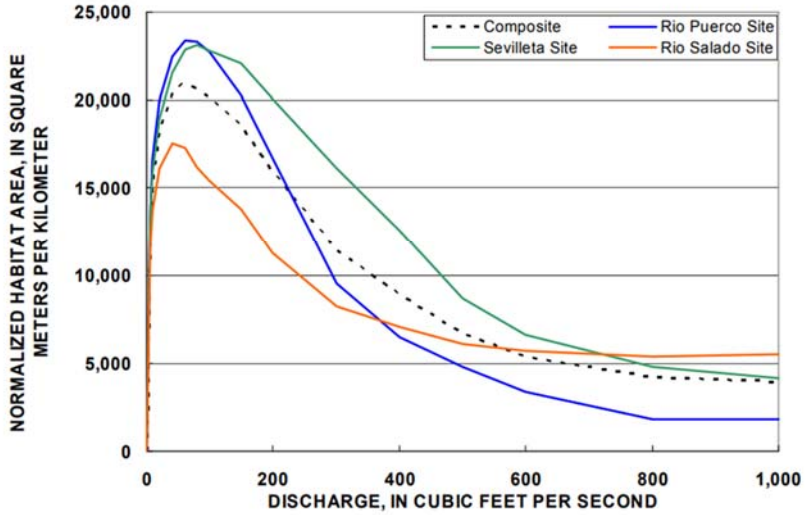


*Figure 48: Habitat area for silvery minnows (H. amarus) from Bovee et al (2008).*

By subreach, I2 and I3 have the highest score and I5 has the lowest. This may be due to the fact that I3 is the most sinuous reach as shown in Figure 22. I2 has the highest width and wetted perimeter, as well as the lowest velocity and depth. These parameters are consistent with good habitat for silvery minnows. I5 has the least amount of jetty jacks installed to channelize the river, so the opposite result would be expected. The density of the jetty jacks in other subreaches doesn't vary greatly, so it does not help explain variations in those subreaches. There are not many obvious trends or geomorphic landmarks that would explain differences in the other subreaches either.

Complex islands, complex bars, wetted side channels, and bedforms decreasing could mean that overall, the channel is becoming less braided and complex. Dry side channels are also becoming more abundant as well as vegetated islands, meaning the main channel is becoming more incised and the side channels becoming abandoned. Vegetated islands also increase if higher flows are also less frequent. Vegetation has time to develop on islands and have strong roots before getting washed away if high flows don't occur often (MEI 2006).

# 6. Shoreline Complexity

Shoreline complexity incorporates some silvery minnow habitat criteria, yet also incorporates geomorphic parameters for its analysis. Because it combines aspects from section 3 and geomorphic characteristics that could fit into section 5, shoreline complexity stands alone as its own section.

## 6.1. Methods

Two aspects of the shoreline were analyzed: the length of the shoreline and habitat features that indicate complex shoreline. The set of data used to analyze these aspects is shown in Table 17.

*Table 17: Years of the photographs used for analyzing the shoreline complexity.*

| | |
|---|---|
| 1992 | February |
| 2001 | February |
| 2002 | February |
| 2005 | June |
| 2006 | January |
| 2008 | July |
| 2012 | January |
| 2016 | October |

These are the years with planforms supplied by the USBR available. Data before 1992 is not used for the same reason it is not used in the habitat criteria analysis. Records of fish population before 1993 is not available, so it would be impossible to relate fish population to geomorphic trends before the early 1990's. April of 2005 and June of 2008 are excluded because planforms were not drawn for these photographs. It is unknown how each year's planform was drawn and how they differed, so there may be inconsistencies that affect the lengths.

Features including complex shoreline (1a, 1b, and 1c), bank attached bars (5a, 5b, and 5c), backwater (4a, 4b), and confluences (7a,7b) were considered to impact shoreline complexity. These points and their scores were used to find a habitat shoreline complexity score. Whatever points fall into each subreach were multiplied by their corresponding score and added up to get an overall score for each subreach in each year. These scores were weighted by area by using the same method as outlined in section 5.2.4.2.

The length of the shoreline is also an indicator of complexity. It was measured using ArcGIS by breaking up the active channel outline provided by USBR into subreaches as shown in Figure 49. The rest of the planform drawings are shown in Appendix D. The cumulative length of the right and left bank was used to compare each subreach in each year. To account for different sizes of the subreaches, the length was weighted. This was accomplished by drawing a straight line between each subsequent subreach delineation line perpendicular to the river. Then the

cumulative shoreline lengths were divided by the straight line and multiplied by 10 to get a weighted length index.

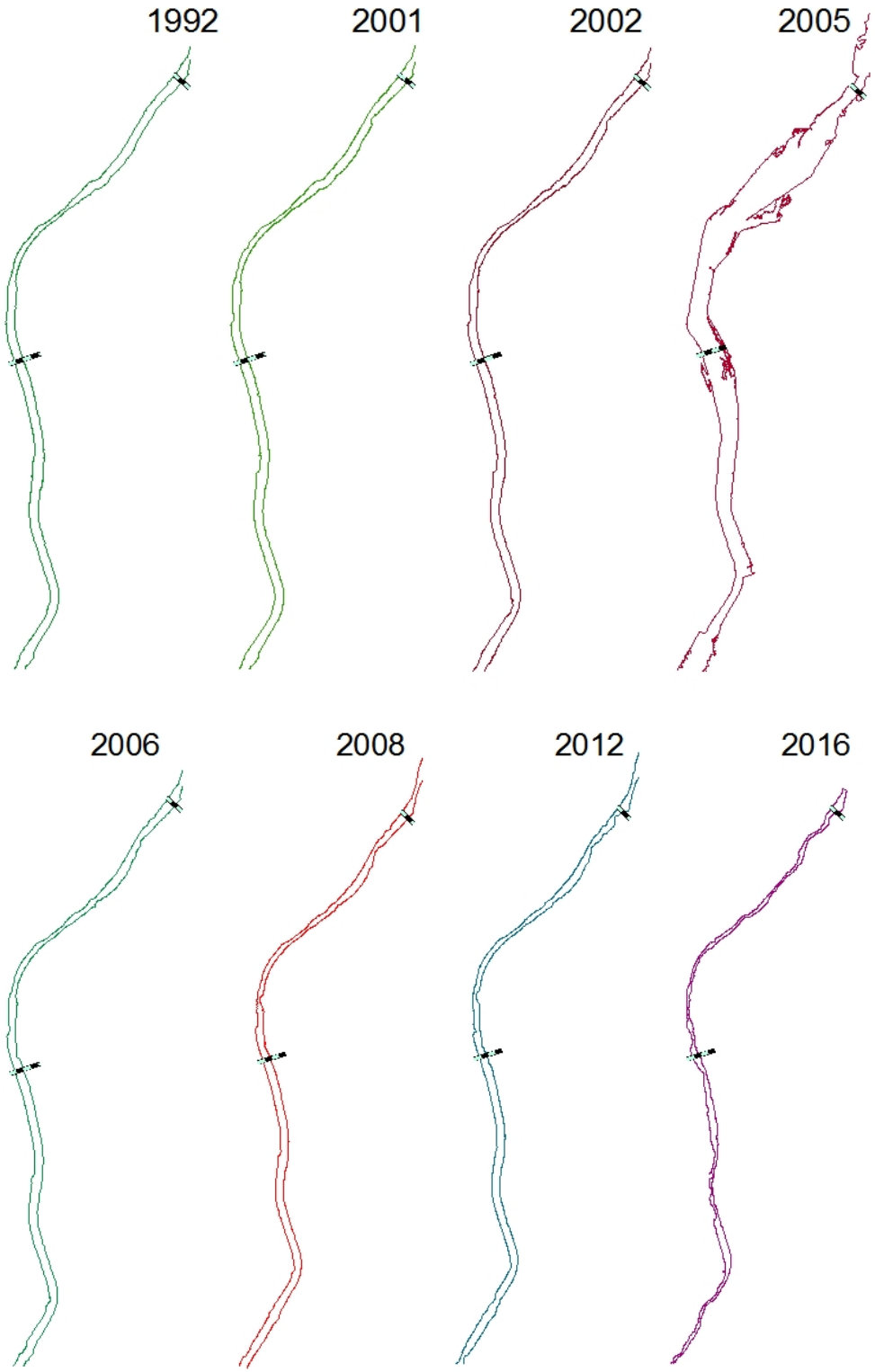


*Figure 49: Subreach I1 shoreline length shown with the planform drawing from USBR for each year.*

The weight length index and the weighted habitat score were then added together to get an overall shoreline complexity score. They were weighted to be on the same order of magnitude so they when they were added up, each would equally impact the overall score. These overall scores were compared across all years and across the comparable years at 650 cfs. The length of each subreach was also compared across every year and in the comparable years with 650 cfs. The individual parameters were also compared to the overall scores for each year and subreach.

## 6.2. Results

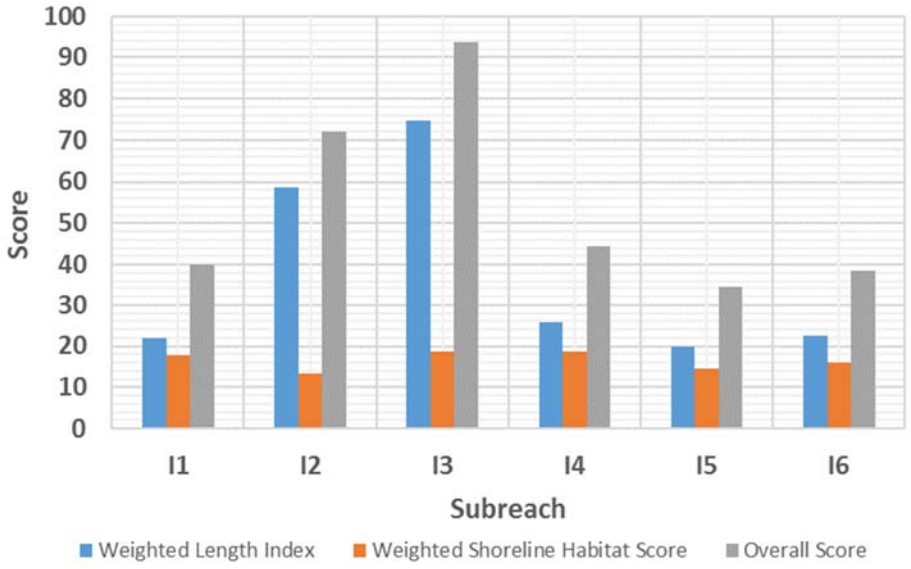


*Figure 50: Two parameters for analyzing shoreline complexity are compared and added up to show the overall score in 1992.*

In Figure 50, the overall complexity scores show that I3 is the most complex, followed by I2. The rest of the scores are very similar to each other. Every year in this subreach follows the same pattern, so the graphs for each year are essentially identical as shown in Appendix D. The shoreline complexity habitat score and the length of the shoreline do not seem to be

correlated.

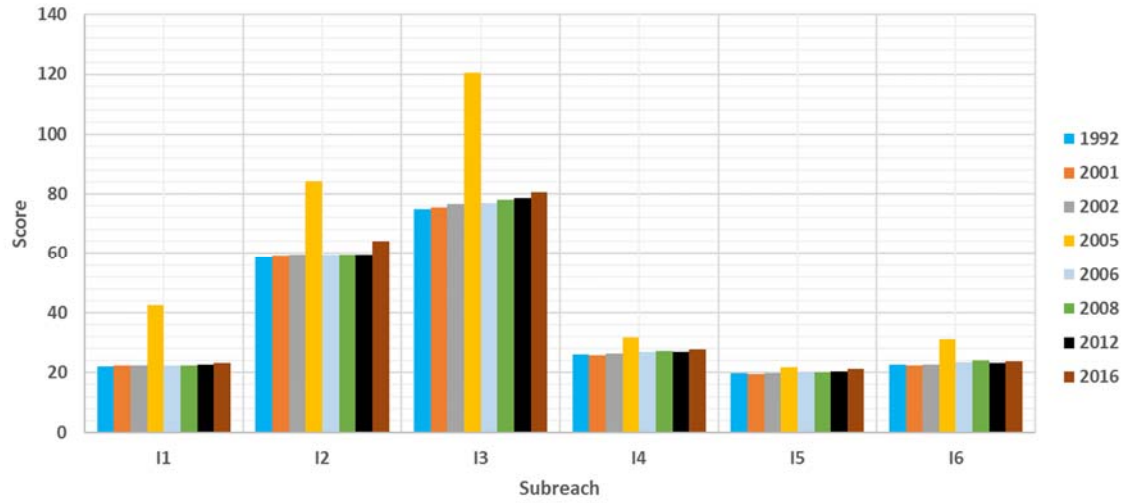


*Figure 51: The weighted length of the shoreline is compared over every subreach and every year.*

When comparing the lengths only across years, 2005 has the highest score and all the other scores are somewhat equal. In some subreaches, there is a slight increase in shoreline length over time.

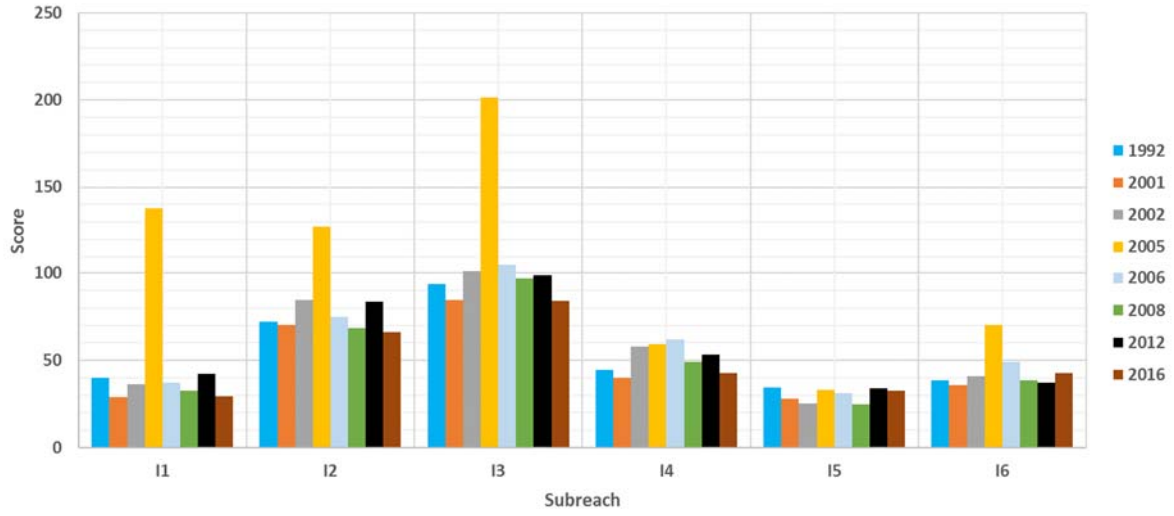


*Figure 52: The overall score for shoreline complexity is compared over every subreach and every year.*

The overall score has more variation among the years, but 2005 still has the highest scores in each subreach.

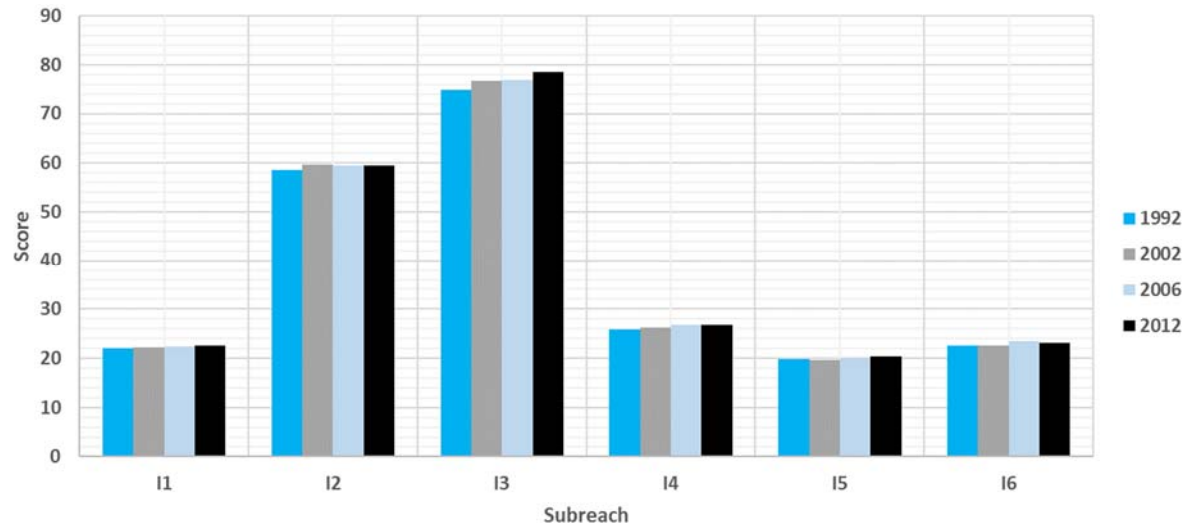


*Figure 53: The weighted length of the shoreline is compared over every subreach during years with a flow around 650 cfs when the aerial photograph was taken.*

There is not much change in any of the subreaches over the years, but in some subreaches the complexity goes up slightly.

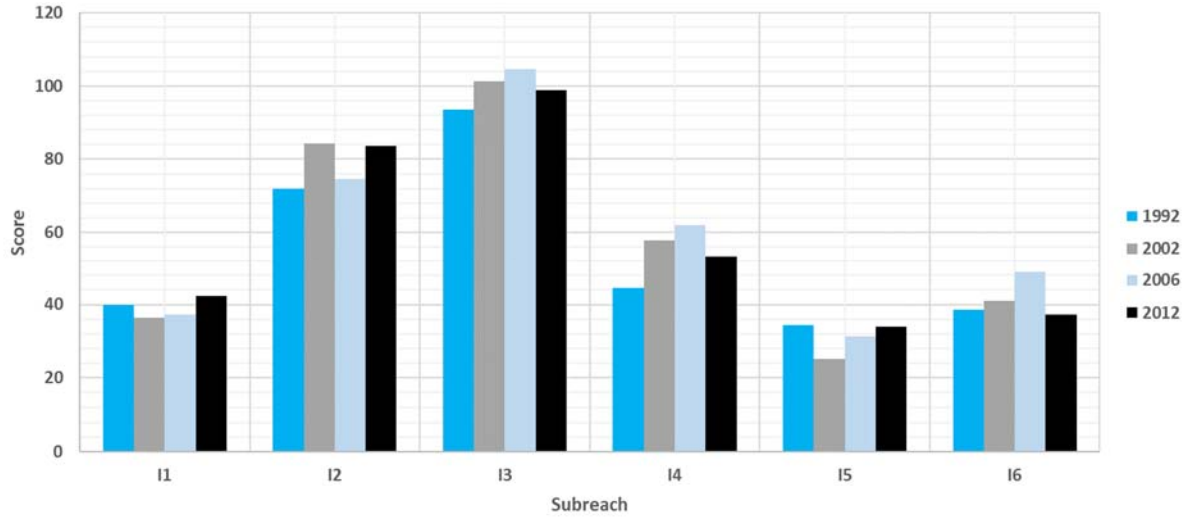


*Figure 54: The overall score for shoreline complexity is compared over every subreach during years with a flow around 650 cfs when the aerial photograph was taken.*

Throughout these years, each subreach has a different trend. There is not much consistency for the overall score.

In each of these figures where the years are compared, the overall trend is the same. I3 is the most complex, followed by I2. The rest of the subreaches have around the same scores and are consistently lower than I3 and I2.

## 6.3. Discussion

I3 has shown to be the most complex subreach in the Isleta reach. This may be due to the fact that I3 is the most sinuous reach as shown in Figure 22. I1 may have a lower score because it is just downstream of the Isleta Diversion Dam. The velocity and energy slope in I1 are higher than the other reaches, and the width is lower in I1 than the other reaches according to Figure 29: Width, depth, velocity, wetted perimeter, energy slope, and bed slope at each subreach for 1972, 1992, 2002, and 2012 at 3000 cfs. These parameters indicate a more incised channel, which would be consistent with the results of lower shoreline complexity. I2 is wider than I1 and has a lower velocity and energy slope than I2 as shown in Figure 28 again. This explains why the complexity jumps up at I2. The width, velocity, depth, wetted perimeter, bed slope and energy slope remain relatively constant from I3 through I6, so the variation in complexity may be due to other factors.

The complexity increasing over time since the 1990's may be due to sinuosity slightly increasing, braiding decreasing and width decreased. Because islands and side channels are not factored into the channel length and complexity, the results are not reflective of braiding decreasing, but instead just sinuosity increasing. This may be why it appears like the complexity is increasing over time.

# 7. Summary of HEC-RAS and GIS Habitat Analysis

To showcase the results for habitat analyses, figures representing one subreach at two flow conditions are presented. The rest of the subreaches at these flow conditions are in the appendix.

Subreach I1 is depicted in Figure 55 and Figure 56 because it is one of the subreaches that provides the best habitat. There is also a great amount of habitat variability in this subreach. This allows the analysis of how the habitats are different and what that difference looks like. Only a portion of the subreach is shown so the points and figures are decipherable.

The two different flow conditions are a low and high flow. The low flow analyzed is in 1992 at 650 cfs in GIS and 600 cfs in HEC-RAS shown in Figure 55. The high flow is analyzed at 4500 cfs in 2005 in GIS and 3500 cfs in HEC-RAS in 2002 shown in Figure 56. The difference in years and flows and the high flow analysis come from limitations in available data. The HEC-RAS simulation includes low, medium and high flows from 1992, 2002, and 2012. The only high flow data from aerial photographs analyzed is in 2005. The closest match for year and flow data to 3500 cfs from 2002 in HEC-RAS is aerial photography from April of 2005 at 4500 cfs. Therefore, the high flow results are not perfectly comparable because there is a difference in time and flow.

The top half of Figure 55 and Figure 56 (a) and (b) are from HEC-RAS and the bottom half (c and d) are from GIS. They both depict a portion of subreach I1. The results show that the HEC-RAS and GIS analyses are somewhat comparable. Where there is a large area of quality habitat from HEC-RAS there tends to be more habitat features mapped in GIS as seen in Figure 55. The trend does not always occur such as in Figure 56 which shows little correlation between the two analyses. This is mainly due to a limitation in seeing where the floodplain is inundated in the aerial photograph. The GIS mapping process is most accurate in the channel, yet HEC-RAS is more powerful at being able to map where the water inundates outside of the channel. Still, previous sections (4.3 and 5.3) show quantitatively how the two methods are closely correlated. These figures are mainly presented to get a visual idea of what the habitat and results look like.

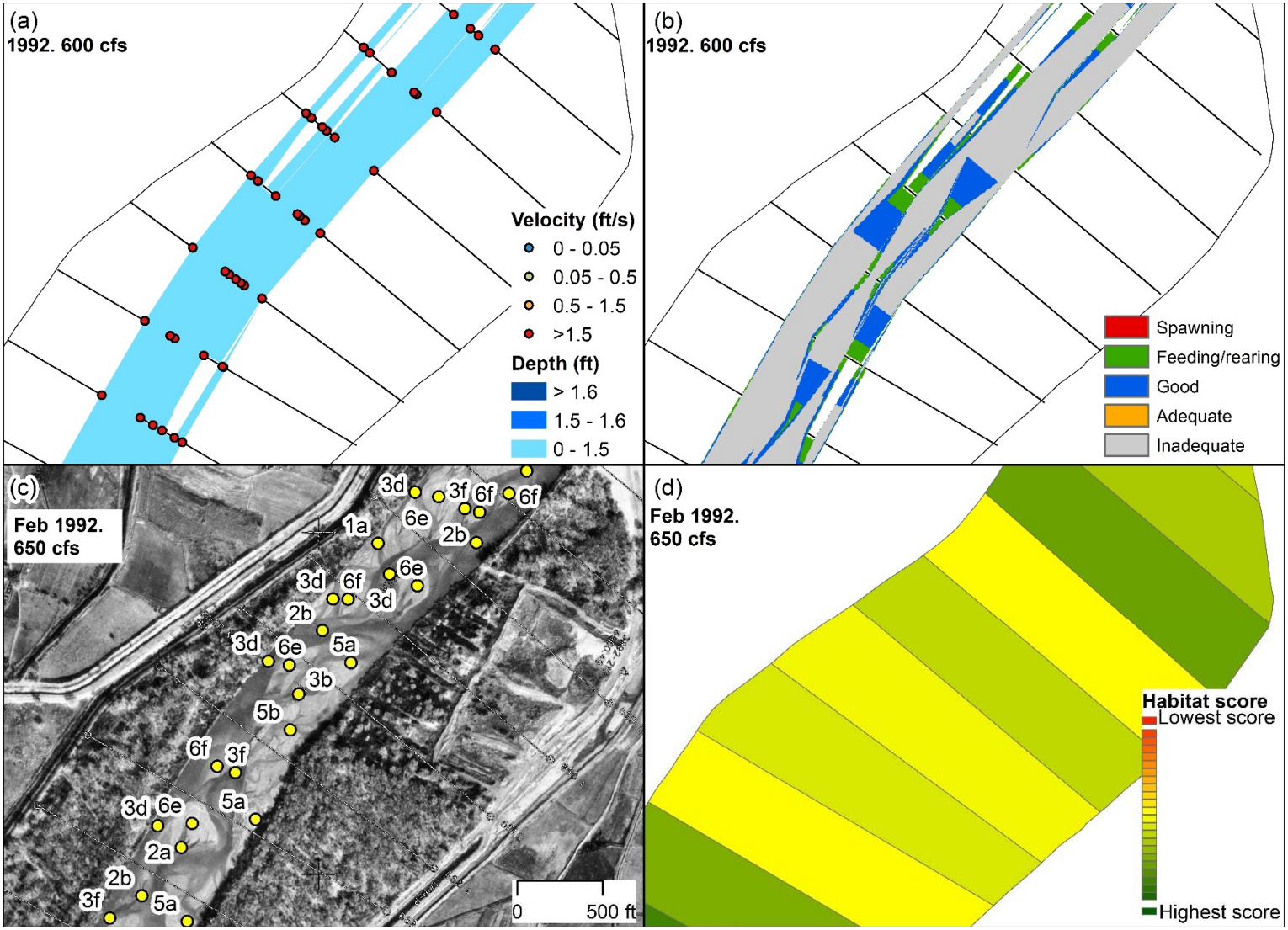


*Figure 55: Summary of HEC-RAS and GIS habitat at subreach I1, aggdeg 657 to 665. (a) Velocity and depth of the simulation. (b) Habitat criteria mapped based on velocity and depth. (c) Habitat features mapped out by points and letters. The description of these points is given in 1)a)i)(1)(a)(i)Appendix B - and section 5.2.3. (d) Habitat color scheme based on habitat features.*

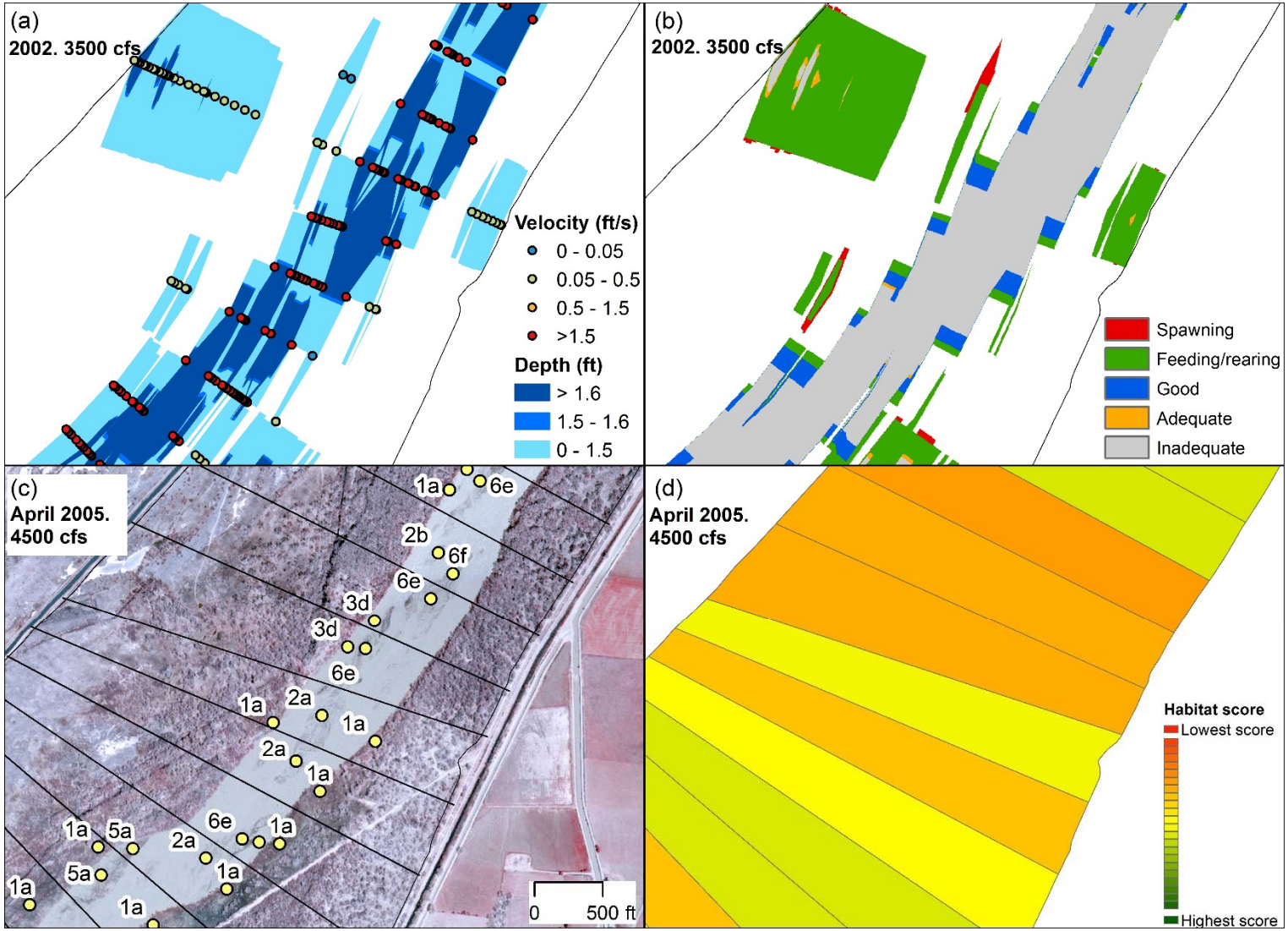


*Figure 56: Summary of HEC-RAS and GIS habitat at subreach I1, aggdeg 666 to 675. (a) Velocity and depth of the simulation at (b) Habitat criteria mapped based on velocity and depth. (c) Habitat features mapped out by points and letters. The description of these points is given in 1)a)i)(1)(a)(i)Appendix B - and section 5.2.3. (d) Habitat color scheme based on habitat features.*

# 8. Conclusion

The Isleta reach was analyzed for hydrologic, hydraulic, geomorphic, and habitat trends between 1918 and 2016. Although, not all analyses spanned this long. For instance, the habitat analysis started in 1992 because fish population data started in 1993 and HEC-RAS data goes back to 1935. Also, sediment and discharge gages don't always date back to 1918. This reach covers about 42 miles from the Isleta Diversion Dam to the Rio Puerco. There have been many geomorphic changes since 1918 due to anthropogenic influences such as installing jetty jack systems in the 1950's and the Isleta Diversion Dam in 1934.

Several techniques were used to analyze trends along the river as well as silvery minnow habitat. Data from USBR was the source of data used for this report. Reports already done on the Rio Grande and input from USBR were used to craft the objectives and goals of this technical report. Hydrologic and hydraulic trends were mainly taken from a report and raw data on this reach from USBR. HEC-RAS and GIS were used to find the geomorphic and river characteristics such as sinuosity, width, braidedness, bed elevation, volume change, and other hydraulic parameters. A conceptual geomorphic analysis was used to understand how the river is changing and how it will change in the future. HEC-RAS was also used to simulate flows in different years to find how much "spawning", "feeding/rearing", or "good" habitat there was. GIS was used to map habitat types and quality over different years of available aerial photography. The geomorphic, HEC-RAS and GIS analyses of the river were broken up into subreaches to get more detailed results than in the previous USBR report by Klein et al. (2018a). The subreaches could be compared between analyses as well to find trends in geomorphology and habitat quality. The major findings are:

- Annual water volume has been reduced recently (since the 2000's). Peak discharges have become less frequent, shorter and have decreased in the past few decades.
- Annual suspended sediment discharge in the Rio Grande and Rio Puerco have decreased since the 1970's. The effective discharge for suspended sediment has also decreased from 900 to 750 cfs since 1995.
- The predominant sediment moving through the reach is sand, then finer material such silts and clay make up less of the total load. The effective discharge for total load has also decreased from 940 cfs to 750 cfs.
- Most subreaches have increased in sinuosity, decreased in width, become more incised, and sediment size has increased. They have also increased in depth and velocity while decreasing in wetted perimeter, energy slope and bed slope.
- A conceptual geomorphic model shows the channel is becoming more incised and less connected to its floodplain. Losing connection to the floodplain is extremely detrimental to the silvery minnow, along with the other geomorphic changes listed above.
- In the HEC-RAS analysis, the best "spawning" and "feeding/rearing" habitat occur when the flows are at 3500 cfs (compared to 600 and 1400 cfs). The "good" habitat has decreased in area over time and is highest in at flows of 600 cfs. The majority of "good",

"spawning" and "feeding/rearing" habitat tend to occur in subreaches I1-I3. While 2002 has the highest amount of "spawning" habitat at 3500 cfs, it has the least amount of "good" habitat at that flow compared to other years.

- For the GIS analysis, the lowest scores are at very low flows when the river is almost dry and for flows around 1500 cfs. The highest scores occur in earlier years or when the flow is high enough to connect the main channel to the floodplain (above 3500 cfs). Over all years I2-I4 have the best scores. When comparing years of photographs with flow at 650 cfs, I1-I4 have the best habitat scores.
    - GIS was used mainly to compare habitats across low flow scenarios because of limited aerial photography. This still may be useful because low flows are becoming the norm and high flows are not as common.
- To compare the GIS and HEC-RAS analyses, the results at 600 cfs were used. The two methods are highly correlated with each other. It is evident that 1992 and 2002 habitats have higher scores than in 2012 for both analyses. Subreaches I1-I3 are the overlapping subreaches from both analyses that provide the best in-channel habitat. Also, flows above 3500 cfs tend to provide the best overall habitat because they connect the channel to the floodplain. Flows around 1400 cfs usually provide the least amount of quality habitat.
    - Now doing a detailed study on subreaches I1-I3 may lead to answers about why they have a high habitat score. This could lead to understanding how to restore the river and improve silvery minnow habitat in other locations.
- There is not a consistent trend with shoreline complexity, but the length has been slightly increasing since the 1990's. June of 2005 stands out as having the highest shoreline complexity because it has the most inundated floodplain.
- Silvery minnow's habitat quality has been decreasing over time due to a more incised channel, increased depth and velocity, increased sediment size and disconnection to the floodplain.

The Rio Grande is naturally very dynamic, yet anthropogenic influences have caused alterations that have accelerated changes unnaturally. This has greatly affected the ecological health and usability of the river. The silvery minnow, for instance, is at the mercy of these changes which are occurring too fast to adapt to. If nothing is done to mitigate this, the silvery minnow will likely go extinct and we will be left with the consequences of losing an important part of an ecosystem. In response to this, many reports such as this one have attempted to understand how the river works to save them. These results can be used to focus on small areas that indicate high habitat quality. The next step could be make an effort to understand why these areas have better habitat and how the river functions, and applying that knowledge to fix the mechanics and geomorphic problems in the Rio Grande.

# References


Baird, D. (2014). Historical Rio Grande Channel Width Design Literature Review Summary, U.S. Department of the Interior, Bureau of Reclamation, Technical Services Center, Sedimentation and River Hydraulics Group. Denver, CO, 42 p.

Baird, D. C. (2016). *Rio Grande silvery minnow habitat restoration design review*, Department of the Interior, Bureau of Reclamation, Technical Services Center, Sedimentation and River Hydraulics Group. Denver, CO.

Bauer, T.R. (2000). *Morphology of the Middle Rio Grande from Bernalillo Bridge to San Acacia Diversion Dam, New Mexico*, Colorado State University, Fort Collins, CO.

Bauer, T.R. (2009). *Sediment Evolution on the Middle Rio Grande, New Mexico*, U.S. Department of the Interior, Bureau of Reclamation, Technical Services Center, Sedimentation and River Hydraulics Group. Denver, CO. 36 p.

Bauer, T.R. and Hilldale, R. (2006). *Sediment Model for the Middle Rio Grande – Phase 2: Isleta Diversion Dam to San Acacia Diversion Dam*. U.S. Department of the Interior, Bureau of Reclamation, Technical Services Center, Sedimentation and River Hydraulics Group. Denver, CO. 295 pp.

Berry, K. L. and Lewis, K. (1997). *Historical Documentation of Middle Rio Grande Flood Protection Projects, Corrales to San Marcial*. Office of Contract Archeology, University of New Mexico, Albuquerque, NM.

Bestgen, K. R., Mefford, B., Bundy, J., Walford, C., Compton B., Seal S., and Sorensen T. (2003). *Swimming performance of Rio Grande silvery minnow. Final Report to U.S. Bureau of Reclamation, Albuquerque Area Office, New Mexico*. Colorado State University, Larval Fish Laboratory Contribution 132, 70 p.

Bestgen, K.R., and Platania S.P. (1991). "Status and Conservation of the Rio Grande Silvery Minnow, Hybognathus amarus." The Southwestern Naturalist. 36 (2), 225-232

Bovee, K.D., Waddle, T.J., and Spears, J.M. (2008). "Streamflow and endangered species habitat in the lower Isleta reach of the middle Rio Grande." *U.S. Geological Survey Open-File Report 2008-1323*.

Cluer, B., and Thorne, C. (2014). "A stream evolution model integrating habitat and ecosystem benefits." *River Research and Applications*, 30(2), 135–154.

Cowley, D.E. (2002). "Water Requirements for Endangered Species- Rio Grande Silvery Minnow (Hybognathus Amarus)." New Mexico Water Resources Research Institute. 97-107

Crawford, C. S., Cully, A. C., Leutheuser, R., Sifuentes, M. S., White, L. H., and Wilber, J. P. (1993). *Middle Rio Grande ecosystem: Bosque biological management plan*, Middle Rio Grande Biological Interagency team, Albuquerque, NM, 320p.

Culbertson, J. K., and Dawdy, D. R. (1964). “A study of fluvial characteristics and hydraulic variables, Middle Rio Grande, New Mexico.” *U.S. Geological Survey, Professional Paper 1498-F*, Washington, D.C., 82 p.

Dudley, R. K., and Platania, S. P. (1997). *Habitat use of Rio Grande silvery minnow*. Division of Fishes, Museum of Southwestern Biology, Department of Biology, University of New Mexico.

Dudley, R.K., Platania, S.P., and Gottlieb, S.J. (2005). *Rio Grande Silvery Minnow Population Monitoring Program Results from 2004*. American Southwest Ichthyological Research Foundation, Albuquerque, NM, 184 p.

Dudley, R. K., Platania, S. P., and White, G. C. (2016). *Rio Grande Silvery Minnow population monitoring results from February to December 2015*, American Southwest Ichthyological Researchers, LLC, Albuquerque, New Mexico.

Easterling Consultants LLC, and Tetra Tech Inc. (2015). *Geomorphic and Hydraulic Assessment of the Rio Grande from the Rio Puerco to San Acacia Diversion Dam 1998 to 2015*, Middle Rio Grande Project Hydrographic Data Collection, U.S. Bureau of Reclamation, Albuquerque, New Mexico.

Happ, S.C. (1948). “Sedimentation in the Middle Rio Grande Valley, New Mexico.” Bulletin of the Geological Society of America. 59, 1191 – 1216

Holmes, R., and Hayes, J., (2011). “Broad-scale Trout Habitat Mapping for Streams (Using Aerial Photography and GIS).” *Cwathron Report, No. 1979*, Nelson, New Zealand, 40 p.

Horner, C. (2016). *Middle Rio Grande Habitat Suitability Criteria*, Colorado State University, Fort Collins, CO.

Klein, M., Herrington, C., AuBuchon, J., and Lampert, T. (2018a). *Isleta to San Acacia Geomorphic Analysis*, U.S. Bureau of Reclamation, Reclamation River Analysis Group, Albuquerque, New Mexico.

Klein, M., Herrington, C., AuBuchon, J., and Lampert, T. (2018b). *Isleta to San Acacia Hydraulic Modeling Report*, U.S. Bureau of Reclamation, Reclamation River Analysis Group, Albuquerque, New Mexico.

Julien, P.Y. (2002). *River Mechanics,* Cambridge University Press, New York

Larsen, A. (2007). *Hydraulic Modeling Analysis of the Middle Rio Grande – Escondida Reach, New Mexico*, Colorado State University, Fort Collins, CO.

Makar, P. (2010). *Channel Characteristics of the Middle Rio Grande, New Mexico*. U.S. Department of the Interior, Bureau of Reclamation, Technical Service Center, Denver, CO, 48 p.

Makar, P. and AuBuchon, J. (2012). *Channel Conditions and Dynamics of the Middle Rio Grande*, U.S. Department of the Interior, Bureau of Reclamation, Upper Colorado Region, Albuquerque, NM, 108 p.

Marshall, M. (2015). “Earth - What is the point of saving endangered species?” *BBC News, BBC*, <http://www.bbc.com/earth/story/20150715-why-save-an-endangered-species> (Jul. 4, 2018).

Massong, T., Paula, M., and Bauer, T. (2010). “Planform Evolution Model for the Middle Rio Grande, NM.” *2nd Joint Federal Interagency Conference, Las Vegas, NV, June 27 - July 1, 2010*.

Medley, C. N., and Shirey, P. D. (2013). "Review and reinterpretation of Rio Grande silvery minnow reproductive ecology using egg biology, life history, hydrology, and geomorphology information" *U.S. National Park Service Publications and Papers.* 133.

MEI. (2002). *Geomorphic and Sedimentologic Investigations of the Middle Rio Grande between Cochiti Dam and Elephant Butte Reservoir*, Mussetter Engineering, Inc., Fort Collins, CO, 220 p.

MEI. (2006). “Evaluation of Bar Morphology, Distribution and Dynamics as Indices of Fluvial Processes in the Middle Rio Grande, New Mexico.” Report prepared for the New Mexico Interstate Stream Commission and the Middle Rio Grande Endangered Species Act Collaborative Program.

Osborne, M. J., Carson, E. W., and Turner, T. F. (2012). “Genetic monitoring and complex population dynamics: insights from a 12-year study of the Rio Grande silvery minnow.” *Evolutionary Applications*, 5(6), 553–574.

Parametrix. (2008). *Restoration analysis and recommendations for the Isleta Reach of the Middle Rio Grande, NM*, Parametrix, Inc. Albuquerque, NM, 292 p.

Perschbacher, J. (2011). *The Use of Aerial Imagery to Map In-Stream Physical Habitat Related to Summer Distribution of Juvenile Salmonids in a Southcentral Alaskan Stream*, University of Alaska Fairbanks, Fairbanks, AK.

Posner, A. J. (2017). *Channel conditions and dynamics of the Middle Rio Grande River,* U.S. Bureau of Reclamation, Albuquerque, New Mexico.

Richard, G. A. (2001). *Quantification and prediction of lateral channel adjustments downstream from Cochiti Dam, Rio Grande*, NM, Colorado State University, Fort Collins, CO.

Russo, B. (2018). “An Endangered Fish Out of Water.” *Earth Island Journal. News of the World Environment*, < http://www.earthisland.org/journal/index.php/elist/eListRead/an_endangered_fish_out_of_water/> (July. 4, 2018)

Scurlock, D. (1998). “From the Rio to the Sierra: an environmental history of the Middle Rio Grande Basin.” *General Technical Report RMRS-GTR-5. Fort Collins, CO: US Department of Agriculture, Forest Service, Rocky Mountain Research Station*, *440 p.*

Swanson, B., Meyer, G., and Coonrod, J. (2010). *Coupling of Hydrologic/Hydraulic Models and Aerial Photographs through Time, Rio Grande near Albuquerque, New Mexico: Report Documentary 2007 Work*. U.S. Army Engineer Research and Development Center, Vicksburg, MS.

Tashjian, P. and Massong, T. (2006). “The Implications of Recent Floodplain Evolution on Habitat within the Middle Rio Grande, NM.” *2006 Federal interagency Sedimentation Conference*, 9 p.

Tetra Tech. (2002). *Development of the Middle Rio Grande FLO-2D Flood Routing Model Cochiti Dam to Elephant Butte Reservoir.* Tetra Tech, Inc. 48 p.

Tetra Tech. (2014). *Ecohydrological Relationships along the Middle Rio Grande of New Mexico for the Endangered Rio Grande Silvery Minnow*. US Army Corps of Engineers, Albuquerque district, Albuquerque, New Mexico, 109 p.

Torres, L.T. (2007). *Habitat Availability for Rio Grande Silvery Minnow (Hybognathus amarus) Pena Blanca, Rio Grande, New Mexico*, University of New Mexico, Albuquerque, New Mexico.

U.S. Bureau of Reclamation. (n.d.). “PROJECTS & FACILITIES.” Central Valley Project - Mid-Pacific Region | Bureau of Reclamation, <https://www.usbr.gov/projects/index.php?id=130> (Aug. 9, 2018).

U.S. Fish and Wildlife Service. (2007). “Rio Grande Silvery Minnow (Hybognathus amarus).” Draft Revised Recovery Plan, Albuquerque, New Mexico, 174 p.

U.S. Fish and Wildlife Service. (2010). “Rio Grande Silvery Minnow Recovery Plan, First Revision” Southwest Region U.S. Fish and Wildlife Service Albuquerque, New Mexico, 210 p.

Varyu, D. (2013). *Aggradation / Degradation Volume Calculations: 2002-2012*. U.S. Department of the Interior, Bureau of Reclamation, Technical Services Center, Sedimentation and River Hydraulics Group. Denver, CO.

Varyu, D. (2016). *SRH-1D Numerical Model for the Middle Rio Grande: Isleta Diversion Dam to San Acacia Diversion Dam*. U.S. Department of the Interior, Bureau of Reclamation, Technical Services Center, Sedimentation and River Hydraulics Group. Denver, CO.

Appendix A - HEC-RAS

A) 1992

I1

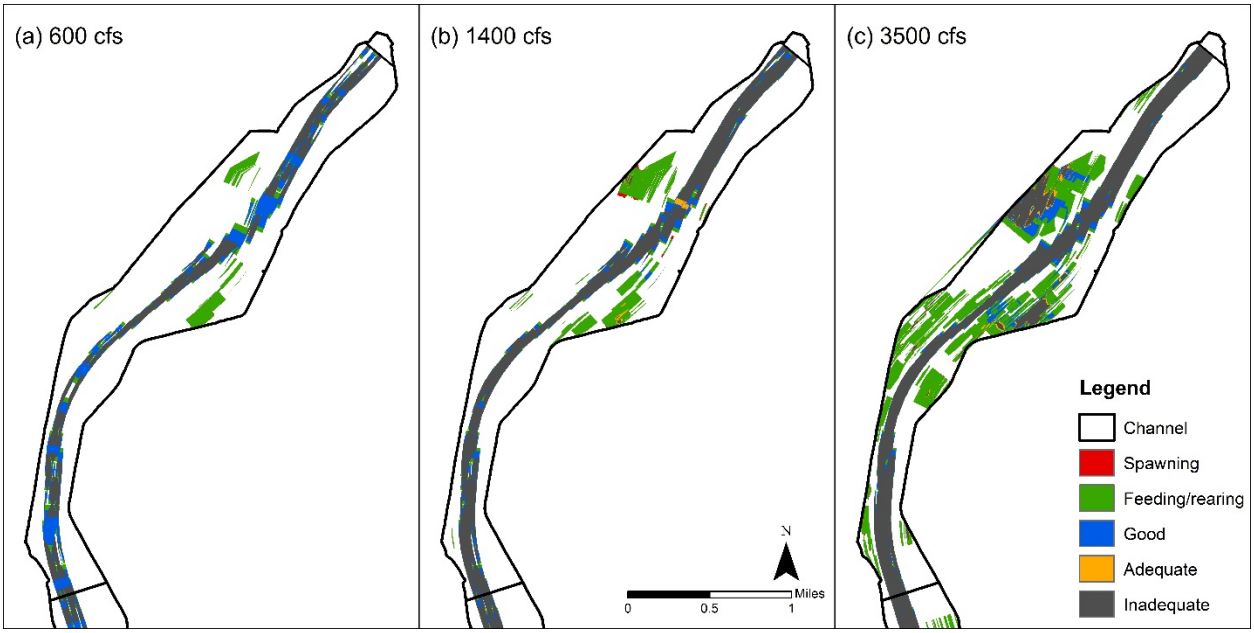


I2

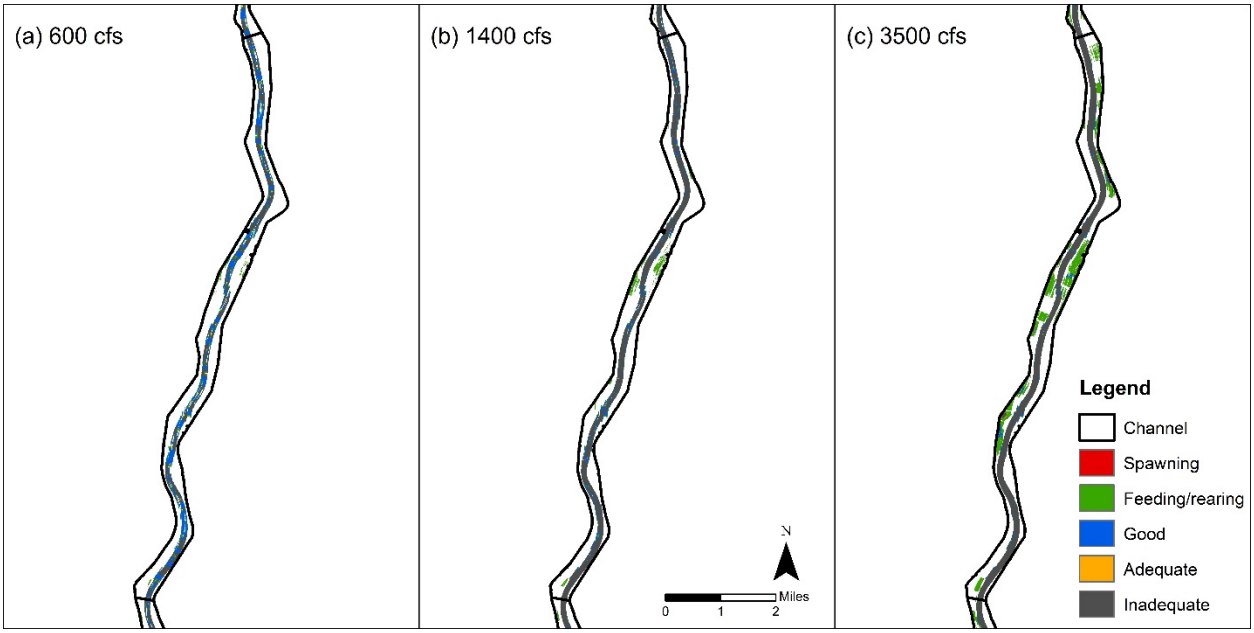

I3

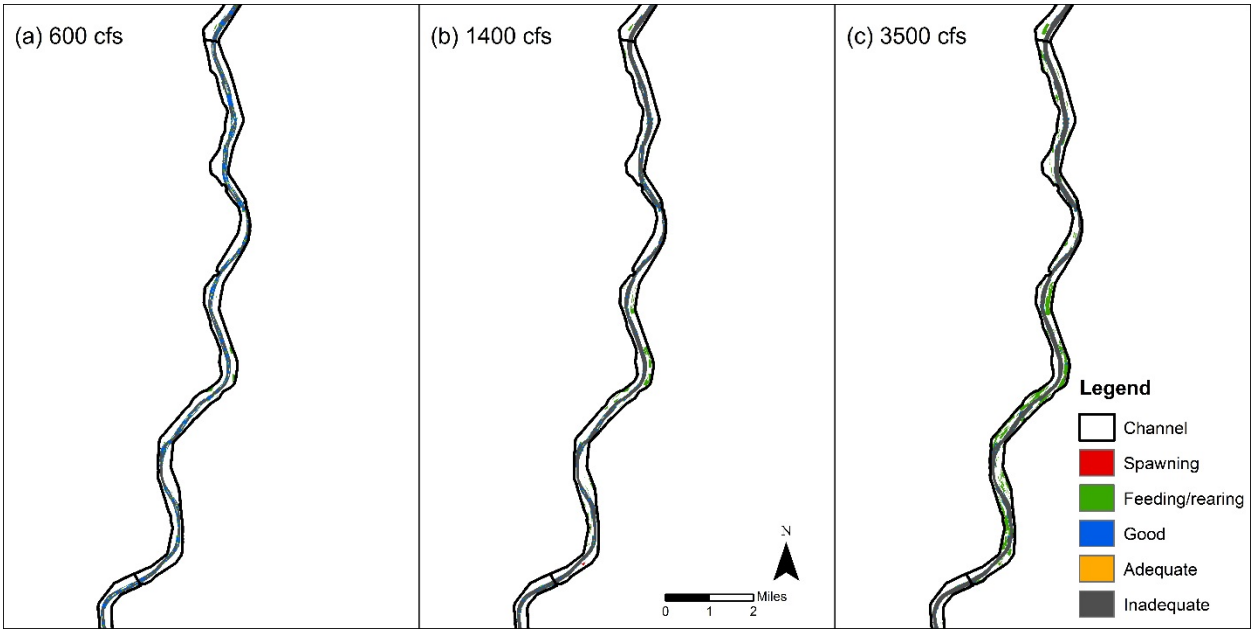
(a) 600 cfs
(b) 1400 cfs
(c) 3500 cfs
N
Miles
0 1 2
Legend
Channel
Spawning
Feeding/rearing
Good
Adequate
Inadequate

I4

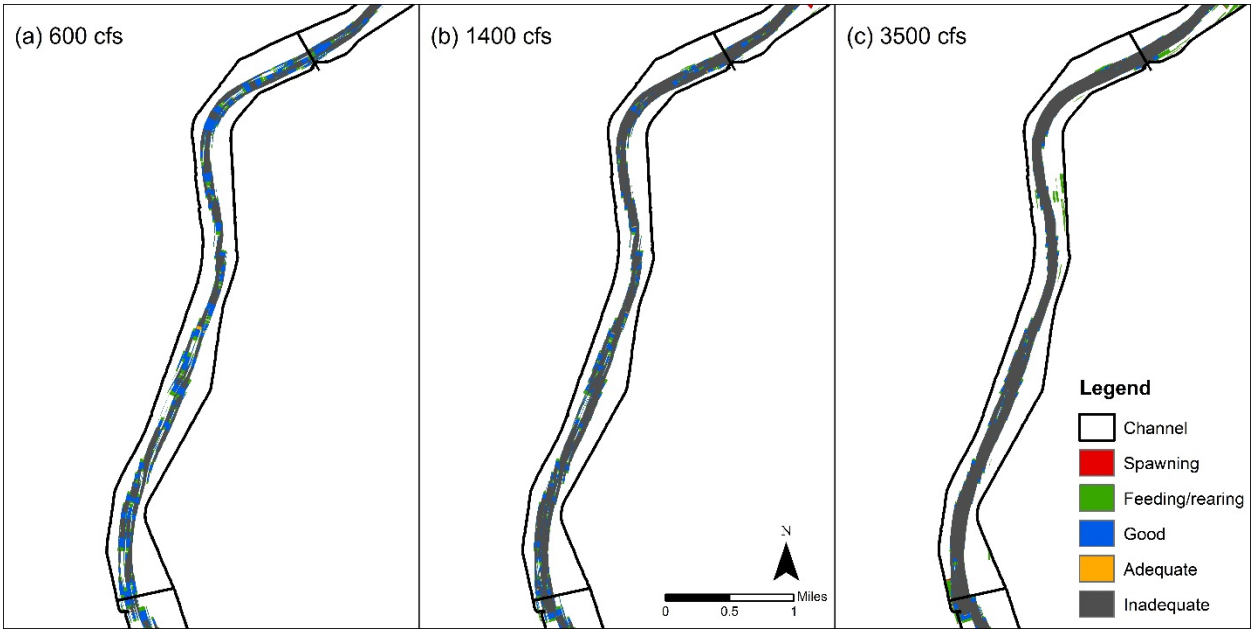
(a) 600 cfs
(b) 1400 cfs
(c) 3500 cfs
N
Miles
0 0.5 1
Legend
Channel
Spawning
Feeding/rearing
Good
Adequate
Inadequate

I5

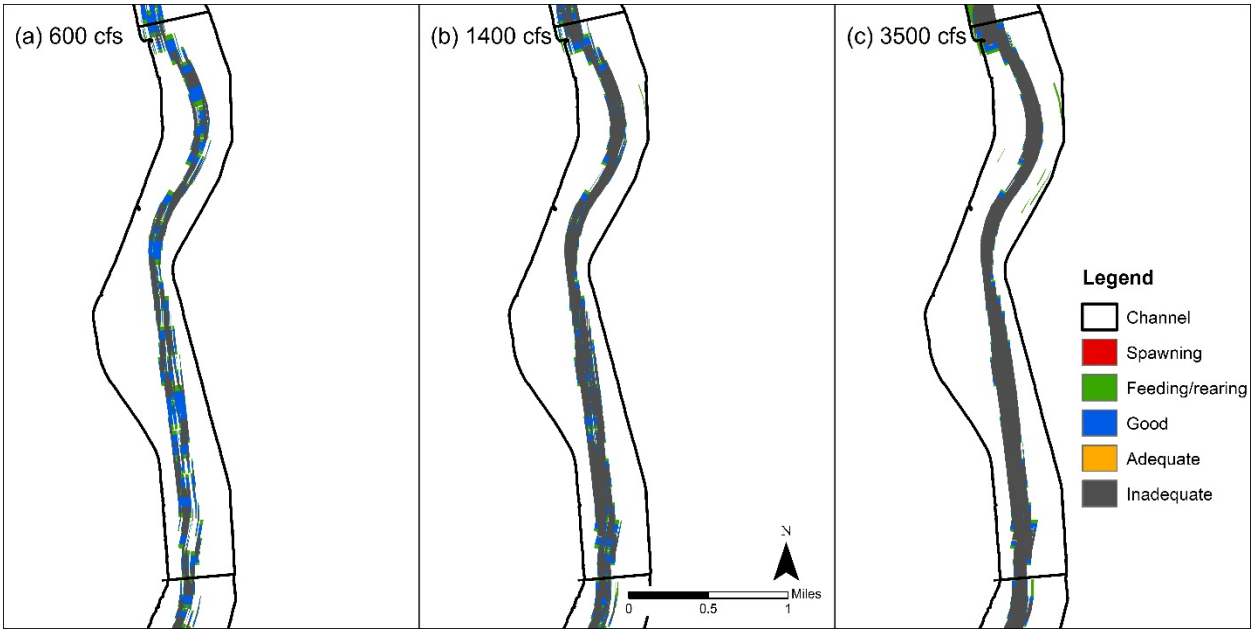
(a) 600 cfs
(b) 1400 cfs
(c) 3500 cfs
N
0
0.5
1
Miles
Legend
Channel
Spawning
Feeding/rearing
Good
Adequate
Inadequate

I6

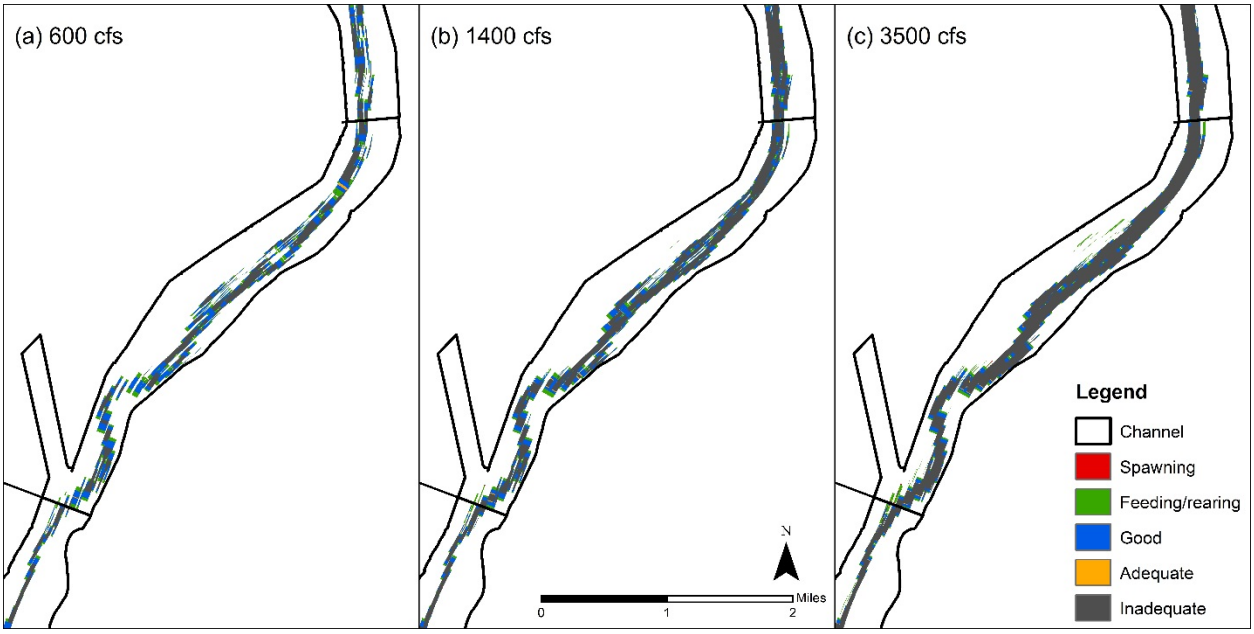
(a) 600 cfs
(b) 1400 cfs
(c) 3500 cfs
N
0
1
2
Miles
Legend
Channel
Spawning
Feeding/rearing
Good
Adequate
Inadequate

B) 2002

I1

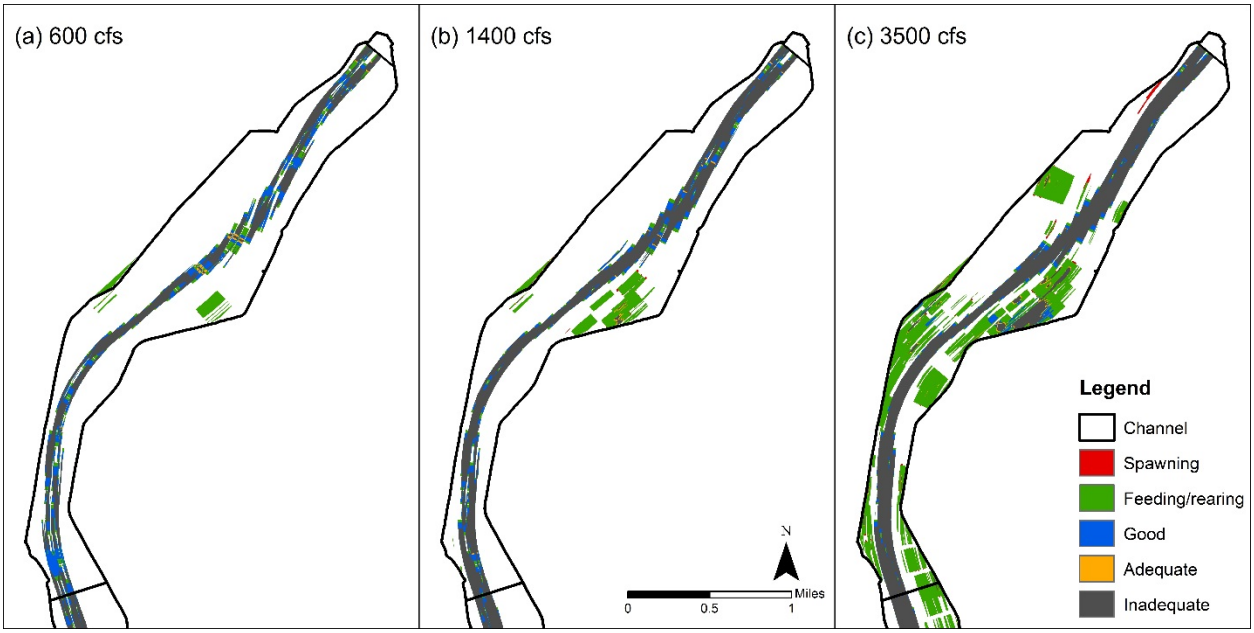
(a) 600 cfs
(b) 1400 cfs
(c) 3500 cfs
N
Miles
0
0.5
1
Legend
Channel
Spawning
Feeding/rearing
Good
Adequate
Inadequate

I2

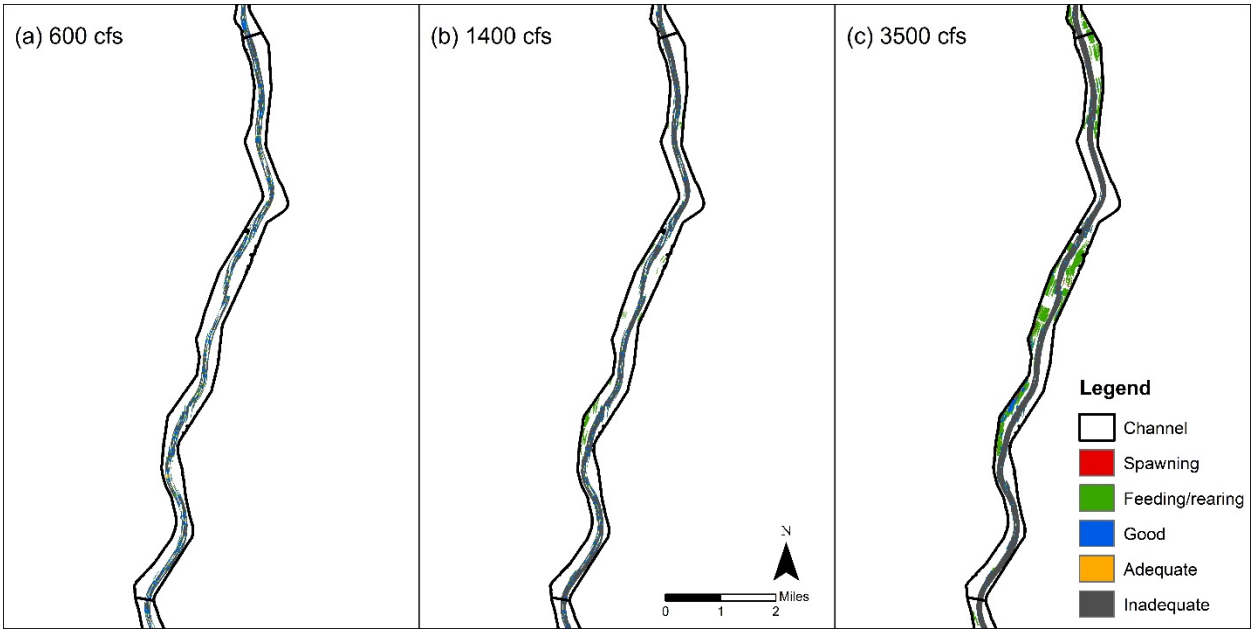
(a) 600 cfs
(b) 1400 cfs
(c) 3500 cfs
N
Miles
0
1
2
Legend
Channel
Spawning
Feeding/rearing
Good
Adequate
Inadequate

I3

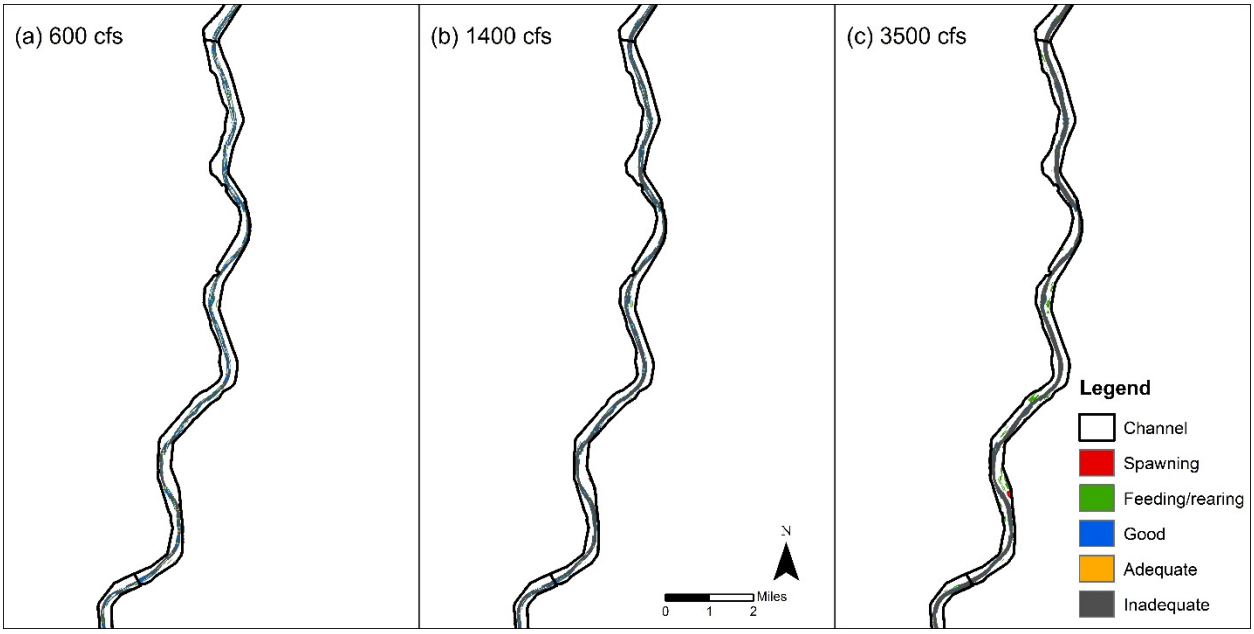
(a) 600 cfs
(b) 1400 cfs
(c) 3500 cfs
N
Miles
0 1 2
Legend
Channel
Spawning
Feeding/rearing
Good
Adequate
Inadequate

I4

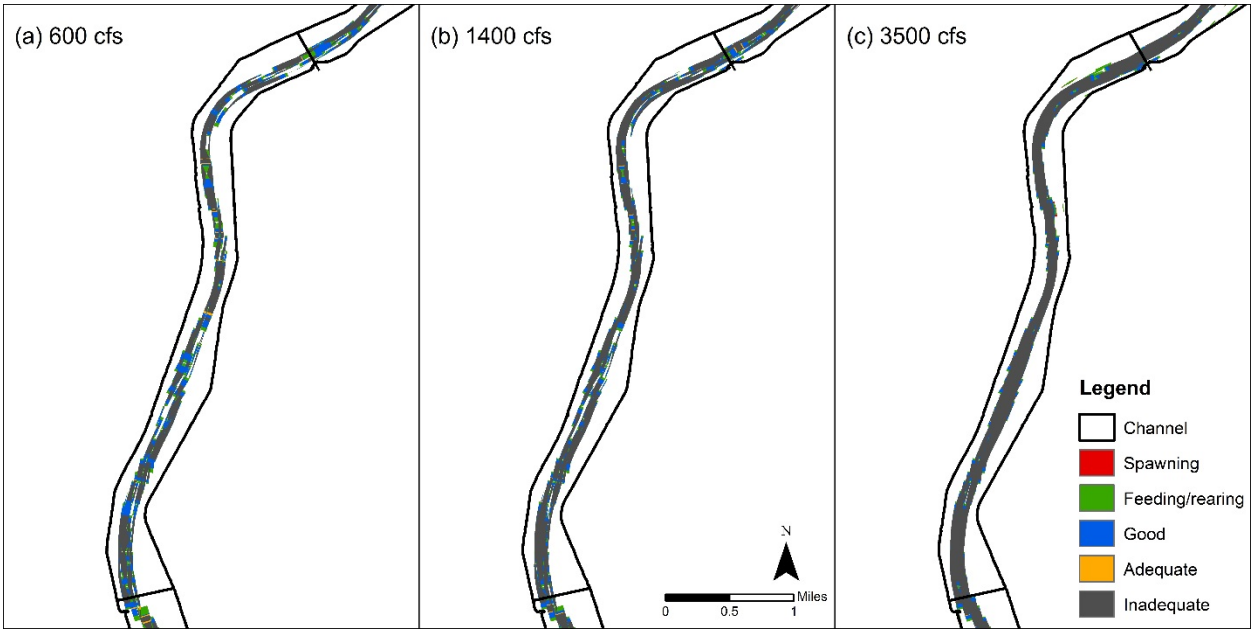
(a) 600 cfs
(b) 1400 cfs
(c) 3500 cfs
N
Miles
0 0.5 1
Legend
Channel
Spawning
Feeding/rearing
Good
Adequate
Inadequate

I5

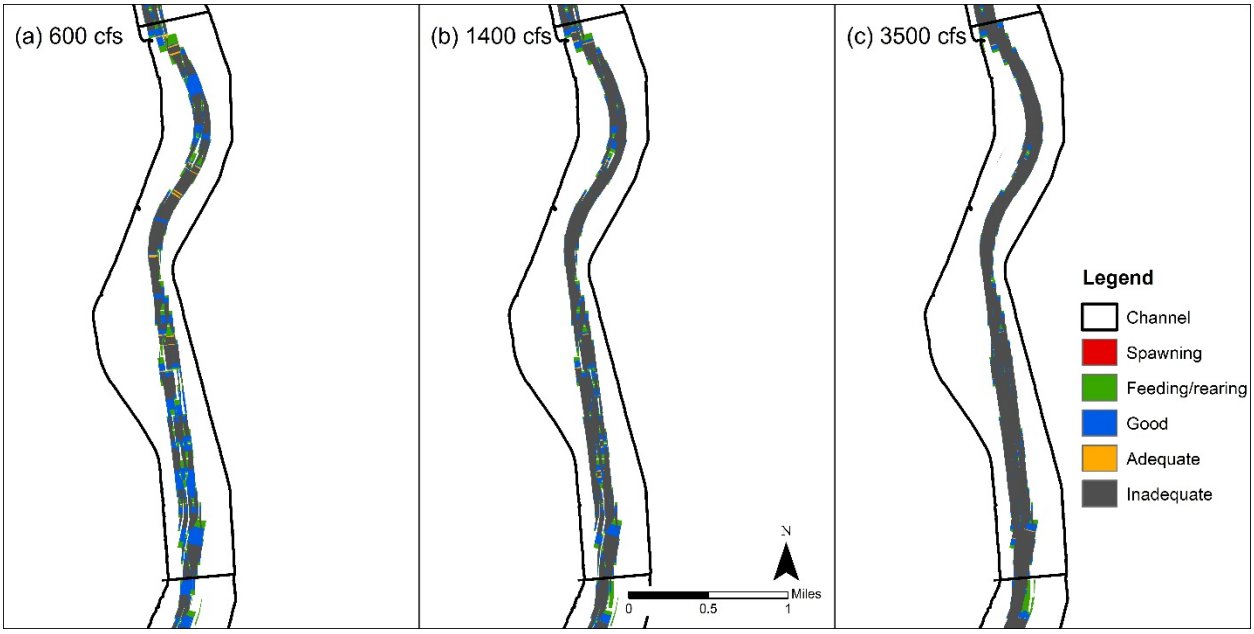
(a) 600 cfs
(b) 1400 cfs
(c) 3500 cfs
N
0
0.5
1
Miles
Legend
Channel
Spawning
Feeding/rearing
Good
Adequate
Inadequate

I6

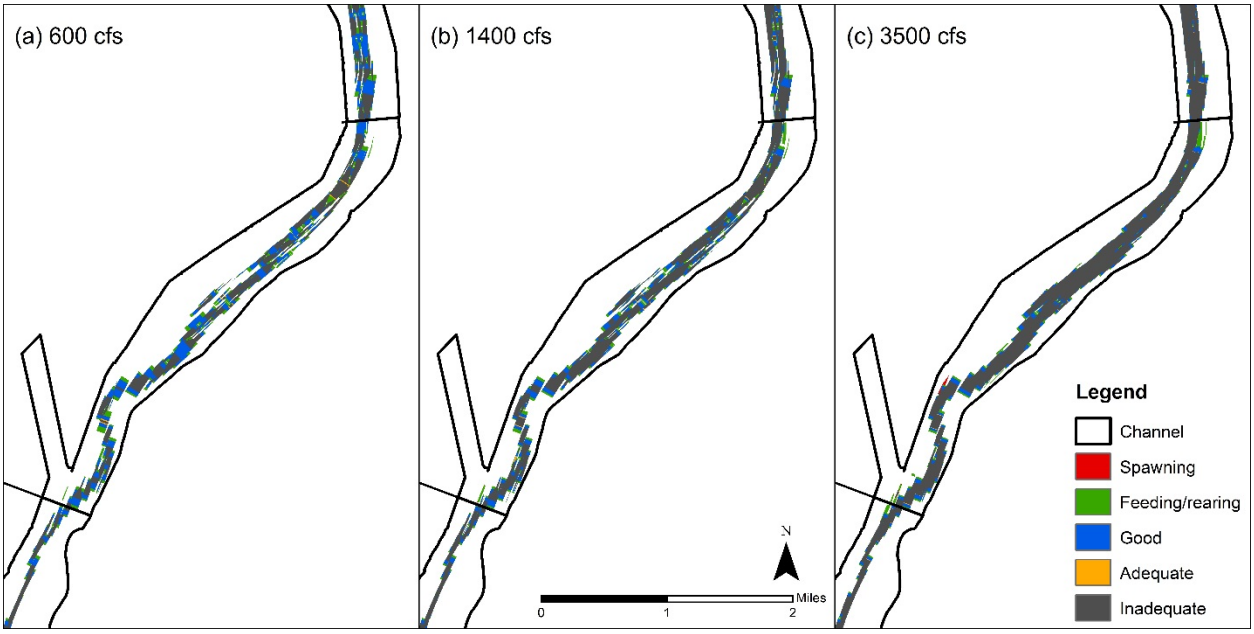
(a) 600 cfs
(b) 1400 cfs
(c) 3500 cfs
N
0
1
2
Miles
Legend
Channel
Spawning
Feeding/rearing
Good
Adequate
Inadequate

C) 2012

I1

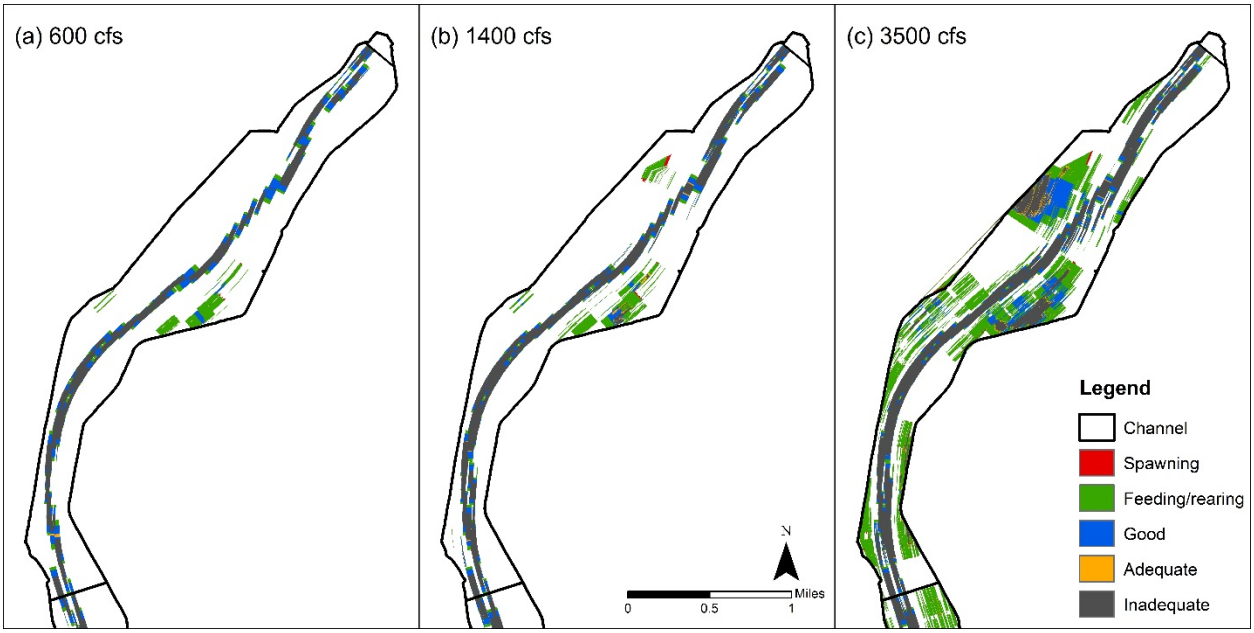
(a) 600 cfs
(b) 1400 cfs
(c) 3500 cfs
N
Miles
0
0.5
1
Legend
Channel
Spawning
Feeding/rearing
Good
Adequate
Inadequate

I2

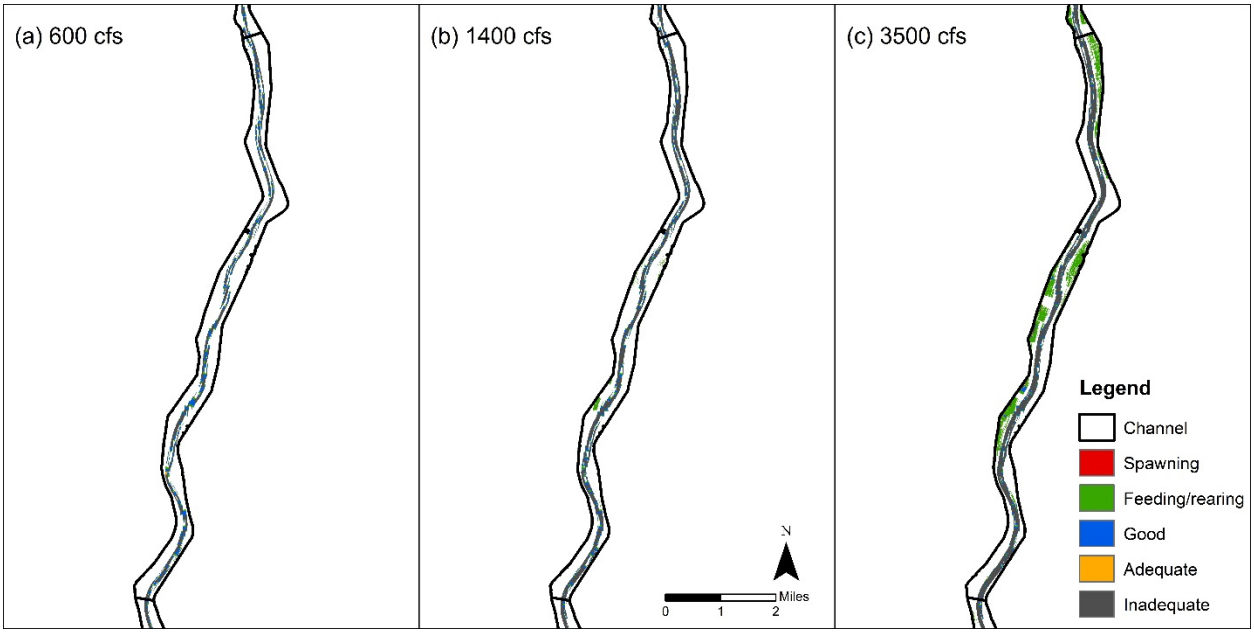
(a) 600 cfs
(b) 1400 cfs
(c) 3500 cfs
N
Miles
0
1
2
Legend
Channel
Spawning
Feeding/rearing
Good
Adequate
Inadequate

I3

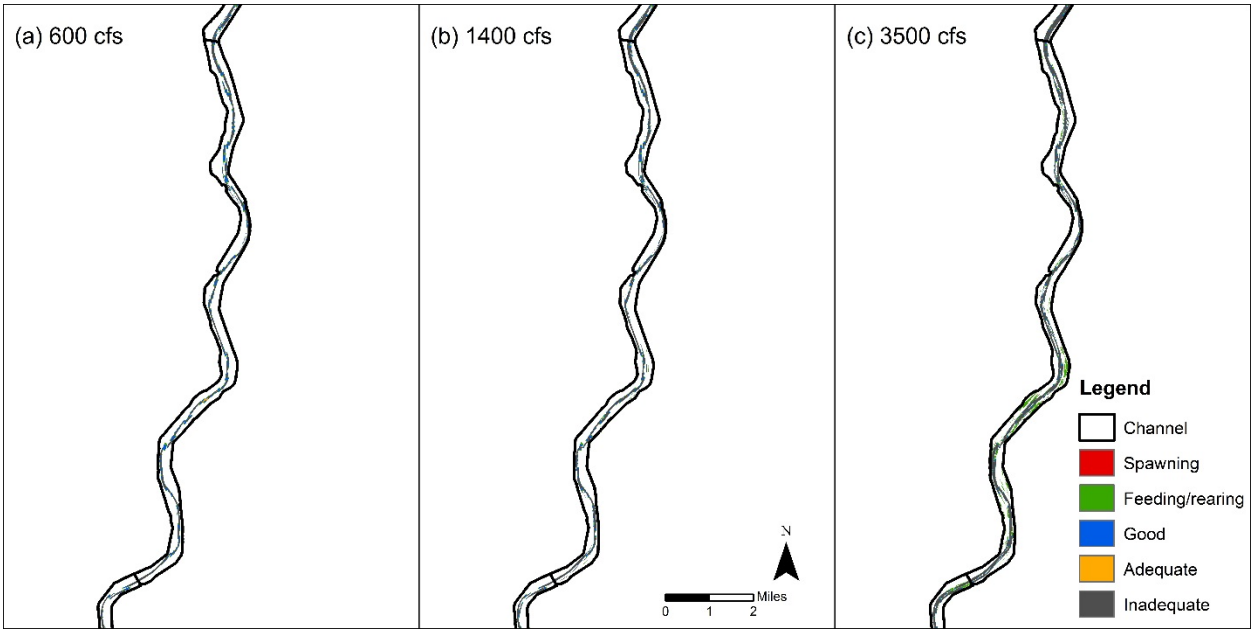
(a) 600 cfs
(b) 1400 cfs
(c) 3500 cfs
N
Miles
0 1 2
Legend
Channel
Spawning
Feeding/rearing
Good
Adequate
Inadequate

I4

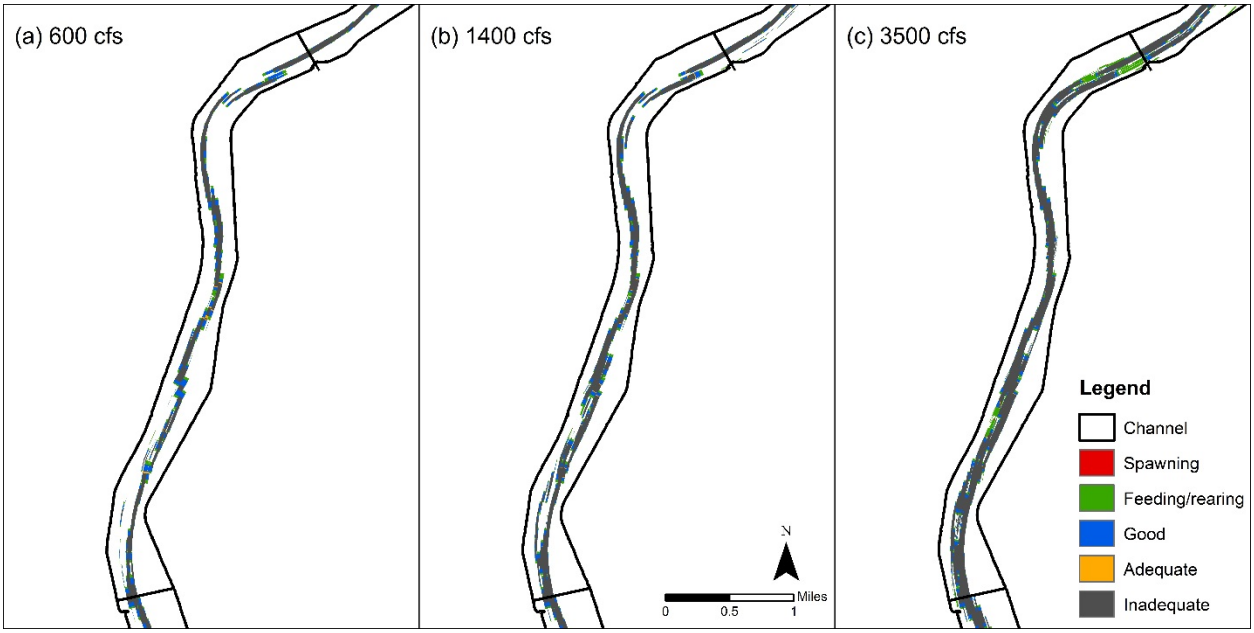
(a) 600 cfs
(b) 1400 cfs
(c) 3500 cfs
N
Miles
0 0.5 1
Legend
Channel
Spawning
Feeding/rearing
Good
Adequate
Inadequate

I5

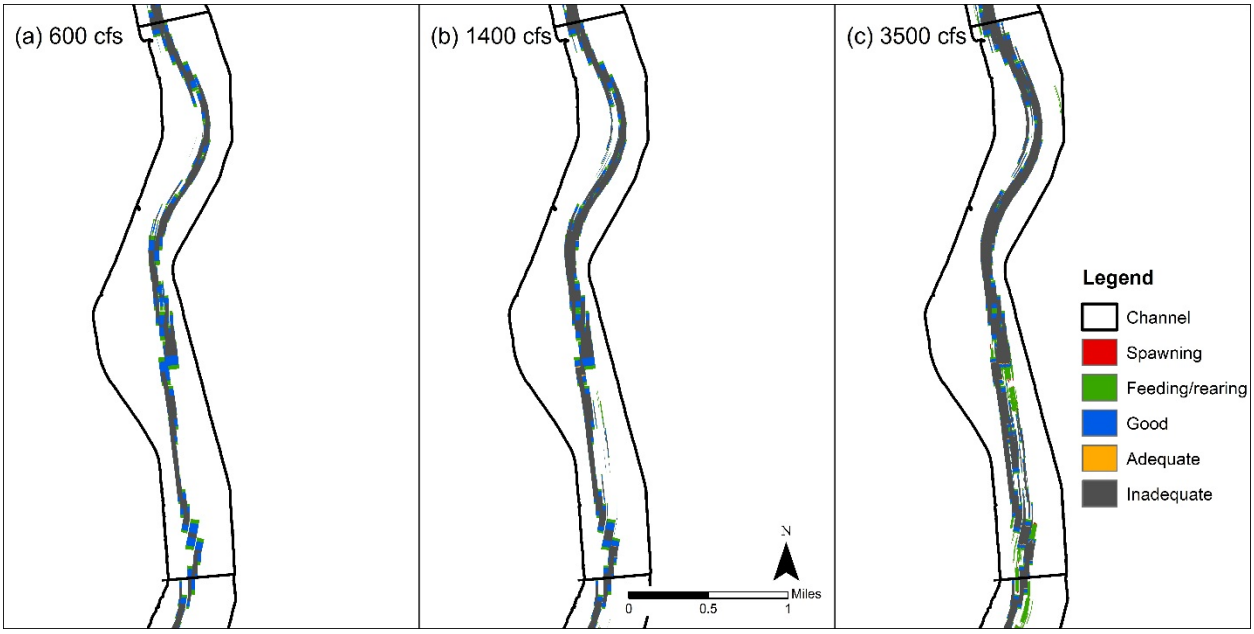
(a) 600 cfs
(b) 1400 cfs
(c) 3500 cfs
N
0
0.5
1
Miles
Legend
Channel
Spawning
Feeding/rearing
Good
Adequate
Inadequate

I6

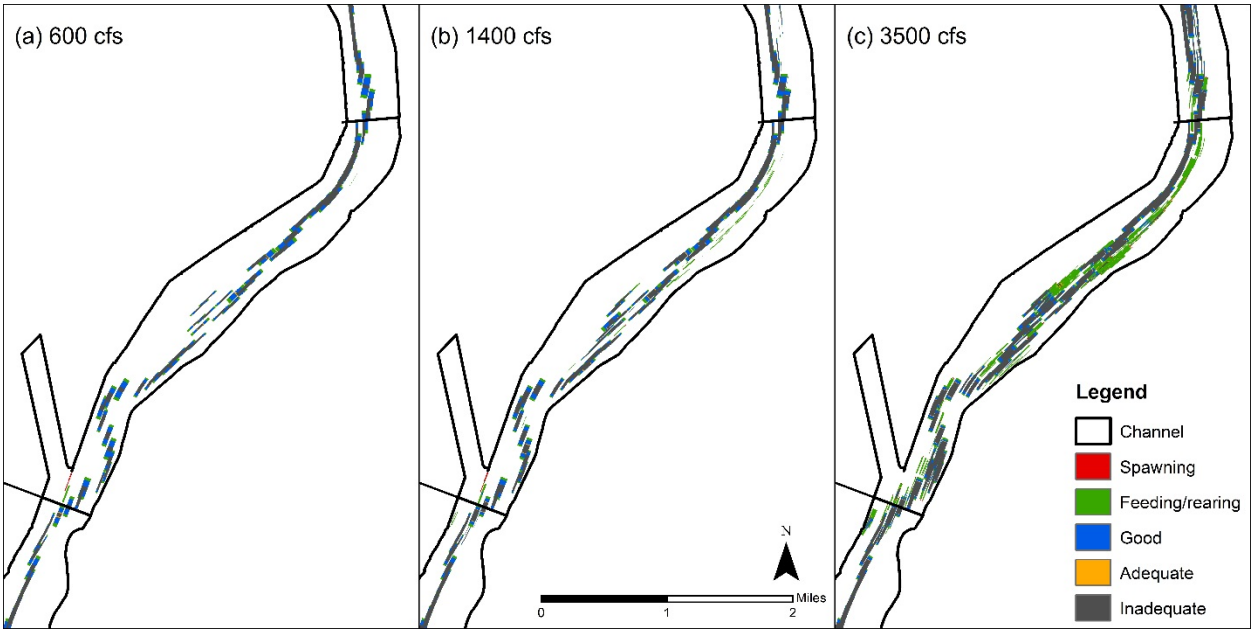
(a) 600 cfs
(b) 1400 cfs
(c) 3500 cfs
N
0
1
2
Miles
Legend
Channel
Spawning
Feeding/rearing
Good
Adequate
Inadequate

Appendix B - Habitat Criteria

Bankline complexity:

*Bankline complexity criteria*

| | |
|---|---|
| 1a. Bankline juts out greatly, forms a small inlet, is rocky or has diverse substrate (vegetated islands, sandy banks and water inundating some parts of the bank). Provides a great amount of habitat, potentially causes eddies. |  |
| 1b. Bankline juts out or caves in slightly and is somewhat diverse. Provides some amount of habitat. |  |
| 1c. Possible access to more complex shoreline during higher flows (outside of active channel so it is less accessible) |  |

*Bankline complexity scores*

| | Shoreline Complexity | | |
|---|---|---|---|
| **Criteria** | 1a | 1b | 1c |
| **Score** | 4 | 3 | 2 |

Complex margins, or shorelines, are very important for silvery minnow habitat because they cause lower velocities, eddies, and shallower waters (Bovee et al. 2008). 1a has the most

complex shoreline with inlets, channels that cause eddies, lower velocities, and diverse water levels. This is not classified as backwater because backwater has a more definite channel away from the main flow. Backwater is also more isolated from the main channel, so it would have lower velocities and would score higher than 1a. 1b offers a refuge, yet it is a simple inlet and the area of complexity is not as large as 1a, so it counts for less habitat points than 1a. 1c is even less diverse and gets the lowest score for bankline complexity. It has the potential to become inundated and provide habitat, but is less accessible than bankline in the active channel. Most banklines analyzed have an active channel outline (provided by USBR) that matches with the water surface. In 2016 though, the water surface is much lower than the active channel so channel complexity is based on the active channel outline instead of the water surface.

Main Channel Complexity:

The clarity and quality of aerial photographs varies across years, within the reaches, and between different flow conditions. This makes it hard to analyze small features of the habitat criteria across the years of photographs provided. For instance, debris piles and bedforms can only be distinguished in highest quality photographs from 2016. The figure below shows the difference in quality of the photographs.

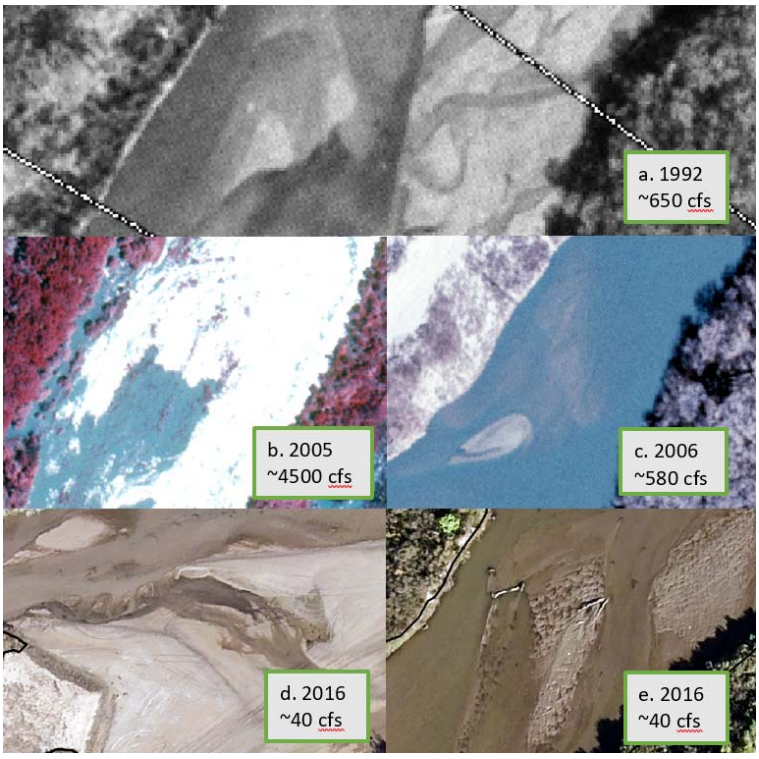


*A set of aerial photography that shows the differences in close up quality. The zoom in each picture is as follows: a. 1:1000, b. 1:1500, c. 1:800, d. 1:600, e. 1:500). 1992 zoomed away by twice as much as 2016 gives a much more pixilated image than in 2016. 2016 has much better resolution even compared to 2006 (and 2008 which is not depicted here). 2005 has areas where light is reflecting off the water that makes it difficult to see what is happening in the channel. It also depicts the variability of flows and how that affects what is seen.*

Therefore, lumping together features that require close up analysis that create main channel complexity is necessary. These features include bedforms, low flow complexity, substrate or formations causing shallow waters, and debris piles.

All of these images vary by a great amount, but they all depict low flow features that are diverse so they could all be identified as the same criteria (2a). Counting these smaller features together does not change the overall score very much because they all serve similar purposes of creating complex flow, eddies, and shallower waters. For example, in 2016 (2d.) more of the river is exposed, so it appears much more complex at a low flow. 2e. is in a higher flow area, yet has debris piles and beforms that cause ripples which could be suitable as well. In the bottom left corner of 2b. and center of 2c. images, bedforms or low geologic features could be the result of what is seen. These look like shallow and physically diverse areas, so they receive a high suitability score as well. In 1992, the complexity is hard to see at a small scale, but shallow areas with various geomorphic features can still be identified.

*Main channel complexity criteria*

| | |
|---|---|
| 2a. Large debris piles/low-flow complexity in the main channel (possibly braided). Large substrate/ formations create shallow depths | 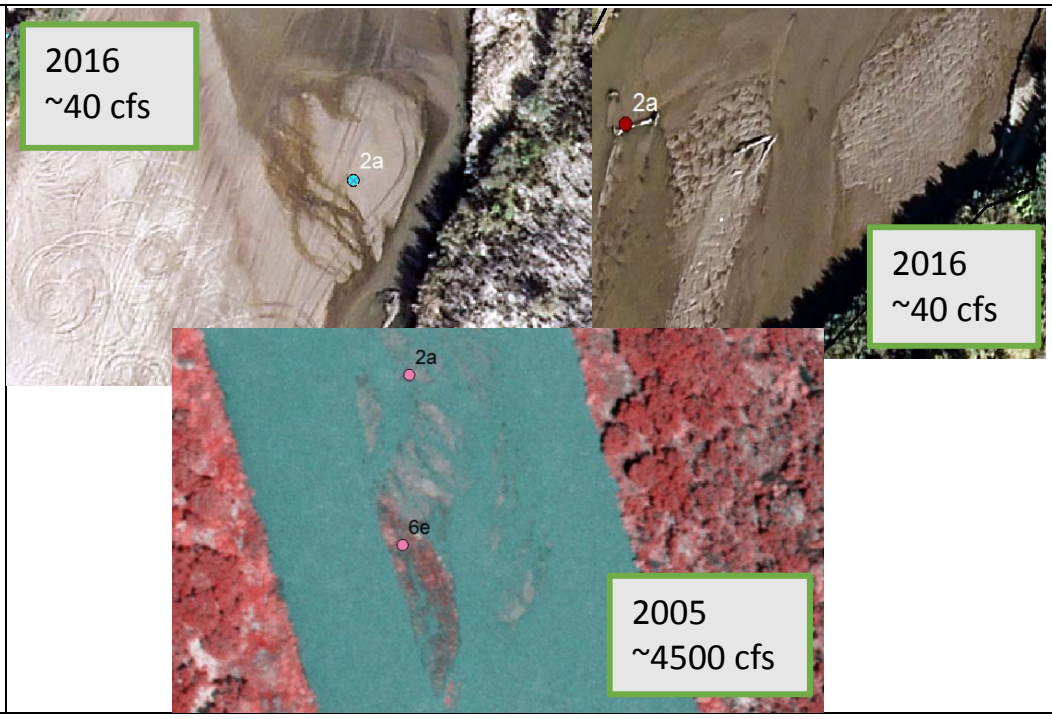 |

| | |
|---|---|
| 2b. Small to Medium sized debris piles/low-flow complexity in main channel. Medium substrate/ formations create shallow depths | 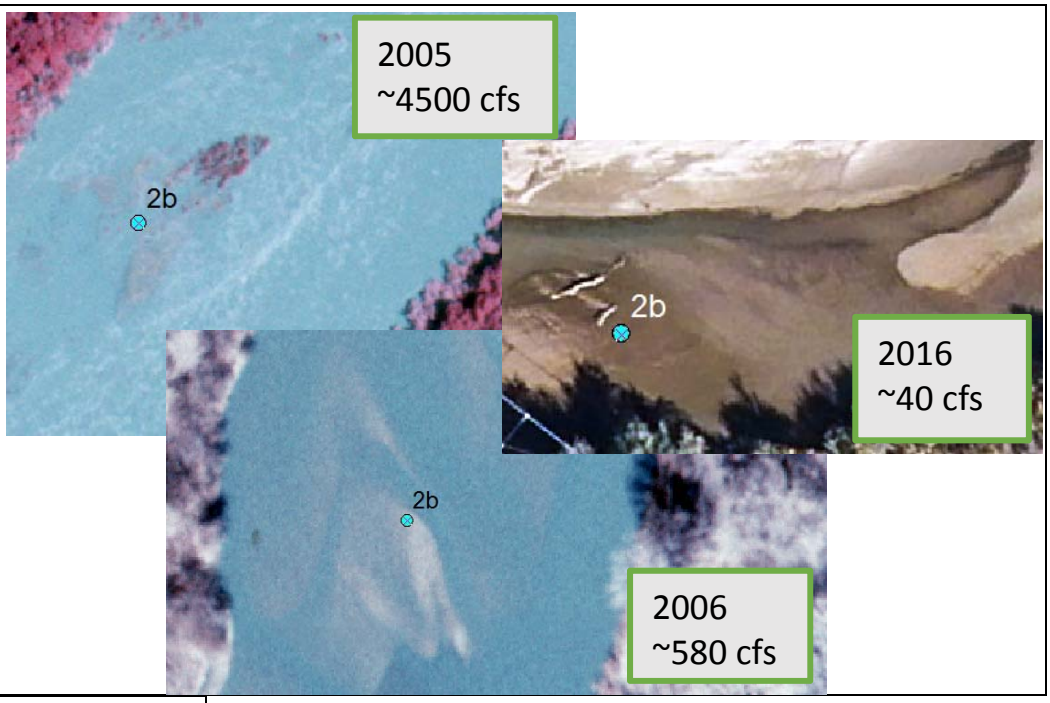 |

| | Main Channel Complexity | |
|---|---|---|
| **Criteria** | 2a | 2b |
| **Score** | 4 | 3 |

*Main channel complexity scores*

In-channel complexity, extensive debris piles, bedforms and formations are depicted in above. Bedforms, channel complexity and debris piles all offer suitable habitat for fish (Bovee et al., 2008, Cluer, Thorne 2013, Tetra Tech, 2014). Therefore, main-channel complexity scores are relatively height. In 2b, there are images of debris piles and substrate formations that are less extensive as those depicted in 2a figures. Because both 2a and 2b are in the main channel that experiences higher velocities, the scores are not as high as backwater or complex side channels. They are still high because they offer refuge to silvery minnows when side channels or backwaters are not accessible at high flows. 2a is given one more point that 2b because it is bigger and generally more complex than 2b.

*Note: 2a is differentiated from an island or mid channel bar based on level of inundation. If the island is underwater so much that it is broken up into too many formations to count, or there is not an obvious continuous stretch of land, it is counted as substrate/formations.

Side channels:

*Side channels criteria*

| | |
|---|---|
| 3a. Dry bed- 3+ parallel side channels are in active channel. Channels appear accessible and wide | 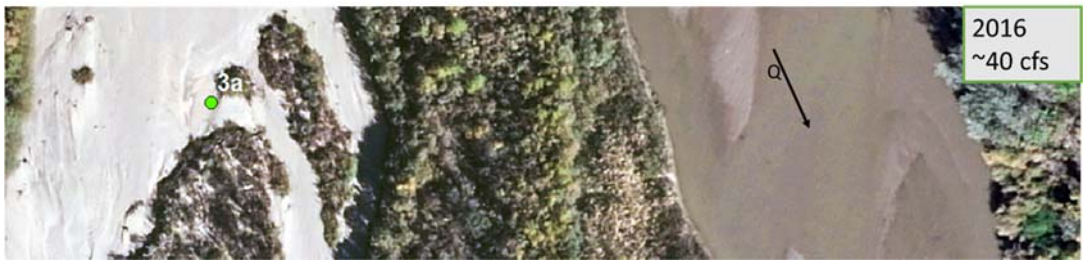 |
| 3b. Dry bed- 1-2 side channels are in active channel and appear accessible- wide (50 + feet) | 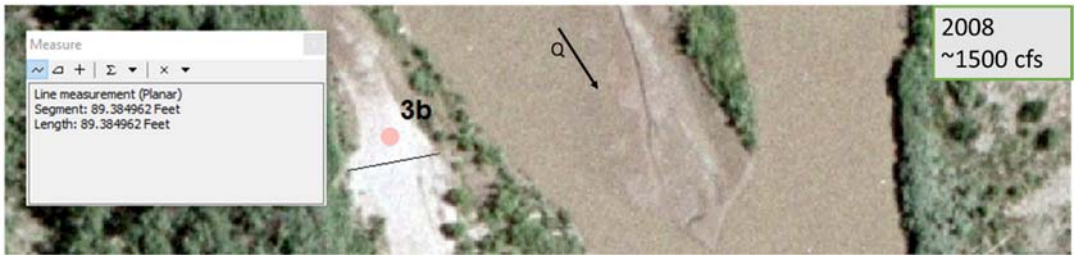 |
| 3c. Dry bed- 1-2 side channels are in active channel and appear accessible- narrow or not as accessible | 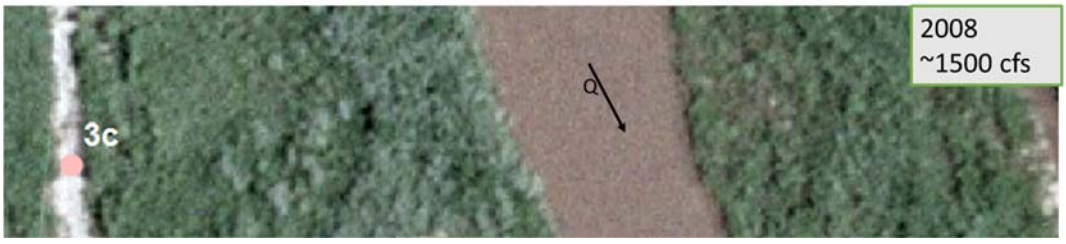 |

| | |
|---|---|
| 3d. Wet channel- simple and generally not braided- single threaded channel |  |
| 3f. Wet channel- Side channels are complex and winding (may cause eddies and slower flows). 2+ channels- braided | 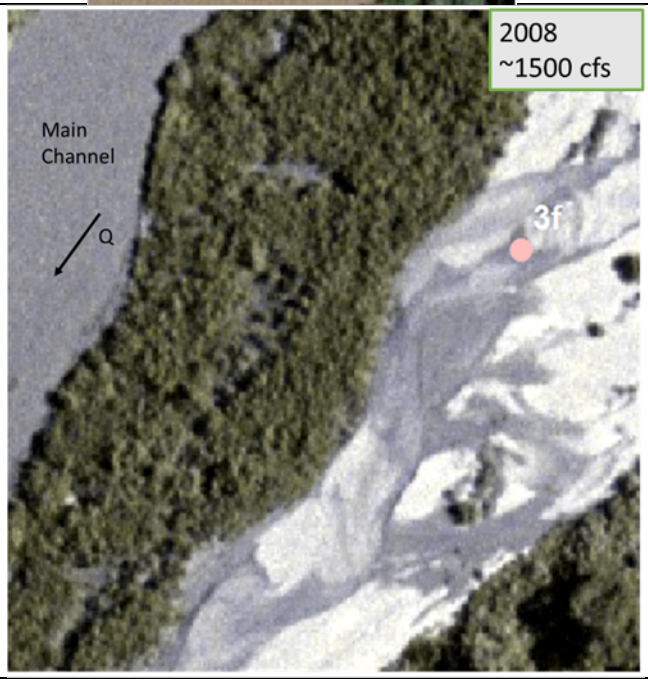 |

*Side channels score*

| | Side Channels | | | | |
|---|---|---|---|---|---|
| **Criteria** | 3a | 3b | 3c | 3d | 3f |
| **Score** | 4 | 3 | 2 | 3 | 5 |

A report by Tetra Tech found that complex, braided and anastomosing channels provide the best habitat suitability for silvery minnows (Tetra Tech 2014). Therefore, the more complex and accessible the side channel is, the greater the habitat score. For instance, 3f has the highest score because it has braided features that create eddies and low velocity flows. 3f is also underwater, so it is proven to be accessible. The next highest ranked is 3a because it is the most complex of the dry channels. If the river gets a large flow, this area could become inundated

and create shallow, low velocity complex channels for silvery minnows to occupy (3a-3d and 3f are within the active channel delineated by USBR). Next, 3b and 3d are all ranked the same. 3b provides habitat during higher flows, but is less complex and accessible than 3a channels. 3d is ranked similarly because while it is more accessible, there are higher velocities and deeper depths at higher flows. Finally, 3c offers the least suitable habitat because the channels are narrower than 3b channels. The more narrow the less habitat area. Also, 3c is narrower because there is a higher density of vegetation, which indicates that this area is less likely to become inundated and provide habitat. Overall, side channels are given relatively high scores because they are essential for high flow situations when the silvery minnow needs to be connected to more diverse areas with slower velocities.

Areas that can become inundated at very high flows are disregarded because they are too hard to analyze the areas beyond the active channel from year to year. The dry channels are identified by being within the active channel. Areas that could become inundated beyond the active channel are too subjective to analyze. For instance, the density of vegetation and previous years of flow areas give an idea of what channels could potentially become inundated. Using LiDAR data also helps with the analysis, but there is only LiDAR available for 2012. This makes analyzing areas that could be inundated in other years inconsistent. Even though potential channels for inundation are highly important for the life cycle of silvery minnows, there is not enough data to effectively analyze them. If there were aerial photographs compared across years that had the same high flow that inundate the floodplain, temporal trends in habitat could be analyzed.

As Middle Rio Grande has become more and more incised over time and peak flows are reducing, the availability of the floodplain habitat is greatly decreasing over the years (Tetra Tech 2014). Because the analysis is focused on the main channel for adult silvery minnows (all that can be analyzed across years at about 650 cfs), channels accessible during a large flood are not considered. This channel would be called 3e, but was removed from the analysis.

*Note: 3f could be confused with 1a because it is near the shoreline. They are differentiated because 3f is generally a complete, yet braided, channel with many offshoots. 1a does not have continuous flow through that section and does not take the form of a channel. 3f is generally more extensive than 1a.

Hydraulic backwater:

*Hydraulic backwater criteria*

| | |
|---|---|
| 4a. Backwater extending back > 100 ft, wide and appear accessible |  |
| 4b. Backwater extending back < 100 ft, not as accessible or wide |  |

*Hydraulic backwater scores*

| | Backwater | |
|---|---|---|
| **Criteria** | 4a | 4b |
| **Score** | 5 | 4 |

The backwater is determined by the active channel outline provided by USBR. In the figures depicting 4a and 4b, the water does not actually flow in these channels, yet it has been delineated as a place where water would normally flow. Backwaters are an essential component of silvery minnow habitat because they provide very low velocities that are near zero. The backwaters are especially important for larvae and juvenile silvery minnows when they first hatch and grow (Bovee et al. 2008). 4a is much larger than 4b so it provides more suitable habitat, and therefore receives a higher score.

Bank-attached bars:

*Bank-attached bars criteria*

| | |
|---|---|
| 5a. Bar is large and provides shallow channels and complex habitat | 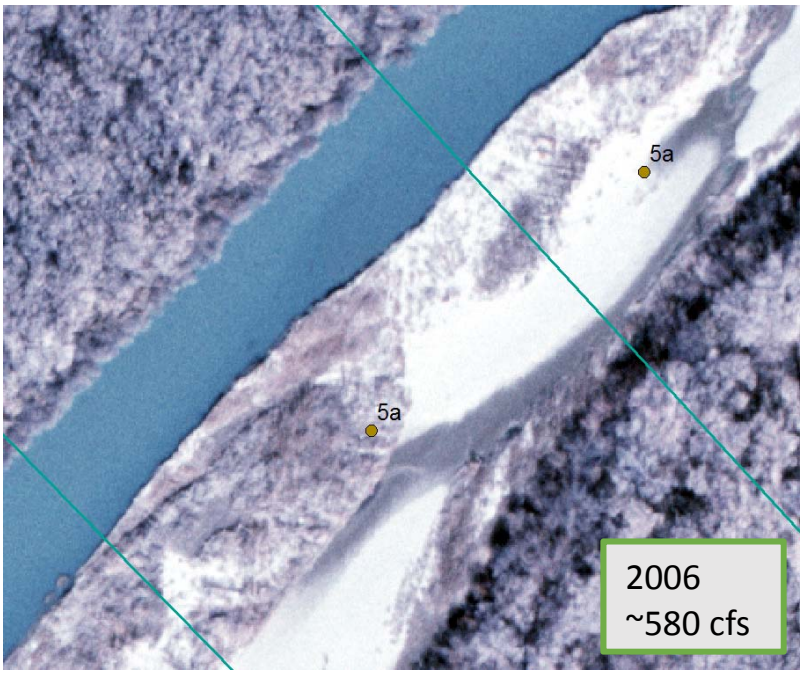 |
| 5b. Bar is small and provides some silvery minnow habitat (some vegetation) | 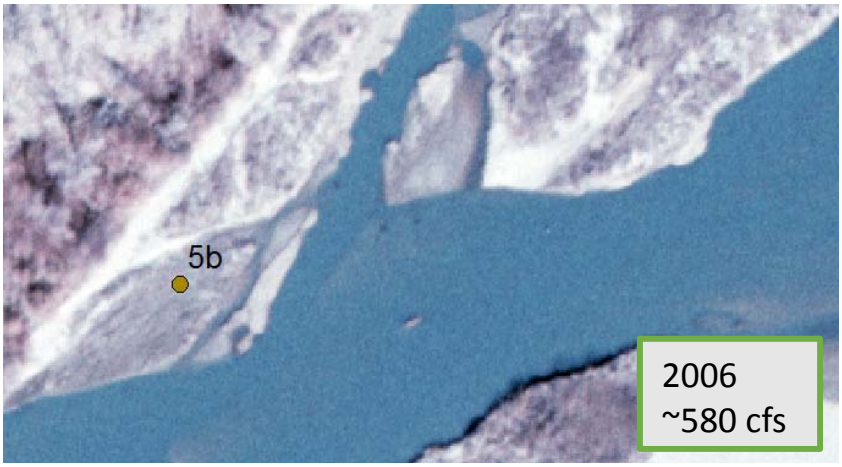 |

| | |
|---|---|
| 5c. Non-vegetated bar with little geomorphic variability |  |

*Bank-attached bars scores*

| | Bars | | |
|---|---|---|---|
| **Criteria** | 5a | 5b | 5c |
| **Score** | 4 | 2 | 1 |

Bars provide some habitat during high flows, yet they do not provide extensive spawning areas for silvery minnows. Because bank-attached bars are not very complex in their topography, only the most complex and extensive structural features provide in-channel habitat. Even when their complexity is evident and may provide some in channel habitat for adults, this does not always translate into optimum spawning habitat (Tetra Tech 2014). Bars still provide important habitat features during higher flows because they offer shallower habitat than the main channel if they become inundated so they are given a relatively high score. The more complex the bar, the more suitable the habitat is for silvery minnows. For instance, 5a is generally characterized by having more complex geomorphic features, small side channels or vegetation that would provide lower velocity areas and shelter from predators (Cluer and Thorne 2014). 5a is similar to 1a (shoreline complexity), so they must be differentiated. 5a is identified as being much larger and wider than 1a. 5b has less of these features, and 5c does provide overall shallower habitat at higher flows, yet it adds little topographic complexity to the habitat.

Islands/Mid-channel Bars:

*Islands/mid-channel bar criteria*

| | |
|---|---|
| 6a. Large and non-vegetated<br>6c. Small and non-vegetated | 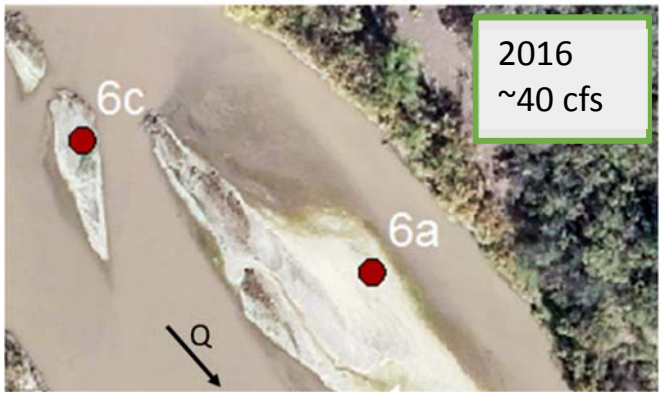 |
| 6b. Large and vegetated<br>6d. Small and vegetated | 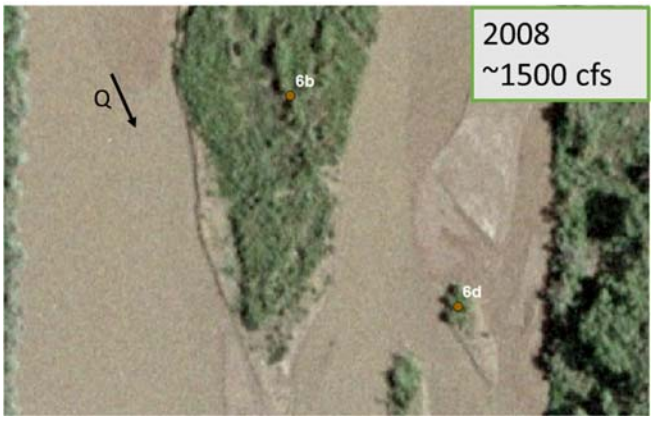 |
| 6e. Large- Some vegetation and some bare ground (Around 50% uniform veg cover over whole island). Could also have shoreline complexity or braided features within island.<br>6f. Small- Some vegetation and some bare ground (Around 50% uniform veg cover over whole island). Could also have shoreline complexity or braided features within island. | 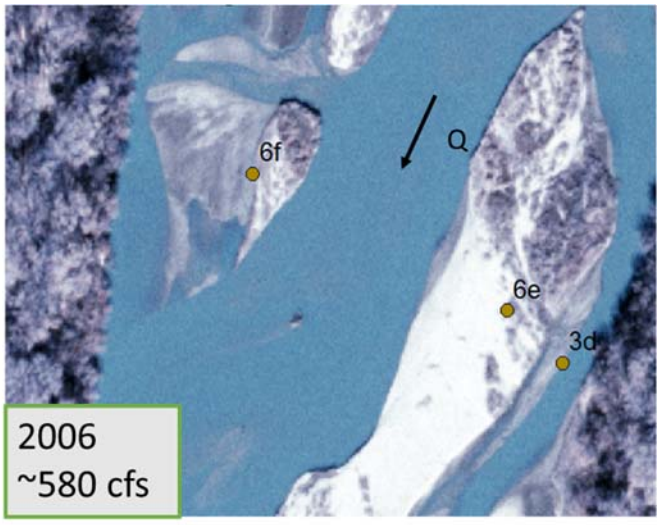 |

*Islands/mid-channel bar scores*

| | Islands | | | | | |
|---|---|---|---|---|---|---|
| **Criteria** | 6a | 6b | 6c | 6d | 6e | 6f |
| **Score** | 3 | 2 | 1 | 1 | 4 | 3 |

Islands in this section area defined as not being attached to the bank and are also referred to as mid-channel bars. An island or mid-channel bar is differentiated from a bank-attached bar based on what it is surrounded by. If there is an obvious, continuous separation from the bar and the shoreline, it is considered an island/mid-channel bar. It can be surrounded by water on both sides, a dry channel on both sides, or water on one side and dry channel on the other. A bank-attached bar has no major side-channels going through it that cause obvious and continuous separation from the bank.

Islands provide habitat to silvery minnows in a similar manner to bank-attached bars. During higher flows, the islands could become partially or fully inundated which helps in-channel habitat, yet is not necessarily most suitable for spawning (Tetra Tech 2014). 6e gets the highest score because it generally has some vegetation, small channels or backwaters within the island providing complex topography and habitat. 6f is a smaller version of 6e so it gets a lower score by one. 6a has no vegetation which indicates it is more accessible at higher flows, and 6b is less accessible because it is densely vegetation. Therefore, 6a has a slightly higher score than 6b. Small islands that are not complex have little to no impact on habitat suitability (Tetra Tech 2014) so these are given the lowest score (6b and 6c). A large island (6a,6b,6e) is considered to reach across one agg/deg polygon, and a small island (6c,6d,6f) spans across half or less of the polygon. Exceptions to this rule may occur when an island is very skinny so it may be considered small instead of large even if it spans across the entire polygon.

Confluences:

*Confluences criteria*

| | |
|---|---|
| 7a. Active confluence- wet | 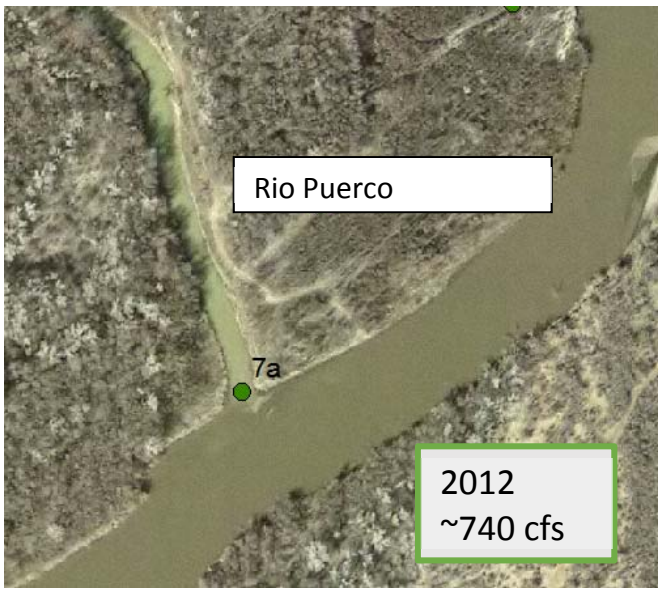 |
| 7b. Active confluence- dry | 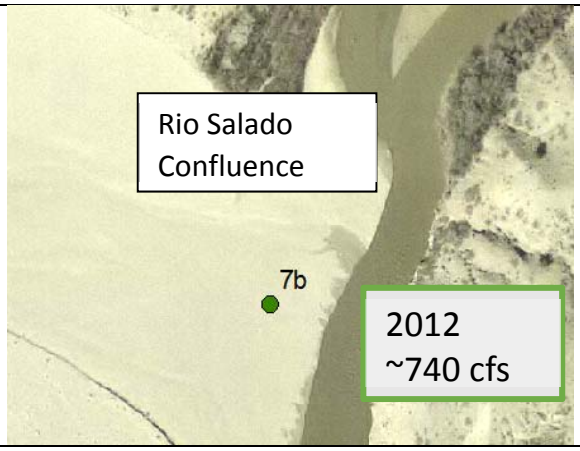 |

*Confluence scores*

| | Wet Confluence | Dry Confluence |
|---|---|---|
| **Criteria** | 7a | 7b |
| **Score** | 4 | 3 |

Confluences are spots where eddies, accelerating and decelerating velocities, sediment deposits, and large wood tend to accumulate. These factors create ecological hotspots (Cluer and Thorne 2014). Confluences are given a relatively high score because of this. If the confluence does not appear to be active or is disconnected from the Rio Grande, it is not included in the analysis. Also, spots where irrigation canals are not counted as confluences because their flow is variable and cannot be compared across years. While these aren't counted as confluences, they are designated as shoreline complexity or backwater depending on how the "irrigation confluence" interacts with the main channel. Wet, active confluences are given a

higher score than dry ones because they provide habitat instead of just channel margin complexity.

Appendix C - Habitat Counts (Years with flows around 650 cfs)

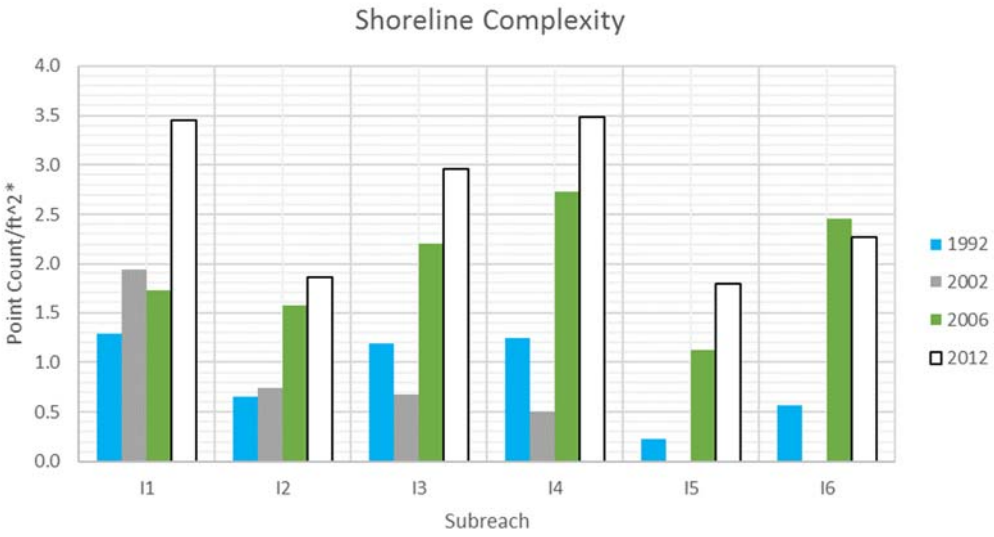


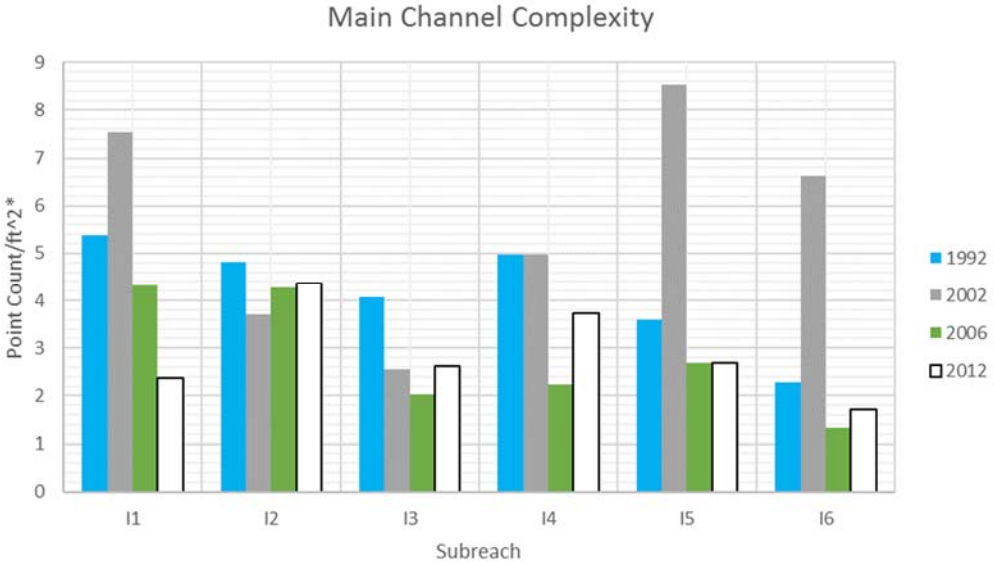

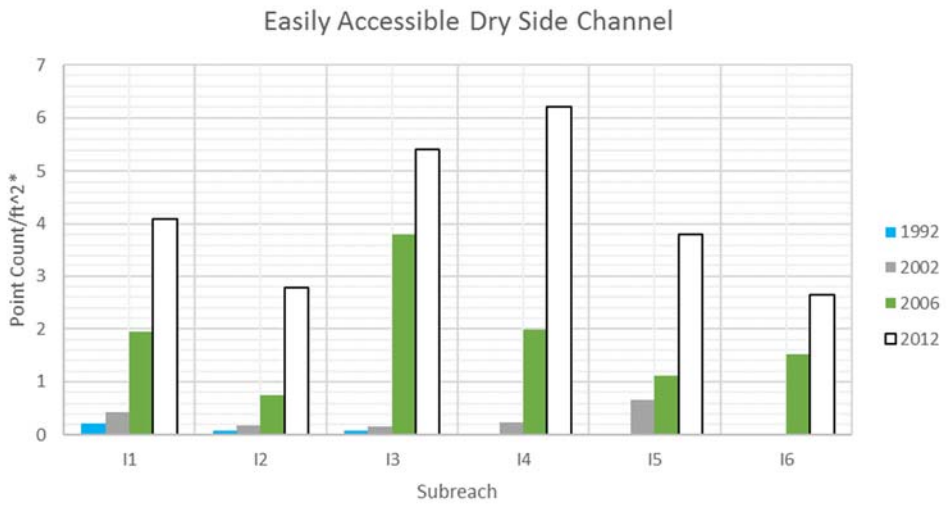
Easily Accessible Dry Side Channel
Point Count/ft^2*
0
1
2
3
4
5
6
7
I1
I2
I3
I4
I5
I6
Subreach
1992
2002
2006
2012

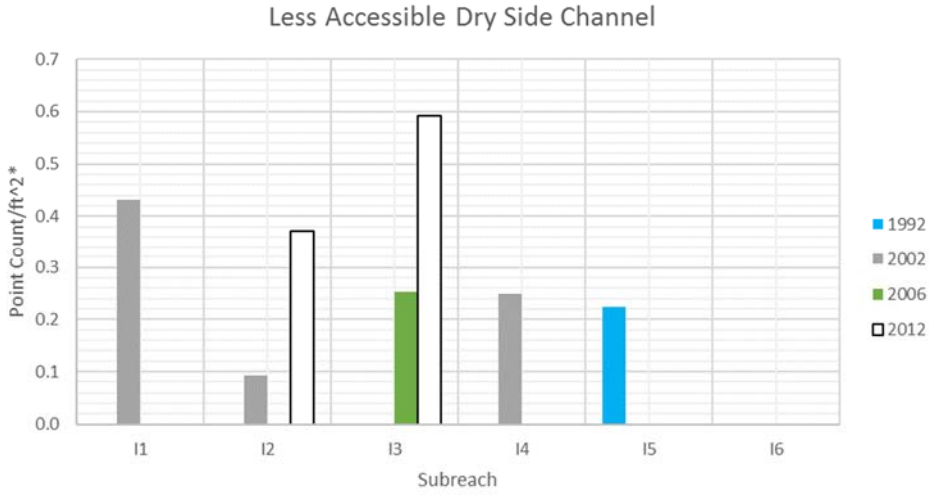
Less Accessible Dry Side Channel
Point Count/ft^2*
0.0
0.1
0.2
0.3
0.4
0.5
0.6
0.7
I1
I2
I3
I4
I5
I6
Subreach
1992
2002
2006
2012

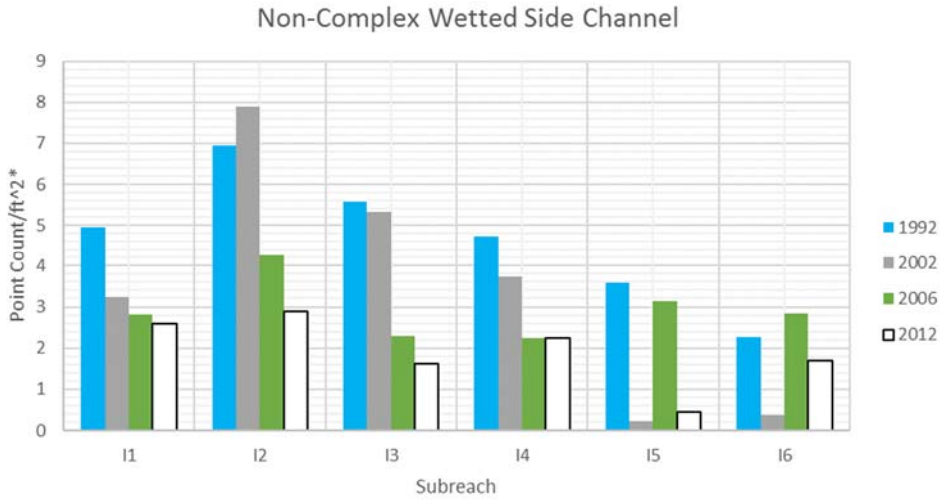
Non-Complex Wetted Side Channel
Point Count/ft^2*
0
1
2
3
4
5
6
7
8
9
I1
I2
I3
I4
I5
I6
Subreach
1992
2002
2006
2012

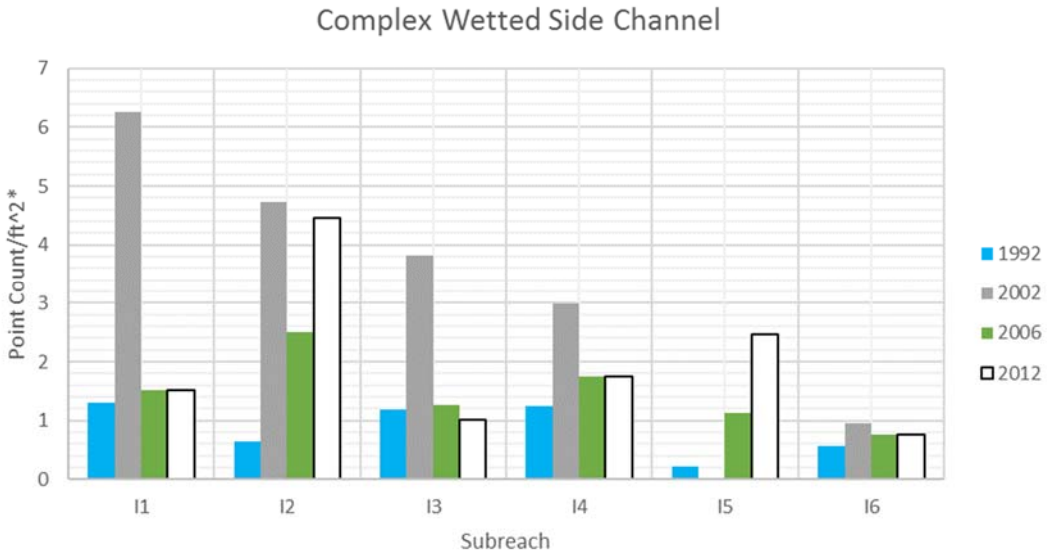
Complex Wetted Side Channel
Point Count/ft^2*
0
1
2
3
4
5
6
7
I1
I2
I3
I4
I5
I6
Subreach
1992
2002
2006
2012

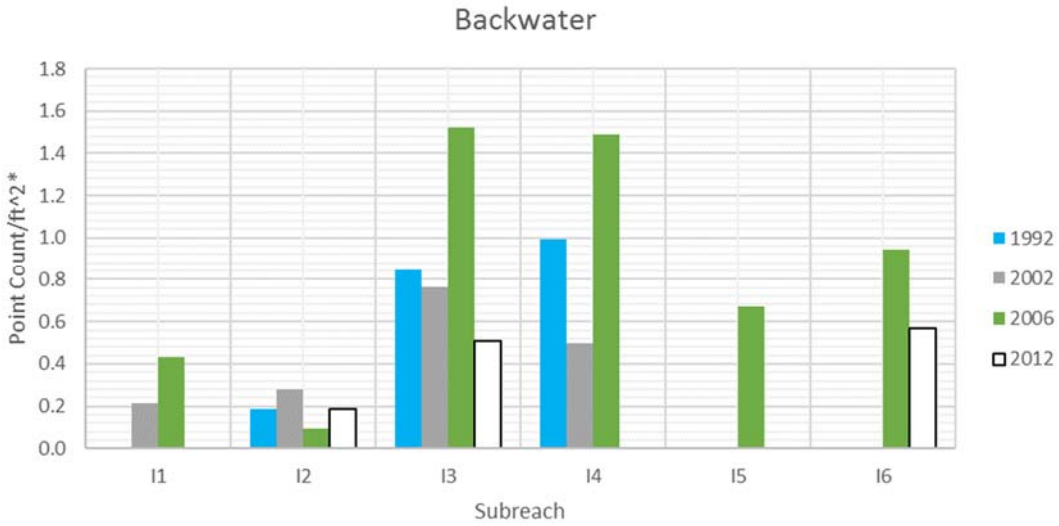
Backwater
Point Count/ft^2*
0.0
0.2
0.4
0.6
0.8
1.0
1.2
1.4
1.6
1.8
I1
I2
I3
I4
I5
I6
Subreach
1992
2002
2006
2012

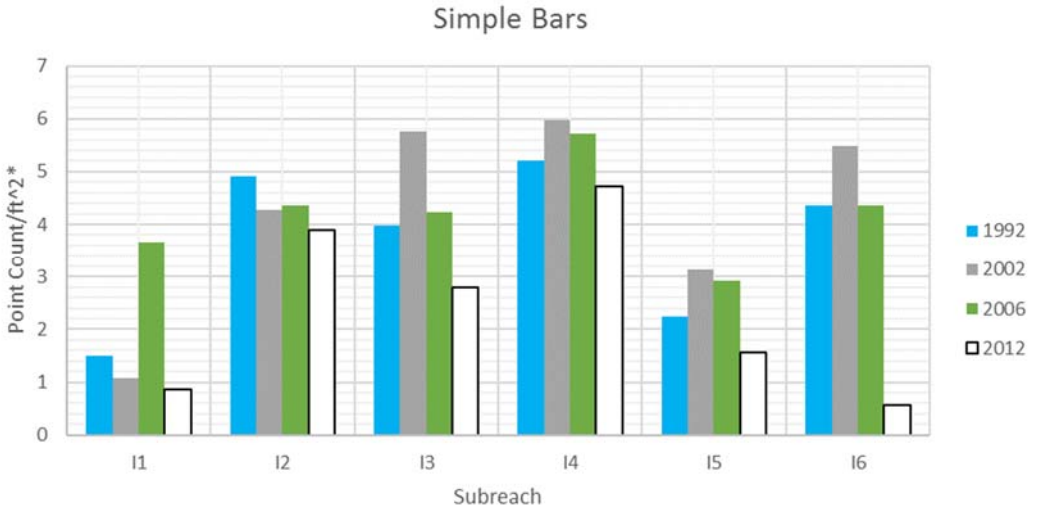
Simple Bars
Point Count/ft^2*
0
1
2
3
4
5
6
7
I1
I2
I3
I4
I5
I6
Subreach
1992
2002
2006
2012

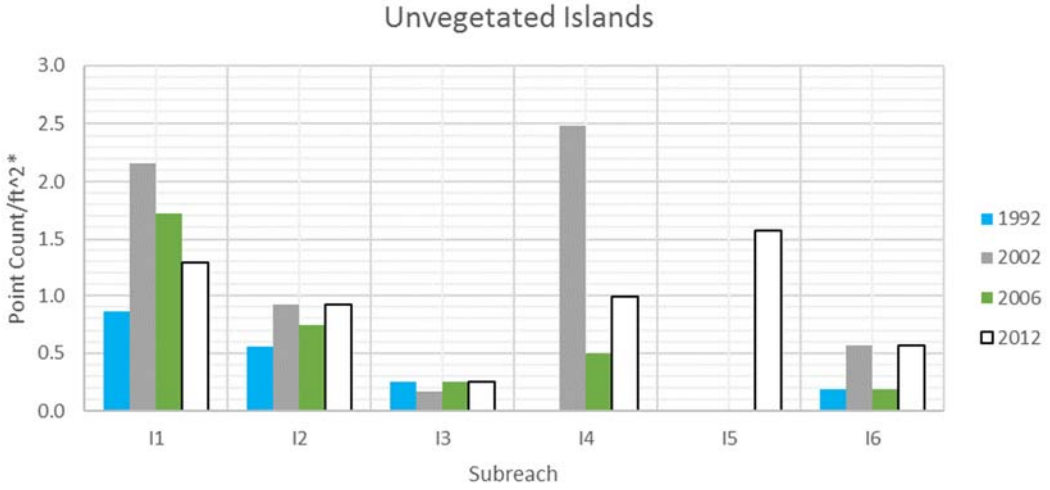
Unvegetated Islands
Point Count/ft^2*
0.0
0.5
1.0
1.5
2.0
2.5
3.0
I1
I2
I3
I4
I5
I6
Subreach
1992
2002
2006
2012

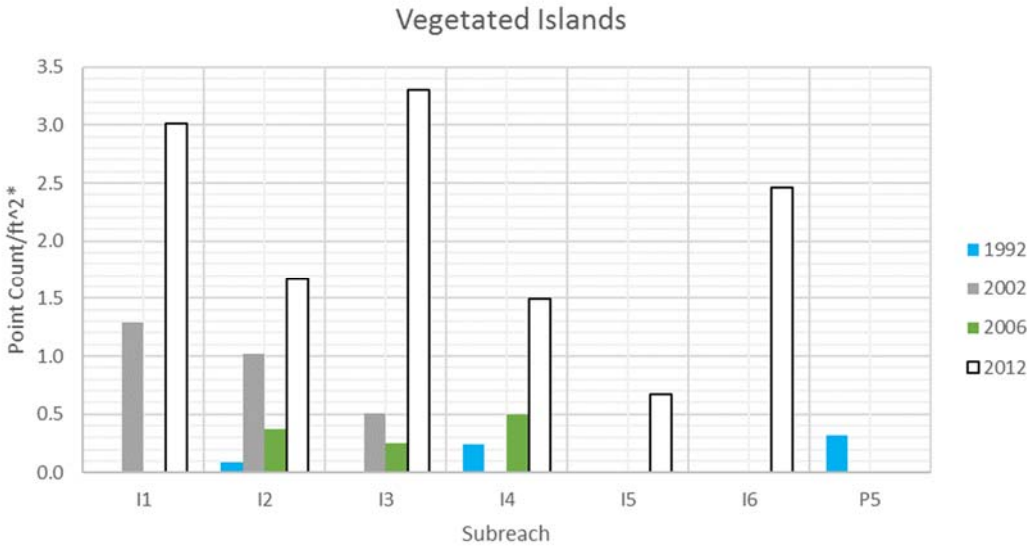
Vegetated Islands
Point Count/ft^2*
3.5
3.0
2.5
2.0
1.5
1.0
0.5
0.0
I1
I2
I3
I4
I5
I6
P5
Subreach
1992
2002
2006
2012

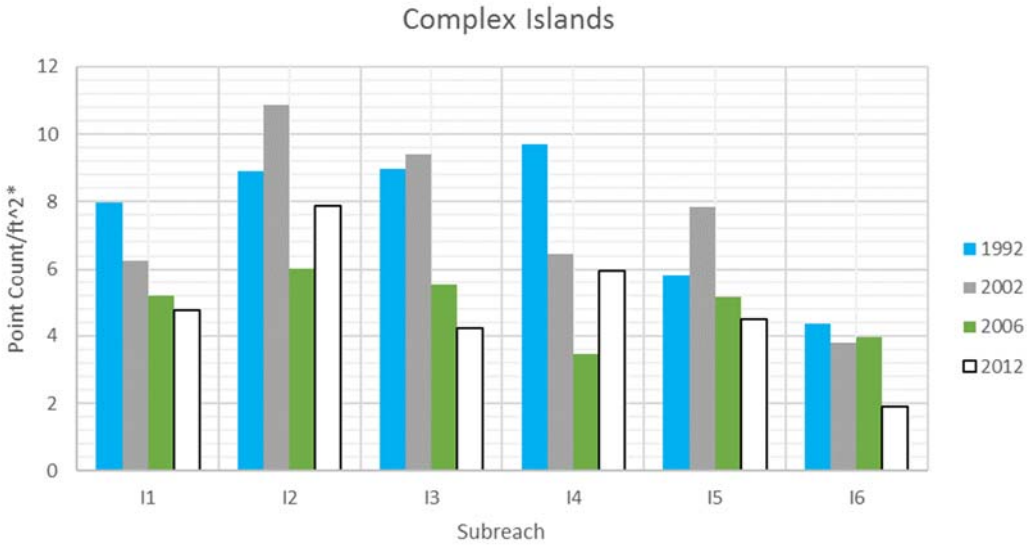
Complex Islands
Point Count/ft^2*
12
10
8
6
4
2
0
I1
I2
I3
I4
I5
I6
Subreach
1992
2002
2006
2012

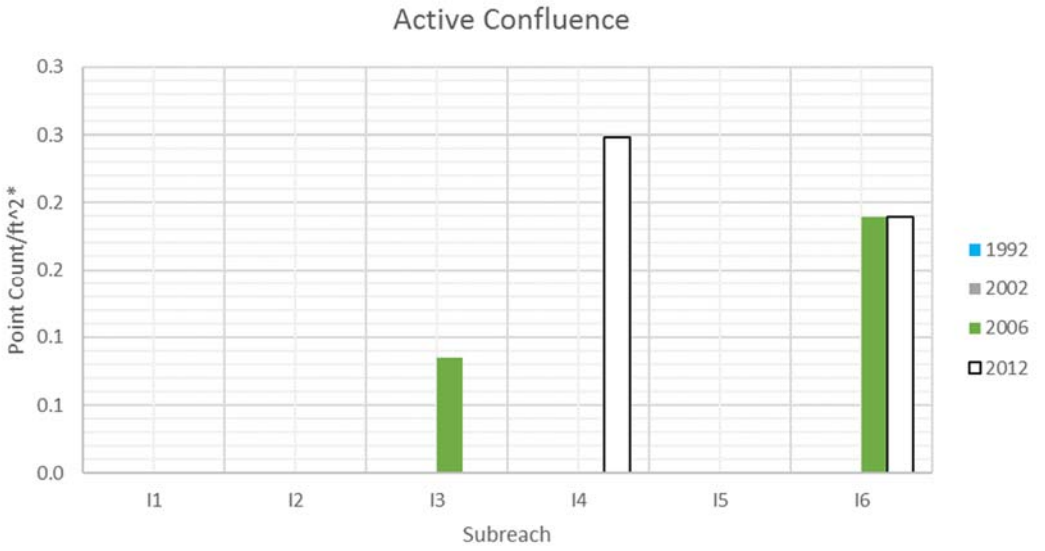
Active Confluence
0.3
0.3
0.2
0.2
0.1
0.1
0.0
Point Count/ft^2*
I1
I2
I3
I4
I5
I6
Subreach
1992
2002
2006
2012

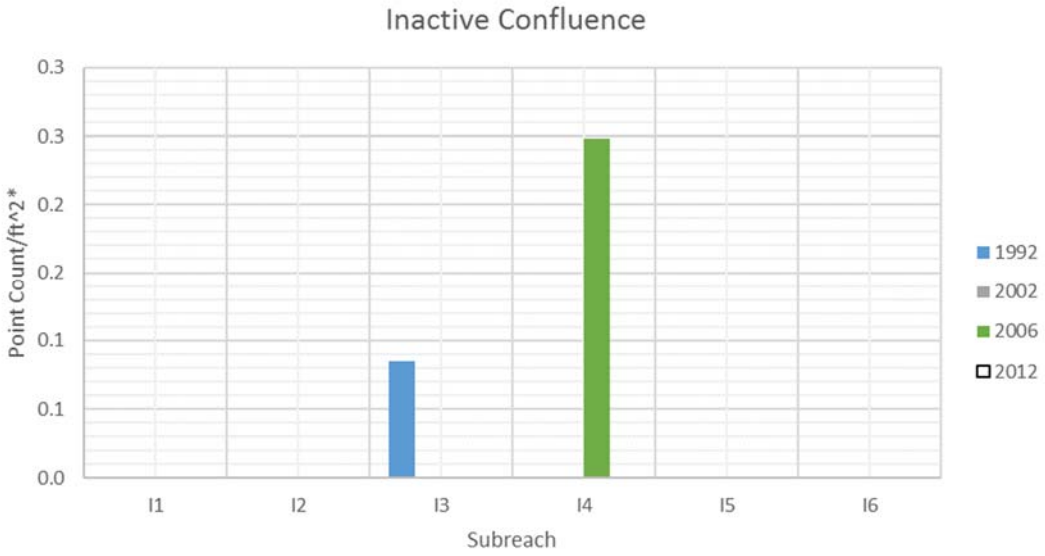
Inactive Confluence
0.3
0.3
0.2
0.2
0.1
0.1
0.0
Point Count/ft^2*
I1
I2
I3
I4
I5
I6
Subreach
1992
2002
2006
2012

## Appendix D - Shoreline Complexity

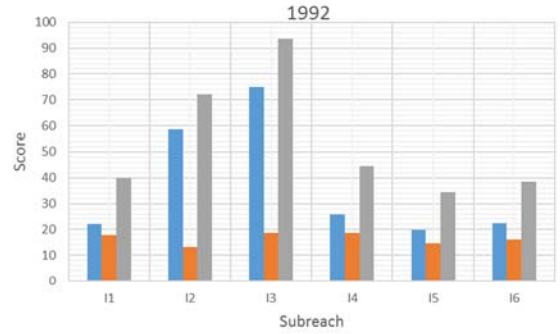


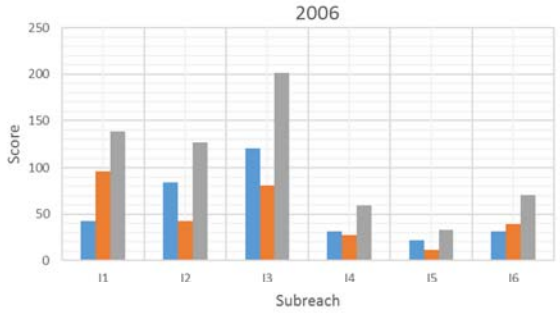


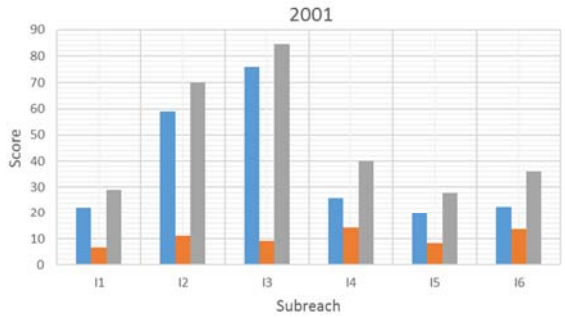


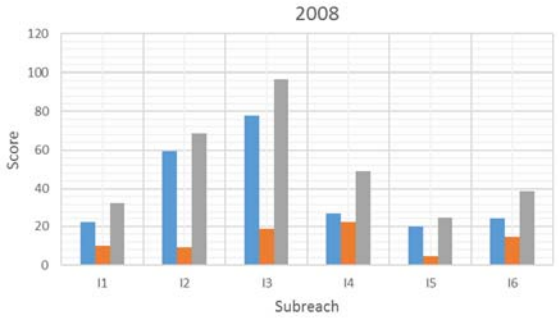


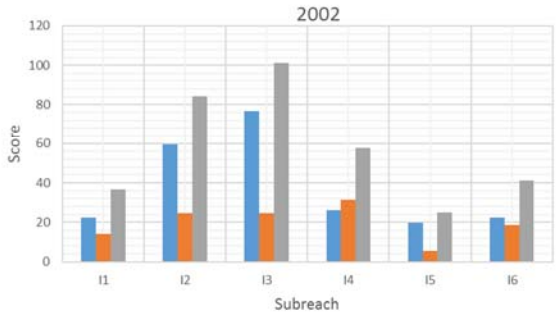


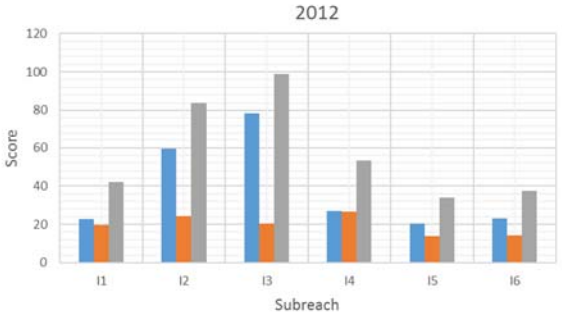


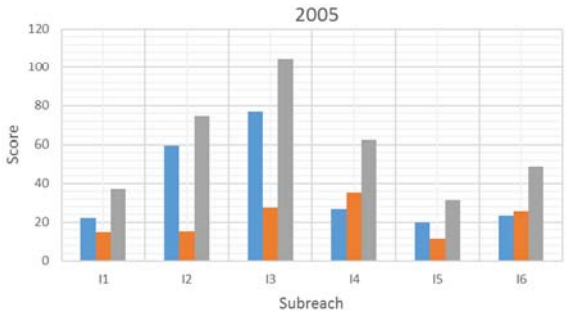


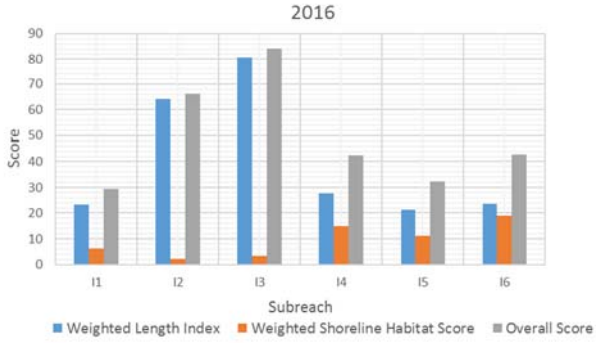

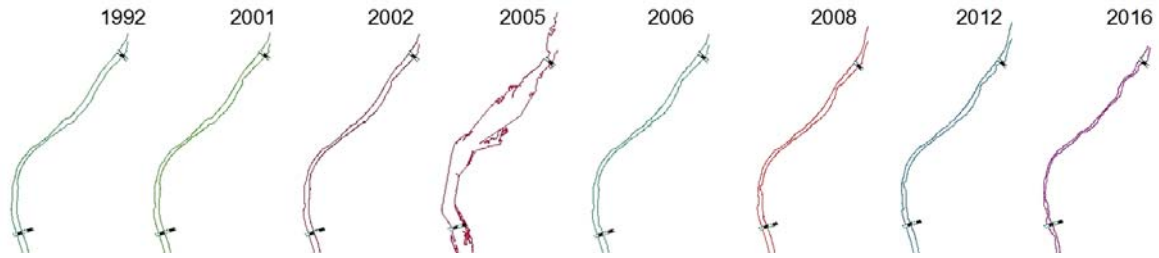
1992
2001
2002
2005
2006
2008
2012
2016

*I1*

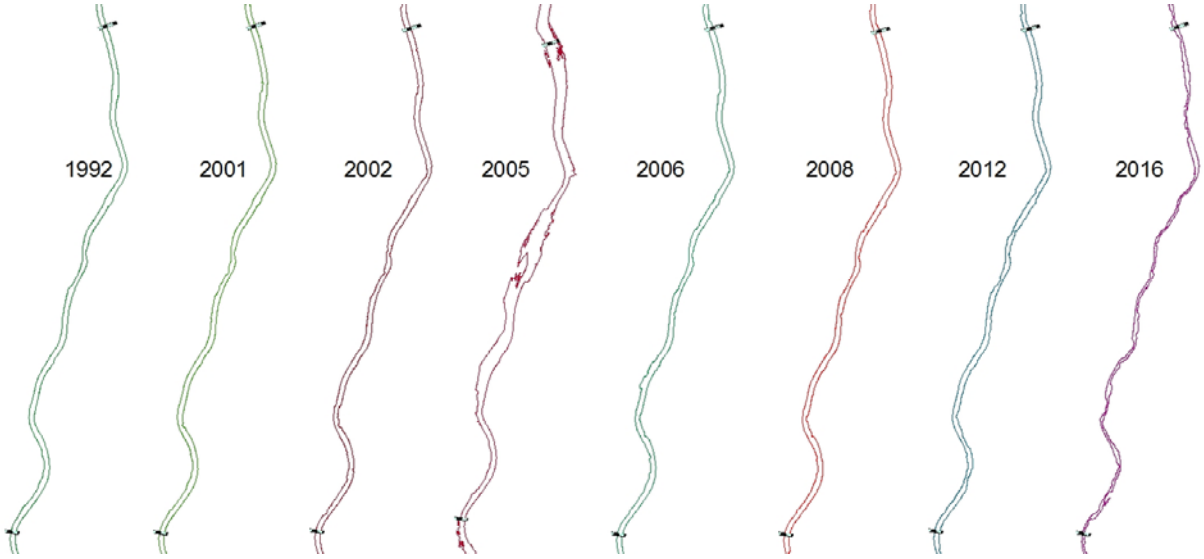
1992
2001
2002
2005
2006
2008
2012
2016

*I2*

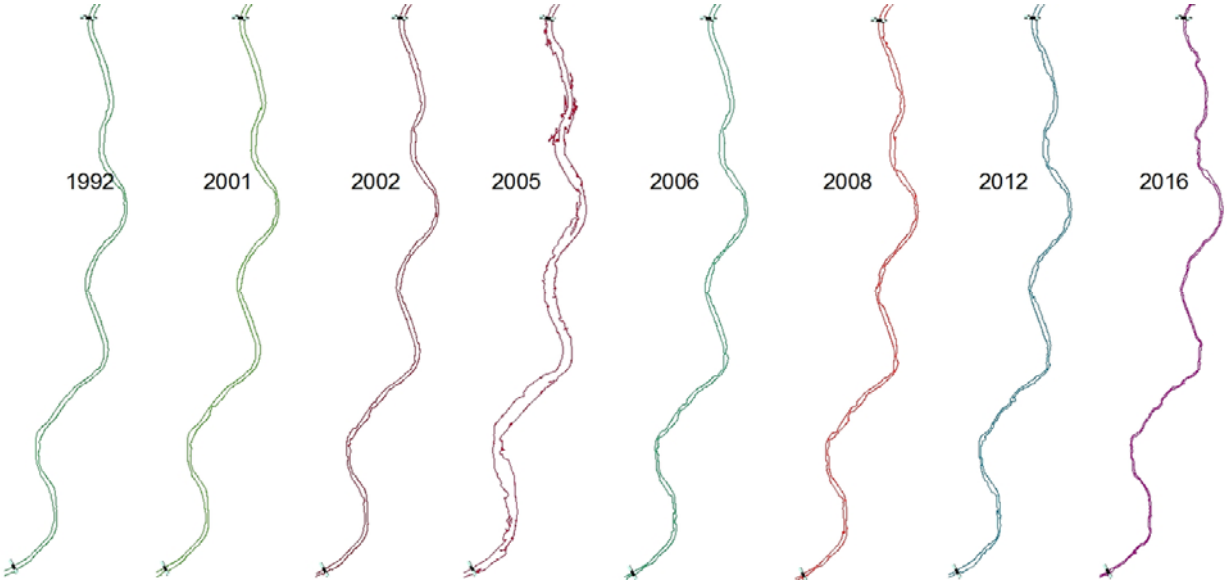
1992
2001
2002
2005
2006
2008
2012
2016

*I3*

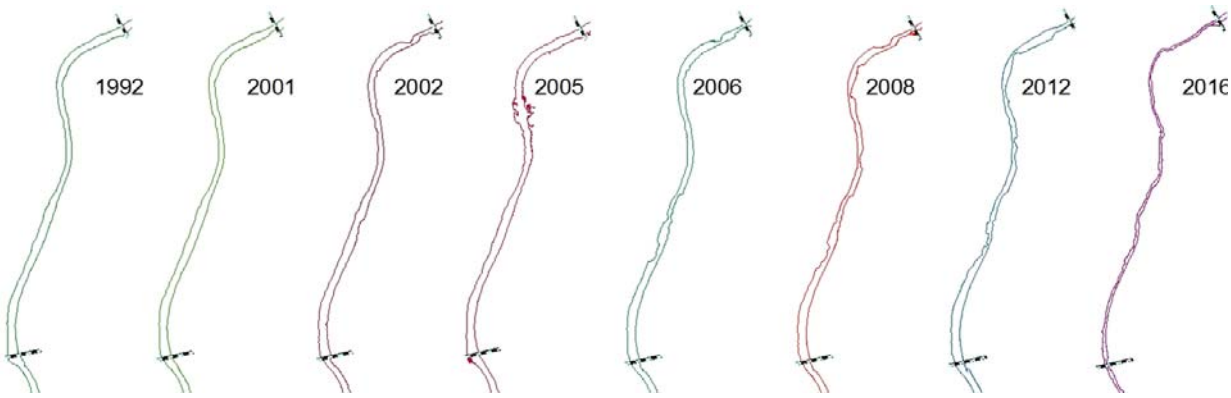
1992
2001
2002
2005
2006
2008
2012
2016

*I4*

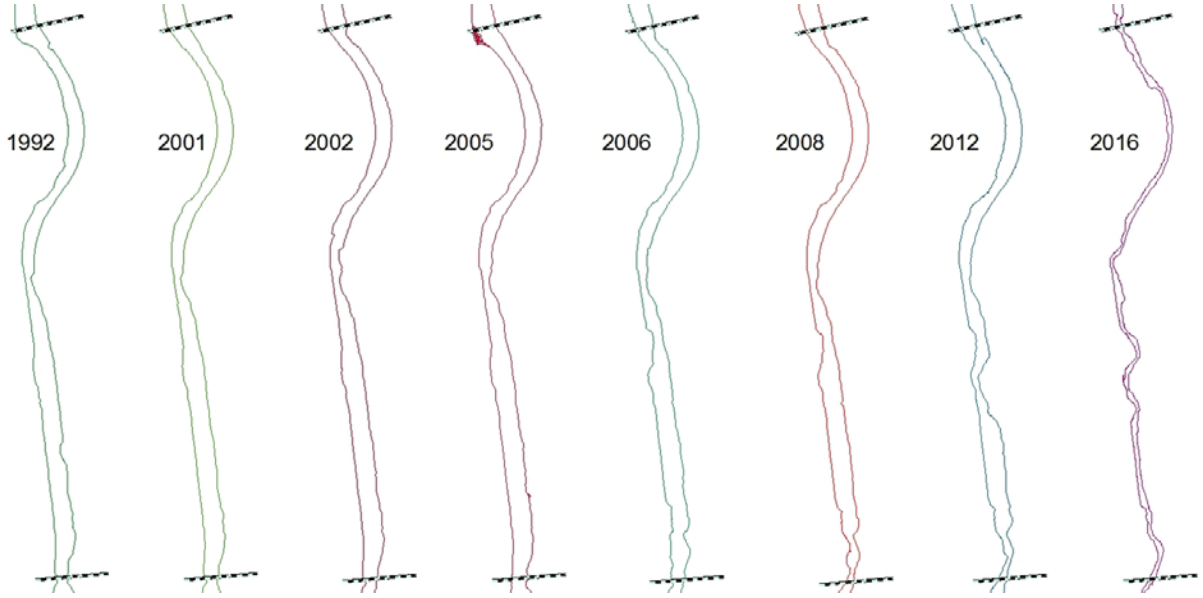
1992
2001
2002
2005
2006
2008
2012
2016

*I5*

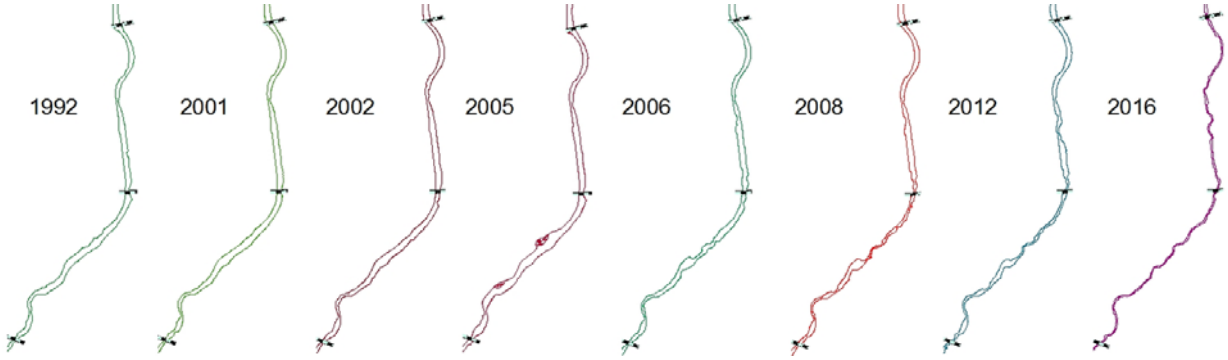
1992
2001
2002
2005
2006
2008
2012
2016

*I6*

## Appendix E - Habitat Score by Subreach (All Years)

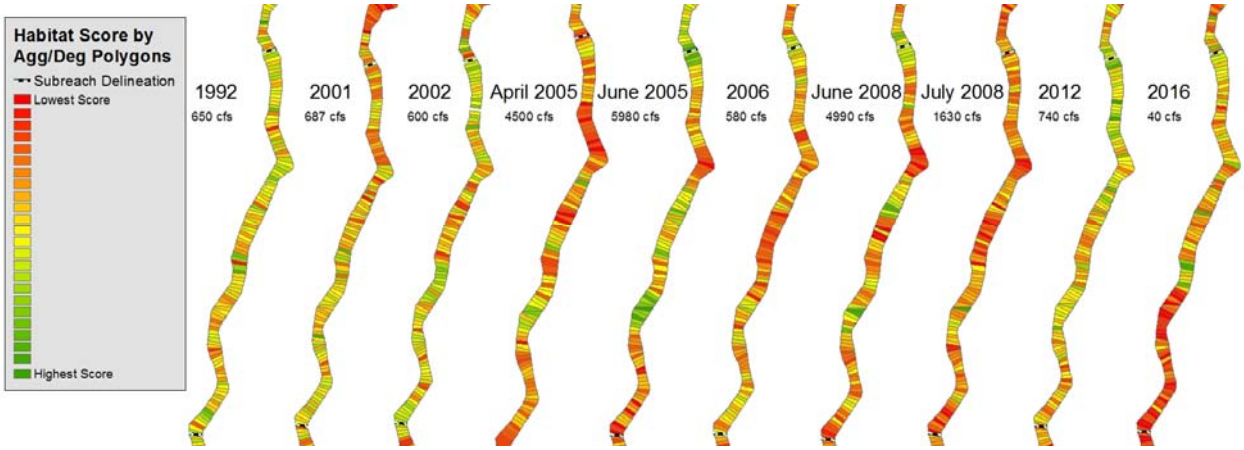


*I2*

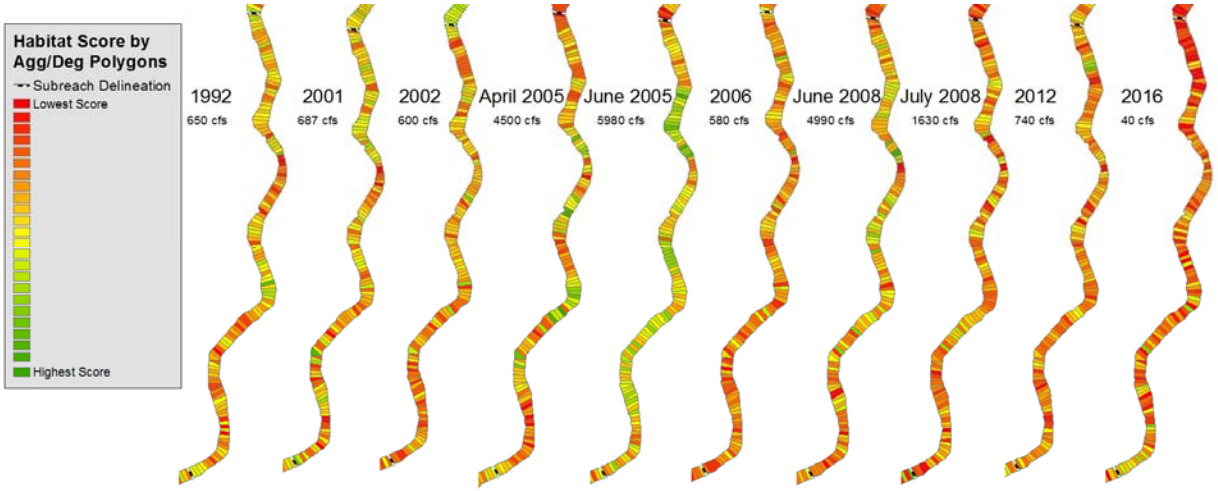


*I3*


*I4*

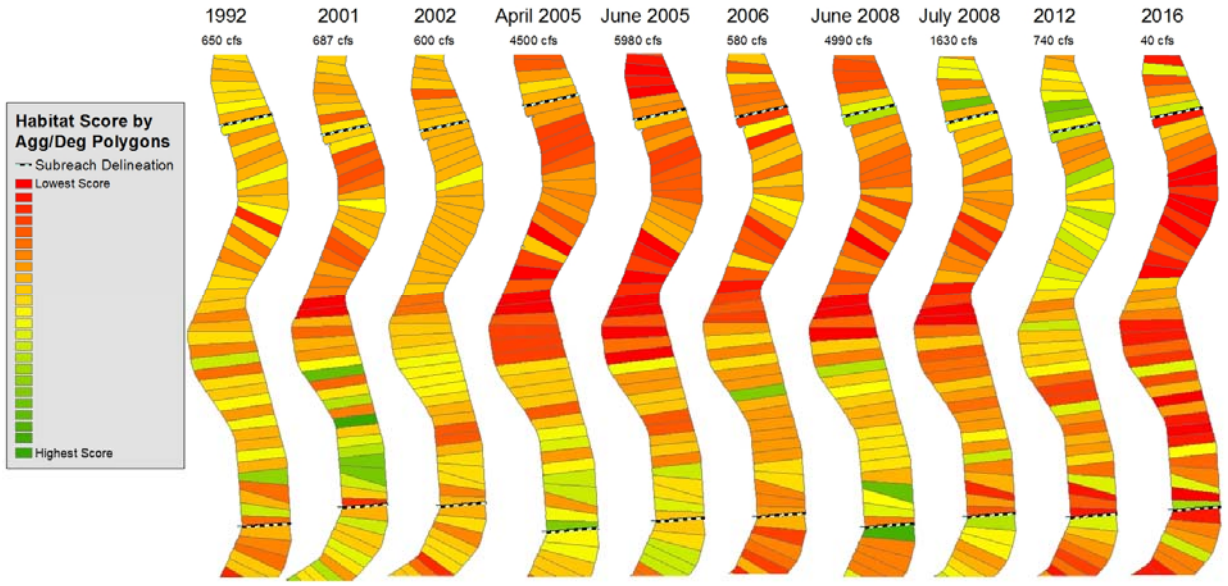
Habitat Score by Agg/Deg Polygons
Subreach Delineation
Lowest Score
Highest Score
1992
650 cfs
2001
687 cfs
2002
600 cfs
April 2005
4500 cfs
June 2005
5980 cfs
2006
580 cfs
June 2008
4990 cfs
July 2008
1630 cfs
2012
740 cfs
2016
40 cfs

*I5*

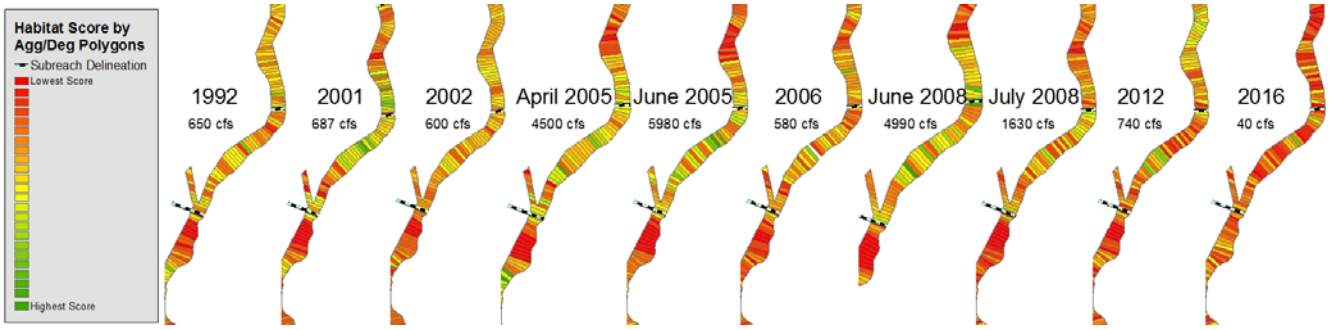
Habitat Score by Agg/Deg Polygons
Subreach Delineation
Lowest Score
Highest Score
1992
650 cfs
2001
687 cfs
2002
600 cfs
April 2005
4500 cfs
June 2005
5980 cfs
2006
580 cfs
June 2008
4990 cfs
July 2008
1630 cfs
2012
740 cfs
2016
40 cfs

*I6*

Appendix F - Habitat Score by Subreach (Years with flows around 650 cfs)

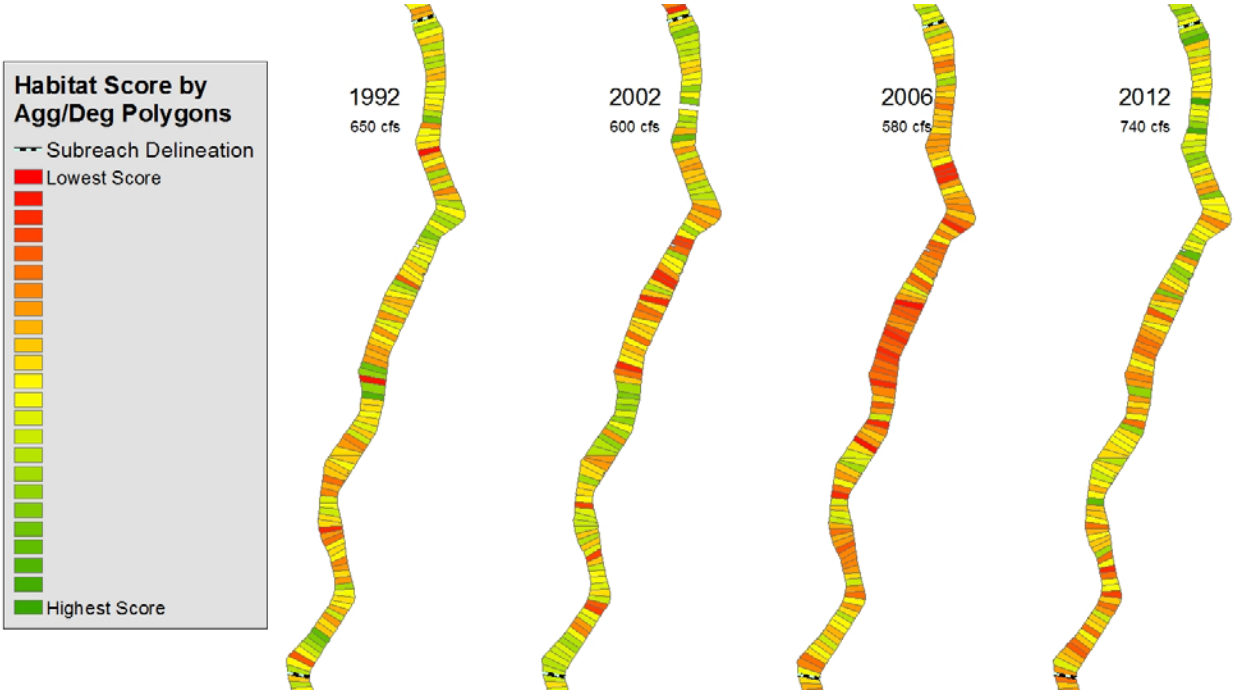


*I2*

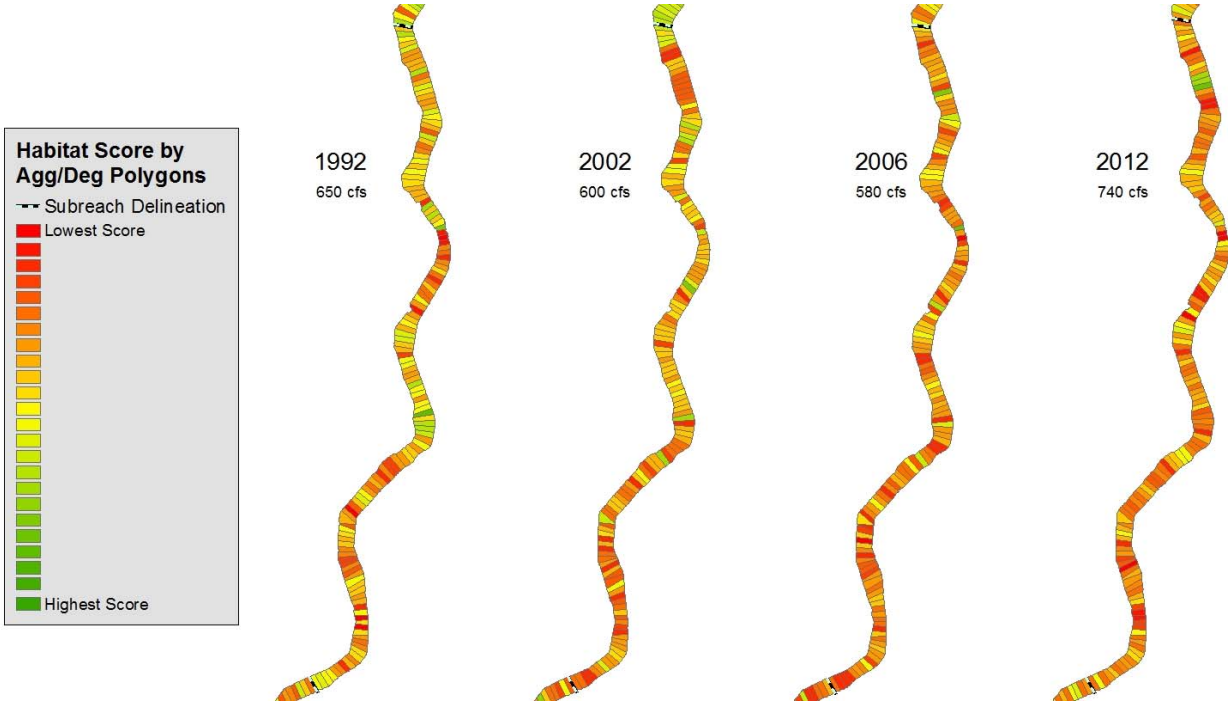


*I3*

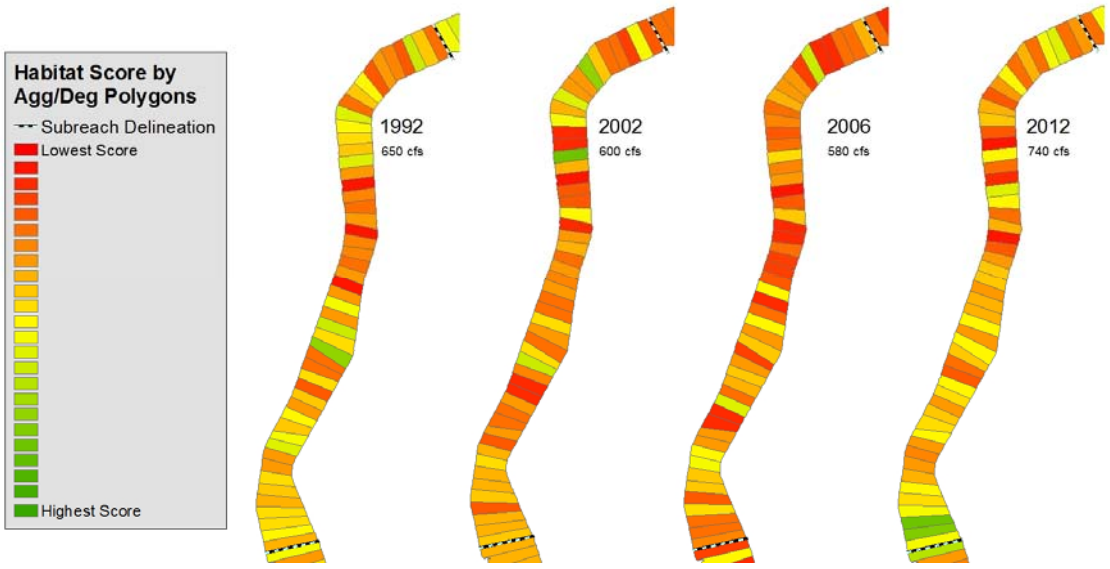
Habitat Score by
Agg/Deg Polygons
Subreach Delineation
Lowest Score
Highest Score
1992
650 cfs
2002
600 cfs
2006
580 cfs
2012
740 cfs

*I4*

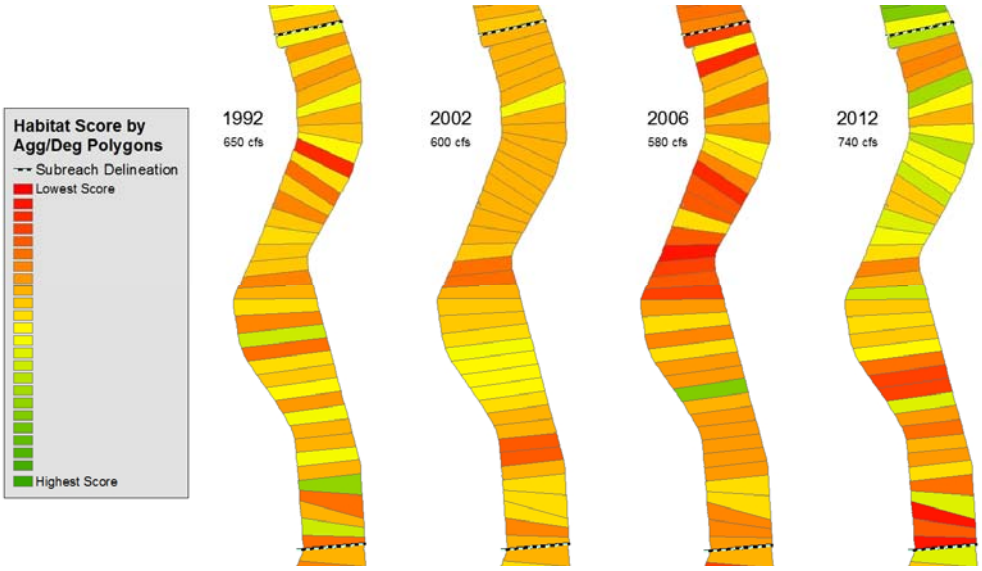
Habitat Score by
Agg/Deg Polygons
Subreach Delineation
Lowest Score
Highest Score
1992
650 cfs
2002
600 cfs
2006
580 cfs
2012
740 cfs

*I5*

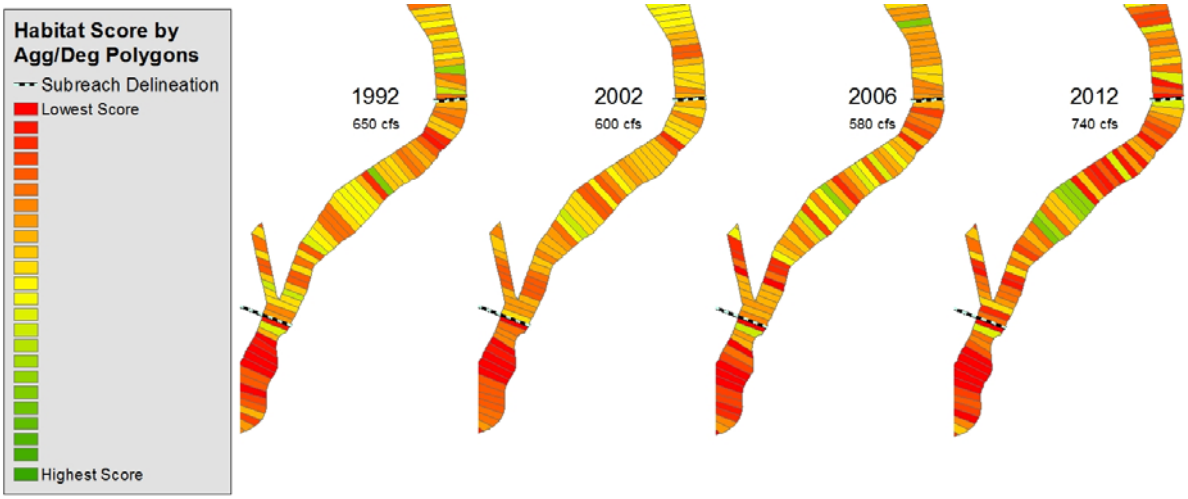
Habitat Score by Agg/Deg Polygons
Subreach Delineation
Lowest Score
Highest Score
1992
650 cfs
2002
600 cfs
2006
580 cfs
2012
740 cfs

*I6*

Appendix G - Summary of HEC-RAS and GIS habitat

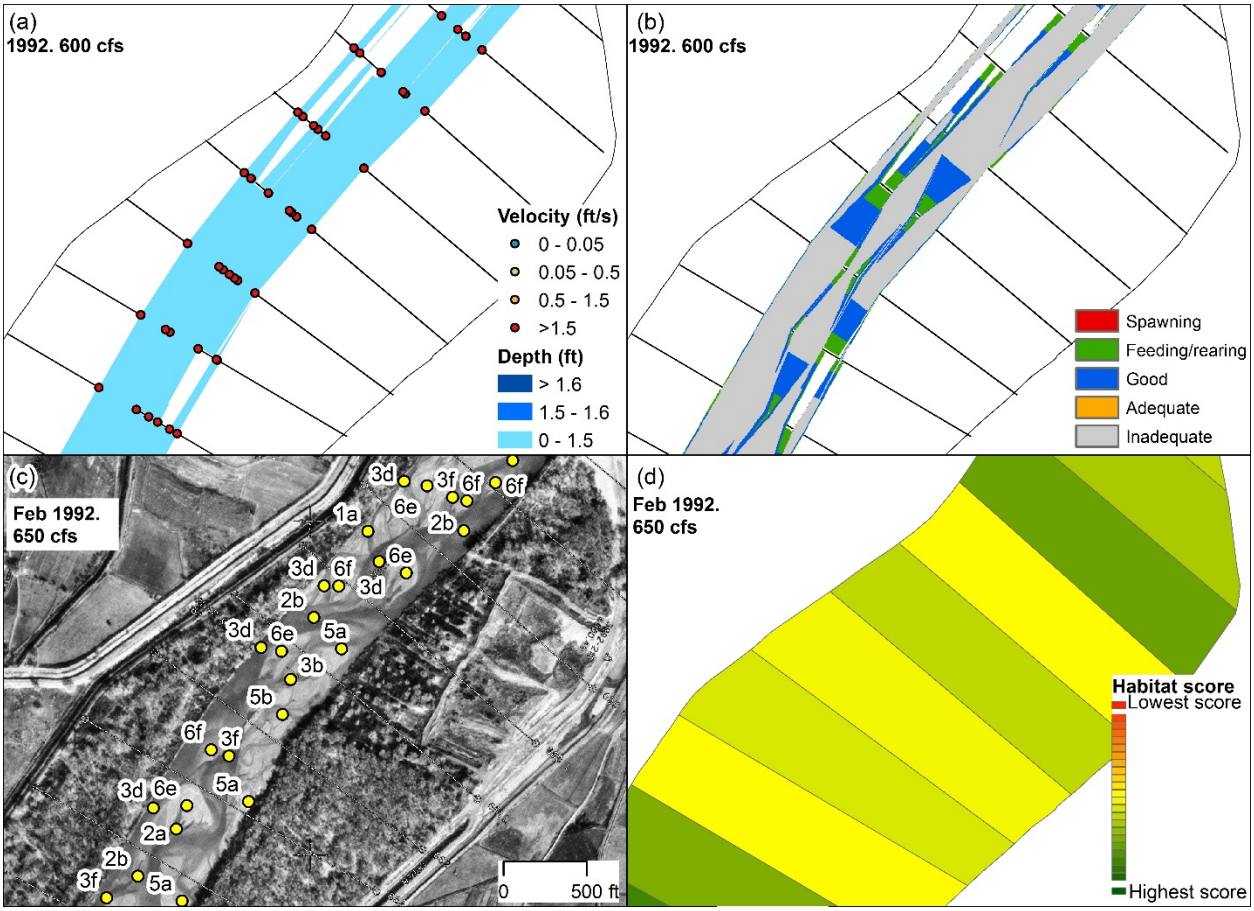


Summary of HEC-RAS and GIS habitat at subreach I1, aggdeg 657 to 665. (a) Velocity and depth of the simulation. (b) Habitat criteria mapped based on velocity and depth. (c) Habitat features mapped out by points and letters. (d) Habitat color scheme based on habitat features.

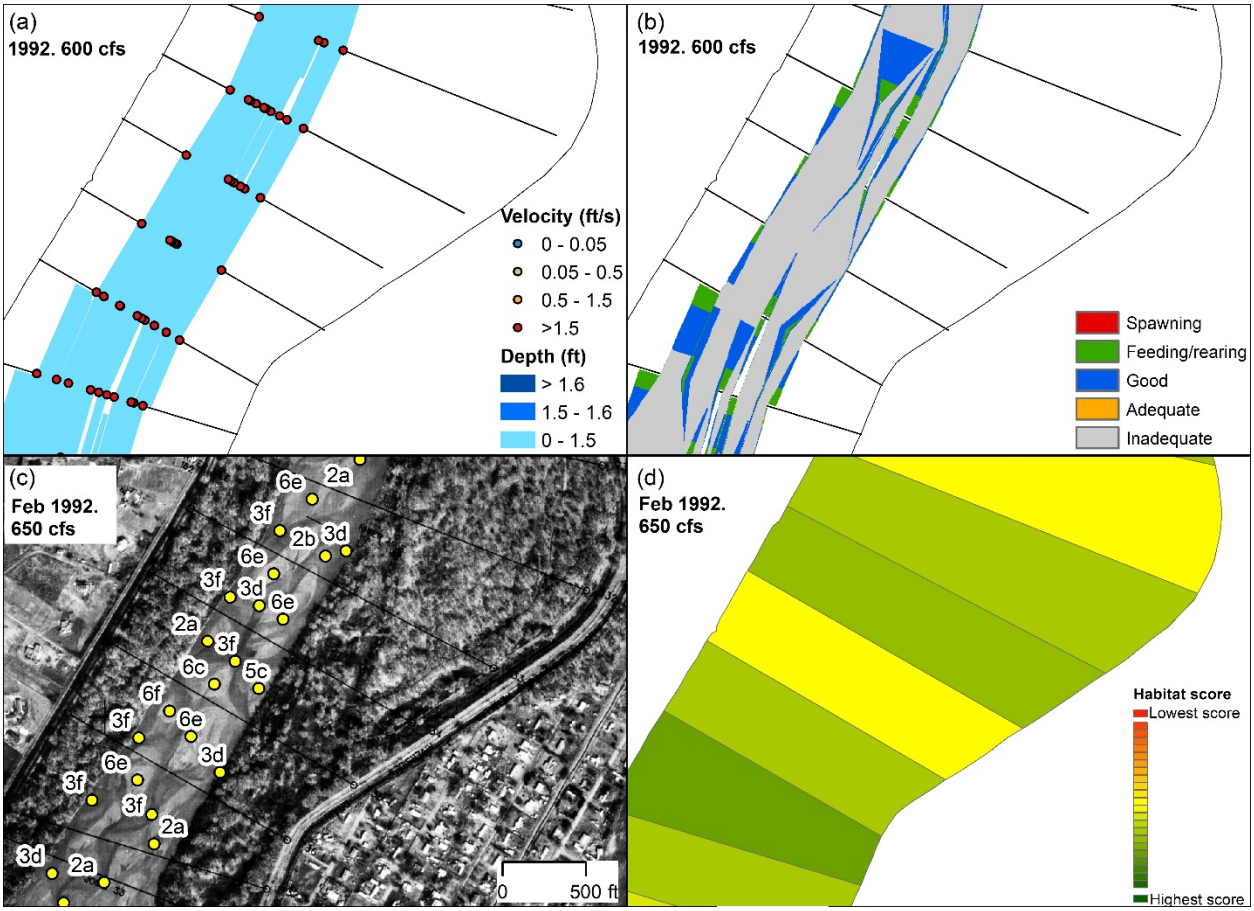


Summary of HEC-RAS and GIS habitat at subreach I2, aggdeg 732 to 737. (a) Velocity and depth of the simulation. (b) Habitat criteria mapped based on velocity and depth. (c) Habitat features mapped out by points and letters. (d) Habitat color scheme based on habitat features.

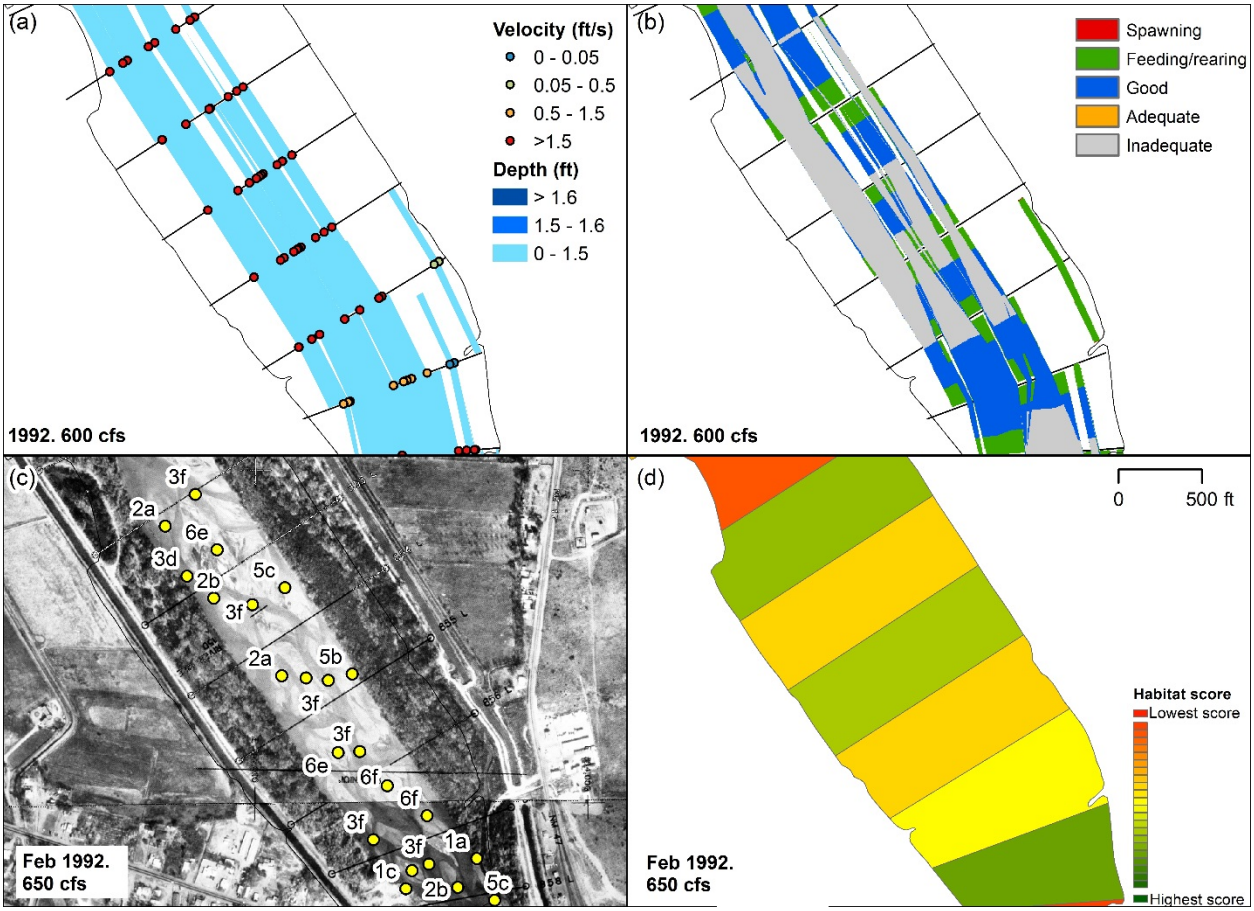


Summary of HEC-RAS and GIS habitat at subreach I3, aggdeg 852 to 858. (a) Velocity and depth of the simulation. (b) Habitat criteria mapped based on velocity and depth. (c) Habitat features mapped out by points and letters. (d) Habitat color scheme based on habitat features.

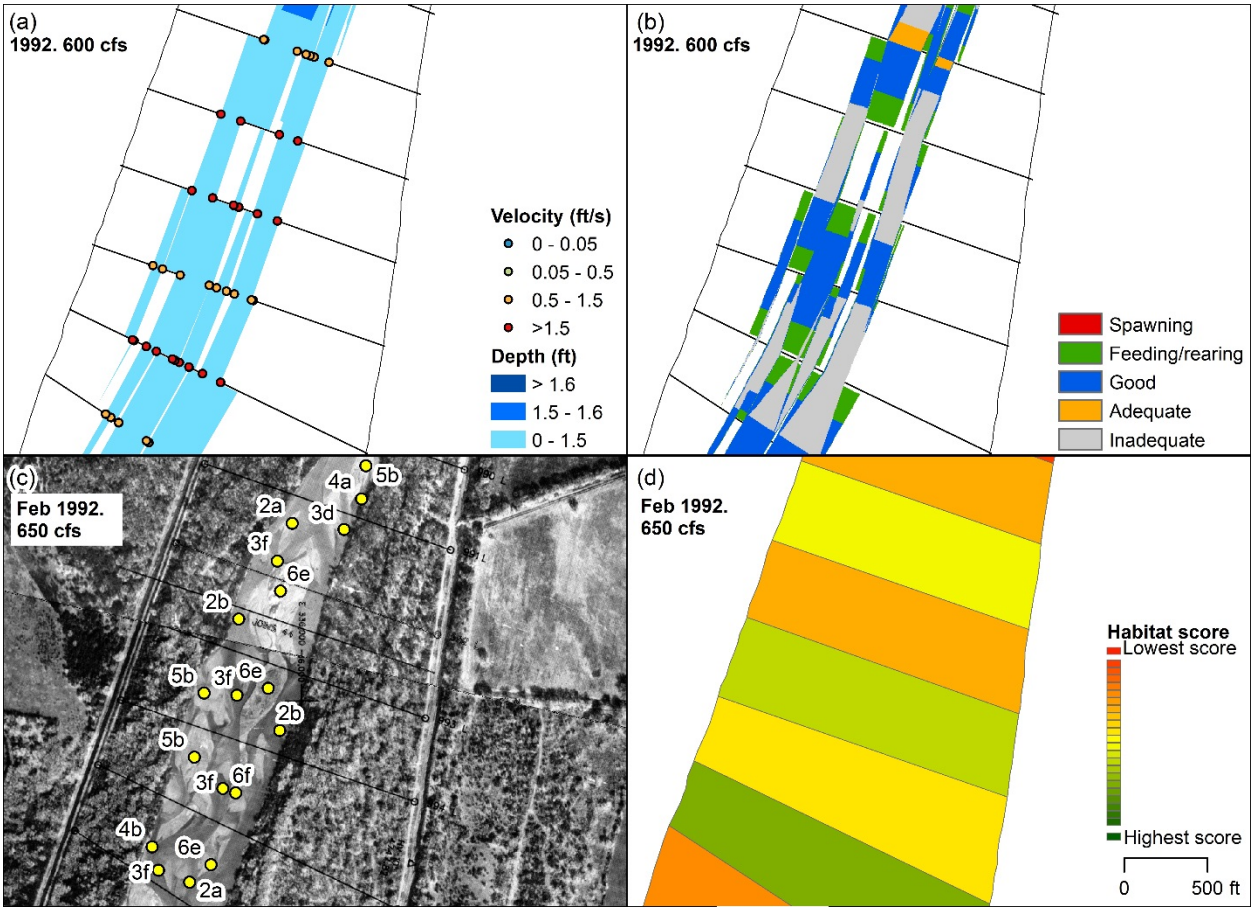


Summary of HEC-RAS and GIS habitat at subreach I4, aggdeg 991 to 996. (a) Velocity and depth of the simulation. (b) Habitat criteria mapped based on velocity and depth. (c) Habitat features mapped out by points and letters. (d) Habitat color scheme based on habitat features.

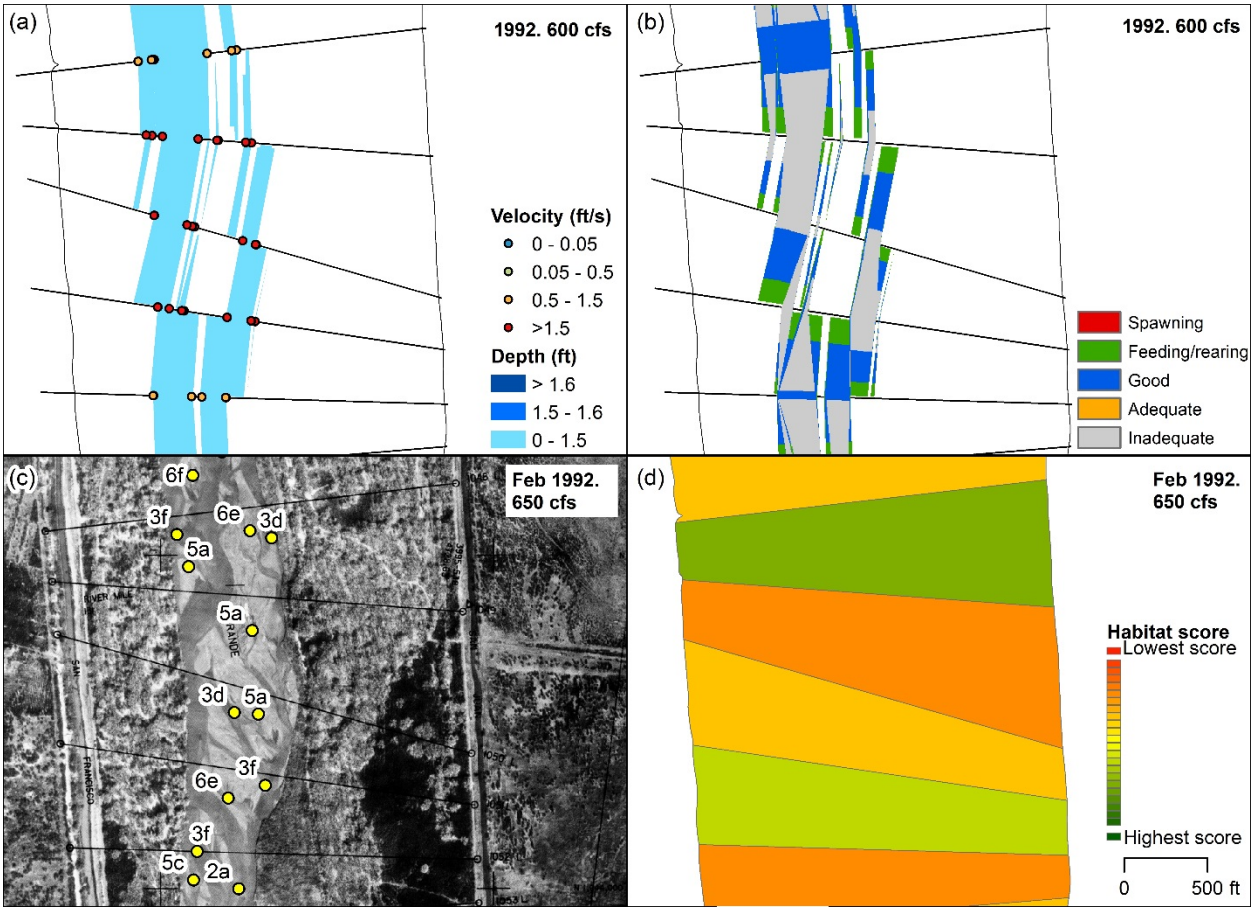


Summary of HEC-RAS and GIS habitat at subreach I5, aggdeg 1048 to 1053. (a) Velocity and depth of the simulation. (b) Habitat criteria mapped based on velocity and depth. (c) Habitat features mapped out by points and letters. (d) Habitat color scheme based on habitat features.

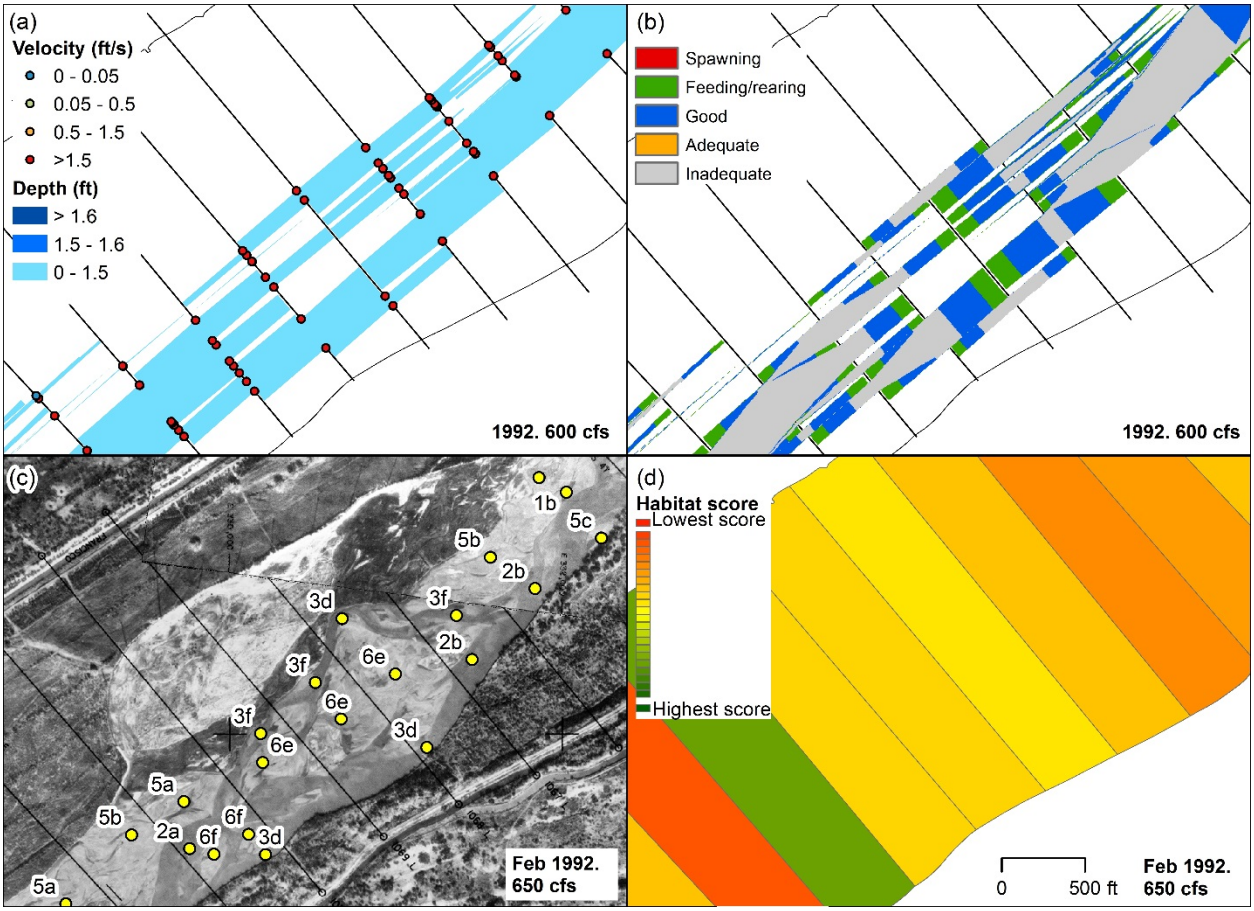


Summary of HEC-RAS and GIS habitat at subreach I6, aggdeg 1064 to 1072. (a) Velocity and depth of the simulation. (b) Habitat criteria mapped based on velocity and depth. (c) Habitat features mapped out by points and letters. (d) Habitat color scheme based on habitat features.